

https://dspace.org/

Analysis of the river flow interaction with gabions

Pepper, Shona Anne

2013-07-12
http://hdl.handle.net/10539/12819

Downloaded from a DSpace repository. https://dspace.org/

ANALYSIS OF THE RIVER FLOW INTERACTION WITH GABIONS

Shona Anne Pepper

A research report submitted to the Faculty of Engineering and the Built Environment, University of the Witwatersrand, Johannesburg, in partial fulfilment of the requirements for the degree of Master of Science in Engineering.

Johannesburg 2013

DECLARATION

I declare that this research report is my own unaided work. It is being submitted to the Degree of Master of Science to the University of the Witwatersrand, Johannesburg. It has not been submitted before for any degree or examination to any other University.

……

Shona Anne Pepper

…… day of ……..…, 2013

ABSTRACT

The study examines the interaction of river flow with gabions in order to optimize their use for the treatment of acid mine drainage (AMD) contamination. The effects of the change in submerged volume, gabion arrangement and number of gabions on the mean residence time and its distribution are studied.

Gabions of dimensions (length x breadth x height) 0.29 m x 0.29 m x 0.175 m and a single gabion of dimensions 0.62 m x 0.62 m x 0.38 m have been tested in a 0.92 m wide flume in the Hydraulics laboratory in the School of Civil and Environmental Engineering at the University of the Witwatersrand, Johannesburg.

The study revealed that a decrease in the submerged volume, gabions arranged in an aligned pattern and increasing the number of gabions produced increased proportions of gabion-flow interaction. Generally, the proportion of gabion-flow interaction remained approximately the same except when twelve gabions, arranged in a staggered pattern, were tested. When testing twelve gabions there was a sudden decrease in the gabion-flow interaction when compared to four and eight gabions. The gabion-flow interaction increased again once the number of gabions was increased to sixteen. These results were confirmed by the results produced from a concentration dispersion model. This model simulated the flow of contaminated fluid ‘particles’ through a channel, which was divided into successive zones.

ACKNOWLEDGEMENTS

I would like to thank:

- My supervisor, Professor C.S. James, for the support and encouragement received while undertaking this degree.
- My co-supervisor, Mr C. Sheridan, for the support received while completing the degree and for the guidance received during testing.
- Mrs T. Booysen, for her assistance with the laboratory processes and equipment.
- Mr. W. Costopoulos and the laboratory technicians for their assistance in the hydraulic laboratory whilst running the experiments.
- Lara Dos Santos, for always making herself available to lend a hand while running experiments.
- My parents and my brother for their support and encouragement throughout my studies.
- Concor Roads and Earthworks for making my studies possible through their support and financial assistance.

CONTENTS

DECLARATION ..... **i**

ABSTRACT ..... **ii**

ACKNOWLEDGEMENTS ..... **iii**

LIST OF FIGURES ..... **vii**

LIST OF TABLES ..... **x**

LIST OF SYMBOLS ..... **xi**

NOMENCLATURE ..... **xiii**

1 INTRODUCTION **1**

1.1 General **1**

1.2 Objectives **2**

1.3 Approach **2**

1.4 Scope **2**

2 LITERATURE REVIEW **4**

2.1 Introduction **4**

2.2 The Formation and Threat of Acid Mine Drainage **5**

2.3 Remedial Acid Mine Drainage Methods **9**

2.3.1 Passive Treatment of Acid Mine Drainage 9

2.3.2 Active Treatment of Acid Mine Drainage 12

2.3.3 Hydraulic Studies 14

3 EXPERIMENTAL METHODOLOGY **20**

3.1 Spectrophotometer Calibration **20**

3.2 Gabion Construction and Arrangements **21**

3.2.1 General 21

3.2.2 Gabion Arrangements 22

3.2.3 Change of Flow Depth 24

3.2.4 Experimental Layout 25

3.3 Data Collection **29**

3.3.1 Injection Scheme 29

3.3.2 Collection Scheme 30
3.4 Test Procedure 32
3.4.1 Residence Time Distribution of the Empty Flume: Control 32
3.4.2 Changing the Flow Depth 32
3.4.3 Changing the Gabion Arrangement 33
3.4.4 Changing the Number of Gabions 34
3.5 Residence-Time Distribution (RTD) Analysis 35
3.5.1 Introduction 35
3.5.2 Measuring the Moments of the RTD for Pulse Input Experiments: 37
3.5.3 Residence-Time Distribution (RTD) Analysis Example 40
4 RESULTS AND DISCUSSION 45
4.1 Residence Time Distribution of the Empty Flume: Control 45
4.2 Changing the Flow Depth 47
4.3 Changing the Gabion Arrangement 51
4.4 Changing the Number of Gabions 54
5 MODELLING THE CONCENTRATION DISPERSION IN A CHANNEL CONTAINING GABIONS 58
5.1 General 58
5.2 Model Design 58
5.3 Model Simulation 60
5.4 Use of the Model to Simulate Experimental Data 62
6 CONCLUSIONS AND RECOMMENDATIONS 67
6.1 Summary and Conclusions of the Present Study 67
6.2 Recommendations for Future River Flow Studies Related to Gabions 68
7 REFERENCES 69
8 BIBLIOGRAPHY 72
9 APPENDIX A: Spectrophotometer Calibration Curve 73
10 APPENDIX B: Residence Time Distribution Analysis 74
10.1 Empty Flume: Control 74
10.2 Changing the Flow Depth 75
10.3 Changing the Gabion Arrangement 84
10.4 Changing the Number of Gabions 93

11 APPENDIX C: Model Coding in VBA..... 105

LIST OF FIGURES

Figure 2.1: Geological cross-section orientated in a North-South direction (McCarthy, 2010) 5
Figure 2.2: Mining methods used for gold mining on the Witwatersrand (McCarthy, 2010) 6
Figure 2.3: Water level rise in the mine void (McCarthy, 2010) 8
Figure 2.4: Passive treatment system conceptual outline (Rees et al, 2004) 11
Figure 2.5: Alkali dosing plant conceptual outline (Rees et al, 2004) 12
Figure 2.6: Short-term treatment processes (in yellow) used in Gauteng, South Africa 13
Figure 2.7: Sulphide formation using bioreactors conceptual outline (Rees et al, 2004) 13
Figure 2.8: Model system of a rectangular rubble mound weir (Michioku et al, 2005) 16
Figure 3.1: Spectrophotometer and calibration concentration samples 21
Figure 3.2: Gabions (0.29 m x 0.29 m x 0.175 m) filled with 26 mm stone 22
Figure 3.3: Plan view of arrangement 1 23
Figure 3.4: Plan view of arrangement 2 24
Figure 3.5: Weir gate control at flume end 25
Figure 3.6: Plan view of the experimental layout for experiment 1 - empty flume 27
Figure 3.7: Plan view of the experimental layout for experiments 2, 3 and 4 - change in flow depth assessment 27
Figure 3.8: Plan view of the experimental layout for experiment 5 - change in flow pattern assessment 27
Figure 3.9: Plan view of the experimental layout for experiment 6 - change in flow pattern assessment 28
Figure 3.10: Plan view of the experimental layout for experiment 7 - change in flow pattern assessment 28

Figure 3.11: Plan view of the experimental layout for experiment 8 - change in the number of gabions assessment (together with experiments 3 and 5)..... 28
Figure 3.12: Plan view of the experimental layout for experiment 9 - change in the number of gabions assessment (together with experiments 3 and 5)..... 29
Figure 3.13: Adjustable injection scheme..... 30
Figure 3.14: Indication of horizontal (left) and vertical (right) mixing..... 30
Figure 3.15: Collection scheme in and out of use..... 31
Figure 3.16: Concentration vs. time graph (C(t))..... 42
Figure 3.17: Concentration vs. time (C(t)) graph for the bypass peak..... 43
Figure 3.18: Concentration vs. time C(t) graph for the flow interaction with gabions peaks..... 44
Figure 4.1: Residence time distribution for experiment 1: empty flume..... 45
Figure 4.2: Plan view of dye flowing in the empty flume experiment..... 46
Figure 4.3: No-slip condition observed during experimentation..... 47
Figure 4.4: Residence time distribution for experiment 2: 16 cm flow depth..... 48
Figure 4.5: Residence time distribution for experiment 3: 13 cm flow depth..... 48
Figure 4.6: Residence time distribution for experiment 4: 10 cm flow depth..... 49
Figure 4.7: Residence time distribution for experiment 5: arrangement 1 using a flow depth of 13 cm..... 51
Figure 4.8: Residence time distribution for experiment 6: arrangement 2 using a flow depth of 13 cm..... 51
Figure 4.9: Residence time distribution for experiment 7: single gabion using a flow depth of 11.2 cm..... 52
Figure 4.10: Flow pattern seen during experimentation - experiment 5: arrangement 1..... 53
Figure 4.11: Flow pattern seen during experimentation - experiment 6: arrangement 2..... 53
Figure 4.12: Flow pattern seen during experimentation - experiment 7: single gabion..... 54

Figure 4.13: Residence time distribution for experiment 5: four gabions using arrangement 1 54
Figure 4.14: Residence time distribution for experiment 3: eight gabions using arrangement 1 55
Figure 4.15: Residence time distribution for experiment 8: twelve gabions using arrangement 1 55
Figure 4.16: Residence time distribution for experiment 9: sixteen gabions using arrangement 1 56
Figure 4.17: Comparison of the mean residence time per unit length for varying number of gabions 57
Figure 5.1: Plan view of channel divided longitudinally into zones 58
Figure 5.2: Flow of particles through zone 59
Figure 5.3: Simulation of relative concentration dispersion through two channel zones 61
Figure 5.4: Simulated concentration vs. time (C(t)) graph for one zone – four gabions 62
Figure 5.5: Simulated concentration vs. time (C(t)) graph for two zones – eight gabions 63
Figure 5.6: Simulated concentration vs. time (C(t)) graph for three zones – twelve gabions 63
Figure 5.7: Simulated concentration vs. time (C(t)) graph for four zones – sixteen gabions 64

LIST OF TABLES

Table 3.1: Experimental layout and configuration..... 26
Table 3.2: Hypothetical set of data representative of eight gabions in a flume.... 40
Table 3.3: Example results..... 42
Table 3.4: Bypass peak analysis 43
Table 3.5: Flow interaction with gabions peak analysis 44
Table 4.1: Flow proportion distribution comparison when changing the flow depth 50
Table 4.2: Flow proportion distribution comparison when changing the gabion arrangement..... 52
Table 4.3: Flow proportion distribution comparison when changing the number of gabions 57
Table 5.1: Model input – proportion of flow in each pathway for each zone..... 65
Table 5.2: Comparison of the experimental and modelled results..... 65

LIST OF SYMBOLS

B_i	Width of Weir at Section i
C_i	Concentration of Sample i Taken at Time t_i
D	Dispersion Number
E_i	Residence Time Distribution Function for Sample i
E(t)	Residence Time Distribution Function / Age Distribution
F	Volumetric Flow Rate for Residence Time Distribution Analysis
F(t)	Cumulative Distribution Function
g	Acceleration of Gravity
h_i	Flow Depth at Section i
h'	Transition Water Depth between Sections at Upstream Weir Face
h''	Transition Water Depth between Sections at Downstream Weir Face
L	Length of Rubble Mound Weir
L_e	Distance from Injection Point to Weir Gate
N	Number of CSTRs in Series Required to Simulate a Given PFR Model
Q	Area Under the C(t) Graph
Q_i	Area Under the C(t) Graph for each Sample i
q	Volumetric Flow Rate for Rubble Mound Weir Calculations
U_i	Velocity at Section i
V_{eff}	Effective Volume
V_S	Volume of the Material's Particles
V_{Total}	Total Volume

V_V	Volume of Voids in the Material
x	Distance from First Gabion to Last Gabion
Δt	Time Interval for the Given C_i Value
δ_i	Velocity Correction Factor at Section i
ε	Porosity/Void Fraction of the Packed Material
λ	Hydraulic Efficiency
ρ	Fluid Density
σ^2	Variance
σ_θ^2	Normalized Variance / Second Moment
τ_{ideal}	Ideal Residence Time
τ_m	Mean Residence time

NOMENCLATURE

ABS	Absorbancy Reading from the Spectrophotometer
AMD	Acid Mine Drainage
CSTRs	Continuous-Stirred-Tank-Reactors
FWT Red Dye	Tracer used to simulate effluent
PFRs	Plug-Flow-Reactors
ppm	Parts Per Million = mg/l
RTD	Residence Time Distribution

1 INTRODUCTION

1.1 General

Acid Mine Drainage (AMD) in South Africa is a topic of growing concern because of the significant threat it poses to the surrounding environment. For this reason, there is a definite urgency in implementing an effective resolution, without which our available water resources could be contaminated with radio-active heavy metals and acid (Godfrey, et al, 2009). Sulfate contaminants could impact both the surrounding agriculture as well as those who utilise the untreated water. An effective resolution will require the development of an economical and efficient water treatment method.

One possible solution to the problem would be to strategically place reactive gabions into the impacted rivers. It is thought that the use of blast furnace slag could neutralise the AMD to acceptable pH levels. This solution appears to be viable as it would potentially minimise environmental waste by using waste products (from the steel production industry) to potentially solve the AMD problem. The objective of this research is to explore whether the strategic arrangement of gabions could be used for the treatment of AMD in rivers. The hydraulic efficiency of the possible gabion arrangements needs to be analysed. The hydraulic efficiency is determined by the ability of each possible gabion arrangement to attenuate the AMD flow long enough for the chemical reaction to take place. The flow interaction with the gabions, both in and around them, must be understood in order to optimise the contact time of the treatment process for various gabion arrangements. It is the understanding of this flow interaction which this research aims to achieve.

The current knowledge base is not adequate when analysing the 2D interaction between soil particles and flow. Some research has been conducted to analyse the effects of limestone filled gabions on the pH levels in acidic water (Arnold et al, 1988). However, this work is limited since there has been no focus on the interaction of flow or the possibility of gabion arrangements to significantly

increase mixing and contact time. In analysing the residence time distribution there has been little contribution to the field of study. Understanding this analysis would better indicate how the flow is interacting in the porous media.

1.2 Objectives

The objective of this research was to assess the impact various gabion arrangements, placed in a river, would have on the residence time distribution of the flow. This investigation describes the effect that the change in flow depth, various gabion patterns and the number of gabions used had on the flow attenuation.

1.3 Approach

In order to assess the effect of the above variables, a series of experiments were run in a flume in the Hydraulics Laboratory of the School of Civil and Environmental Engineering at the University of the Witwatersrand. Variables were altered so that patterns and inferences could be noted and made. Three different flow depths, three different patterns and four changes in the number of gabions used were tested in the flume.

All experiments were conducted in the same flume with the same flow rate of 9.92 l/s. The concentration of the impulse of tracer, FWT Red Dye, was kept constant at 25 000 ppm. Samples were collected across the full width of the flume at particular time intervals. These samples were subsequently analysed in a spectrophotometer.

1.4 Scope

Chapter 2 presents a review on the current AMD situation, the various remedial solutions and previous work conducted on the treatment of acidic discharge in rivers and flow through rockfill.

Chapter 3 describes the experimental techniques, data acquisition and the data processing. The test procedure for all of the experiments run is included in this chapter. Information on the residence time distribution theory of analysis is also provided with an example illustrating the use of this theory.

Chapter 4 presents the results and discussion for all of the experiments which were conducted. The experiments conducted assessed the effect of a change in flow depth, flow pattern and the total number of gabions used.

Chapter 5 presents a model that simulates the conducted experiments and aids the understanding of the dispersion of flow through the gabions. This model was compared to the experiments which investigated the effect of the change in the number of gabions used.

Conclusions and recommendations are made in Chapter 6.

2 LITERATURE REVIEW

2.1 Introduction

Acid Mine Drainage (AMD) is highly acidic water which usually contains high concentrations of sulfates, metals and salts (Godfrey et al, 2009). It is caused by pyrite/sulfide ores which are oxidised in an aquatic environment (WPCAMR, no date):

- Pyrite reacts with water and oxygen forming dissolved ferrous iron, acidity and sulfate

  $4FeS_{2(S)} + 14O_{2(g)} + 4H_20_{(l)} \longrightarrow 4Fe^{2+}_{(aq)} + 8SO_4^{2-}{}_{(aq)} + H^+_{(aq)}$ (2.1)

- Ferrous iron is oxidised to ferric iron

  $4Fe^{2+}_{(aq)} + O_{2(g)} + 4H^+_{(aq)} \longrightarrow 4Fe^{3+}_{(aq)} + 2H_2O_{(l)}$ (2.2)

- Ferric iron is hydrolysed to insoluble iron hydroxide. The net reaction is

  $4FeS_{s(s)} + 15O_{2(g)} + 14H_2O_{(l)} \longrightarrow 4Fe(OH)_{3(s)} + 8SO_4^{2-}{}_{(aq)} + 16H^+$ (2.3)

  Pyrite + Oxygen + Water $\longrightarrow$ Iron Hydroxide + Sulfate + Acid

AMD is not a problem specific to South Africa. It is experienced throughout the world where mining activity exists. Examples of this are: the Rio Tinto River in Spain, which has been an important copper mining area for the last 5 000 years, is one of the oldest AMD sites (Galan et al, 1999) and at Cerro Rico de Potosi II in South America (Strosnider et al, 2011). AMD poses one of the major environmental challenges by mining activities in South Africa. In our water-scarce environment it is important that the fresh water supply is protected. This acidic water is one of the consequences of mining activity. It is this effluent which poses such a threat to the environment, as it pollutes our available fresh water supply. Underground mine shafts, runoff and discharge from open pits and mine waste dumps, tailings and ore stockpiles are the main sources from which AMD is produced (Godfrey et al, 2009). The Witwatersrand gold mining area is a large contributor to this environmental problem. Underground water is an immense reservoir system that is interconnected. Once a mine is closed the AMD still continues to contaminate the water supply due to decant (Godfrey et al, 2009). Decant occurs due to the rising levels and subsequent overflow of the AMD. Once

a mine closes the pumping system used to remove the AMD will no longer function. It is due to this that overflow occurs (McCarthy, 2010).

2.2 The Formation and Threat of Acid Mine Drainage

In Gauteng the Main Reef layer attracted the most mining activity due to the abundance of gold. This layer can be seen in Fig. 2.1, together with the Kimberley Reef, where limited mining took place.

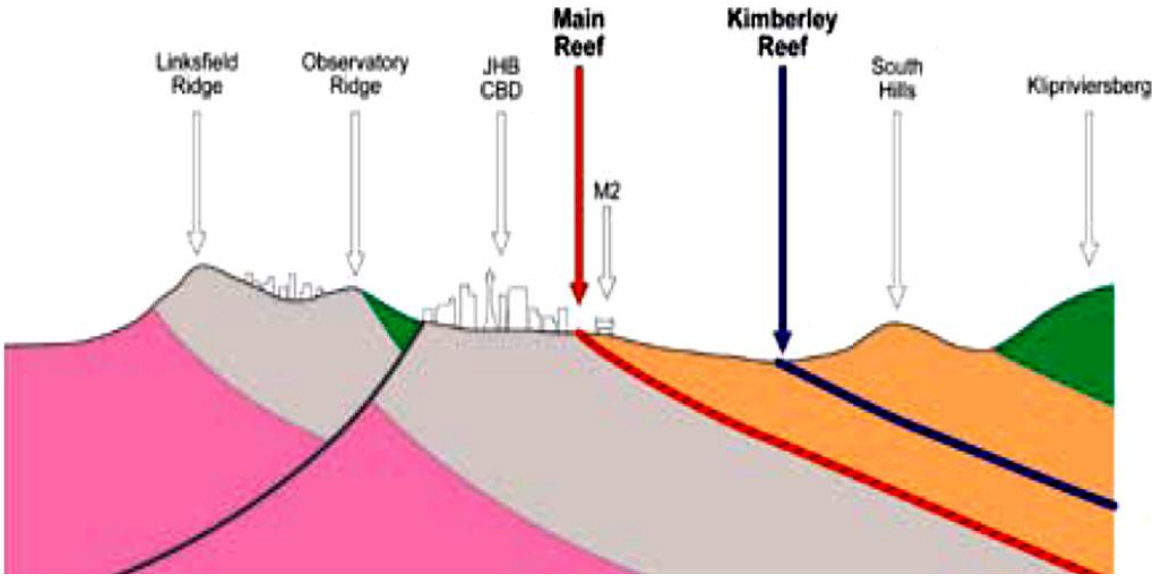


Figure 2.1: Geological cross-section orientated in a North-South direction (McCarthy, 2010)

As mining activity increased the need to mine deeper became apparent, as the gold-bearing rock at the current levels had all been mined. This led to the use of vertical shafts with horizontal tunnels (Fig. 2.2), which were dug to reach the ore-bearing reef (McCarthy, 2010). As mining activity increased the additional shafts were made, all the while extracting the gold-bearing rock (McCarthy, 2010).

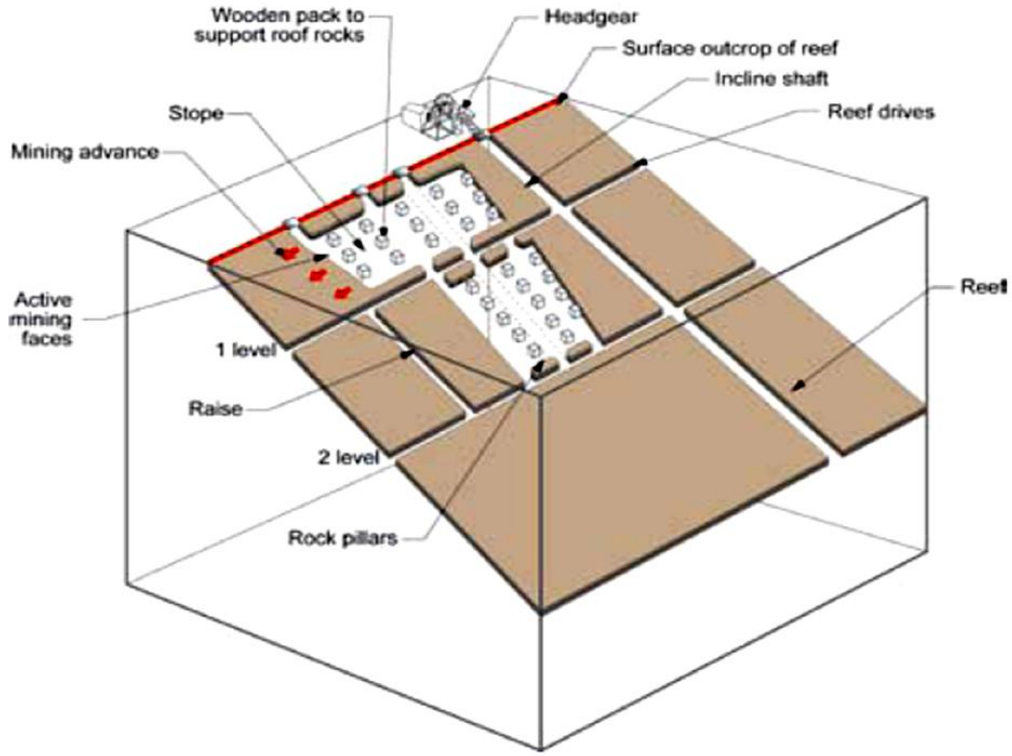


Figure 2.2: Mining methods used for gold mining on the Witwatersrand (McCarthy, 2010)

When the mines were in operation the inflow of water was channelled into sumps by using gullies (McCarthy, 2010). This inflow was constantly being pumped out of the void and to the surface, before the chemical reaction, whereby the acidic water is produced, could occur (McCarthy, 2010). The void is the term used for the underground cavities, caused by mining processes. The pumping of water out of the voids had to occur at a rate equal to the inflow of water into the mine so as to avoid the flooding of the mine works (McCarthy, 2010). Only once mining operations ceased did AMD become of such a high concern because the pumping then stopped, which led to the rising levels of underground water and the subsequent AMD problem because the exposed rock in the void had the three pre-requisites for AMD formation: pyrite, moisture and oxygen.

The development of an effective and efficient AMD treatment process is urgently required. The contamination of the valued fresh water supply is occurring at a rapid rate. According to McCarthy (2010) the level of AMD in Gauteng will continue to rise at an average rate, throughout the year of 15 m per month (Fig.

2.3). As the voids fill the water will flow into the higher areas and decant at low discharge points. McCarthy (2010) also believes that this rise in AMD will completely fill the voids by the year 2013. This means that the AMD problem is even more of a threat than originally thought. Once the voids fill, the decantation of AMD will be widespread (McCarthy, 2010).

The AMD problem is no doubt one of great concern and does require an efficient solution, however, one must also analyse the validity of McCarthy's (2010) views with regards to the rate at which the AMD is currently rising. This rate of AMD rise appears to be alarming. He does not, however, mention whether or not the AMD will continue to rise at that rate indefinitely. If not, then at what point will the AMD stop rising and how far reaching would the damage potentially be?

In order for a solution to be proposed, one needs to understand the composition of AMD which is significantly different within various areas (Robb and Robinson, 1995). Iron pyrite, found in the Main Reef mined rocks, becomes sulfuric acid when it is exposed to oxygenated water (McCarthy, 2010). This acid breaks down other minerals and their metals then dissolve into the sulfuric acid (McCarthy, 2010). It is this solution of acid and heavy metals which proves to be both toxic to the environment and corrosive to man-made structures.

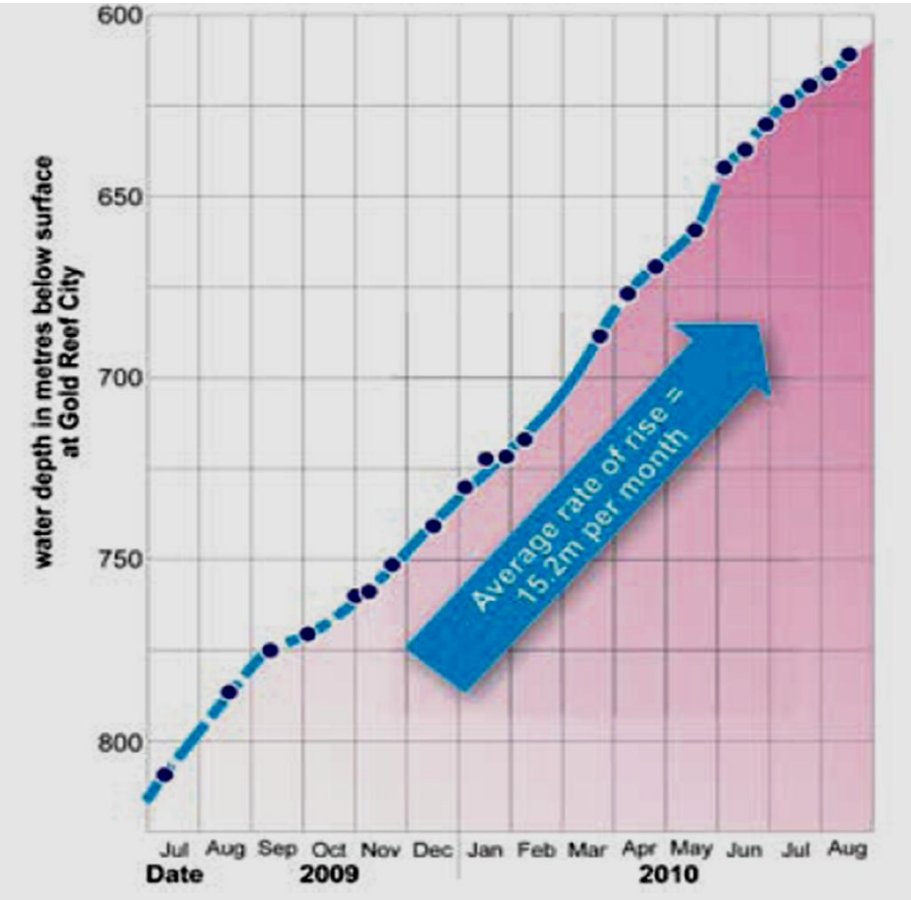


Figure 2.3: Water level rise in the mine void (McCarthy, 2010)

The AMD filling the mine voids pose not only a threat to the fresh water supply, but potentially also to the surrounding buildings which have deep basements. Once these mine voids fill up it is possible for the decant to flood the surrounding basements.

If an effective solution is not found soon the AMD could rapidly decant into the aquifers of many communities; this could threaten the quality of the fresh water for drinking and agricultural processes from the groundwater.

From all of the evidence presented above it is apparent that the AMD problem is severe. It may, however, not show quite how urgently a solution is required. The above papers mention the increasing rise in AMD levels and the potential for

decant in the very near future. There have, however, been instances where AMD has already decanted into our fresh water supplies. On the 24th of January 2011 it was reported that AMD had polluted the dams in the Kromdraai area, which is situated in the Cradle of Humankind (Karolia, 2011). The residents told reporters that the AMD had been flowing into the dams and has already poisoned the fish in one of their dams (Karolia, 2011). This is very concerning as the AMD problem has now become one which requires an immediate effective solution due to the contamination of their fresh water supply and possible food sources.

The AMD threat is severe and previously investigated remedial methods have proven to be inadequate. Some of these methods are discussed in Chapter 2.3.

2.3 Remedial Acid Mine Drainage Methods

2.3.1 Passive Treatment of Acid Mine Drainage

Arnold et al (1988) investigated the effects of limestone filled gabions on the pH of a mountain trout stream which had a pH between 4.5 and 5.3. The trout stream is found in the Clearfield and Elk counties of north-central Pennsylvania. The gabions were placed across the full width of the stream, thereby creating a weir effect. The results proved to be insignificant as the limestone only increased the pH by 0.5 units for a period of two weeks. Once the two-week period had passed, the effect of the limestone gabion barrier became untraceable. Additional problems arose due to the high material grain size distribution (grading) which lowered the porosity to a point where the gabion weir acted more as a dam. Arnold et al (1988) have suggested, however, that the method could be improved upon, by using a uniform sized (5 cm in diameter) stone which contains a high calcium content (>95%). This improvement has not yet been investigated.

Arnold et al (1988), however, did not consider that the free surface flow interaction with the flow within the gabions fill material might have a greater effect on the neutralization performance. The analysis of the free surface flow

interaction would give a better understanding of the expected behaviour of the gabion structure. They also did not investigate what percentage of the gabion fill was unreacted after the two week period had passed. This would give a good indication of the flow interaction within the gabion. Pattern placement of individual gabions, to improve mixing, was also not investigated.

Additional AMD remedial treatment solutions have been reviewed by Robb and Robinson (1995). These methods include: active and passive treatment, anoxic limestone drains (ALD), anaerobic wetland systems as well as manganese and aluminium removal. Robb and Robinson (1995) suggest that these methods are inadequate due to: the infancy in understanding the wetland system operation, land availability, high capital and running costs of active systems and the lack of complete polluted water treatments due to the fact that the above methods serve only to partially treat the AMD.

Possible AMD treatment strategies have been investigated in a case study 8km east of Aberystwyth in West Wales. The two adits (horizontal entrances to an underground mine) at the Cwmrheidol abandoned metal mine site, have contributed large quantities of zinc and lead to the Rheidol watercourse (Rees et al, 2004). According to Rees et al (2004) the water emanating from the mine has a pH of 3 and contains high levels of iron, copper, zinc, cadmium and lead. It is for this reason that the evaluation of various remedial methods was required. Rees et al (2004) evaluated three different remedial options. These included: passive treatment options, alkali dosing and sulfide formation using bioreactors.

Based on the guidelines available, the most suitable passive treatment for this investigated site, proved to be the Reducing and Alkalinity Producing System (RAPS) (Rees et al, 2004). This process operates by passing water vertically through a compost bed which is positioned on top of a layer of limestone. In order for the RAPS to be effective, the high iron and acidity loadings need to be significantly lowered. Rees et al (2004) state that limestone channels would lower

these loadings, while simultaneously optimizing bacterial iron oxidation, and settlement lagoons could be used to capture the precipitates. The processes predicted to occur were (Rees et al, 2004): the addition of bicarbonate alkalinity to the mine water from the dissolution of limestone, the increase in pH and alkalinity and the oxygenation of the mine water will lead to ochre precipitation and metal removal (specifically iron), the settlement lagoon will then trap the precipitates thereby limiting their transport to the RAPS. The RAPS will increase the alkalinity through bacterial processes and the sulfide produced by these processes will cause metals to precipitate as sulfides, the settlement lagoon will finally trap and accumulate the precipitates from the RAPS and site cut-off drains will prevent their discharge into the Afon Rheidol. The outline of the passive treatment system is depicted in Fig. 2.4.

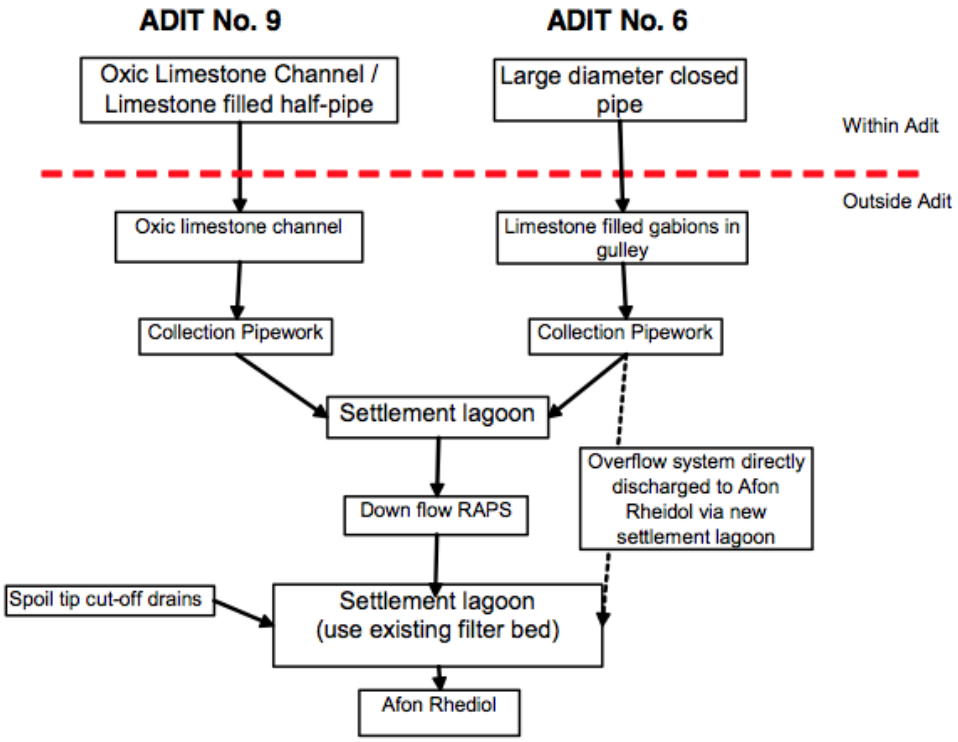


Figure 2.4: Passive treatment system conceptual outline (Rees et al, 2004)

2.3.2 Active Treatment of Acid Mine Drainage

The High Density Sludge (HDS) process was used for the alkali dosing treatment option (Rees et al, 2004). This process is one where the mine water is recirculated with hydroxide sludge before lime is introduced. This form of treatment requires an approximate area of 40 m x 40 m and also requires a method of collecting and transporting of the mine water and storing the sludge. The outline of the alkali dosing plant can be seen in Fig. 2.5.

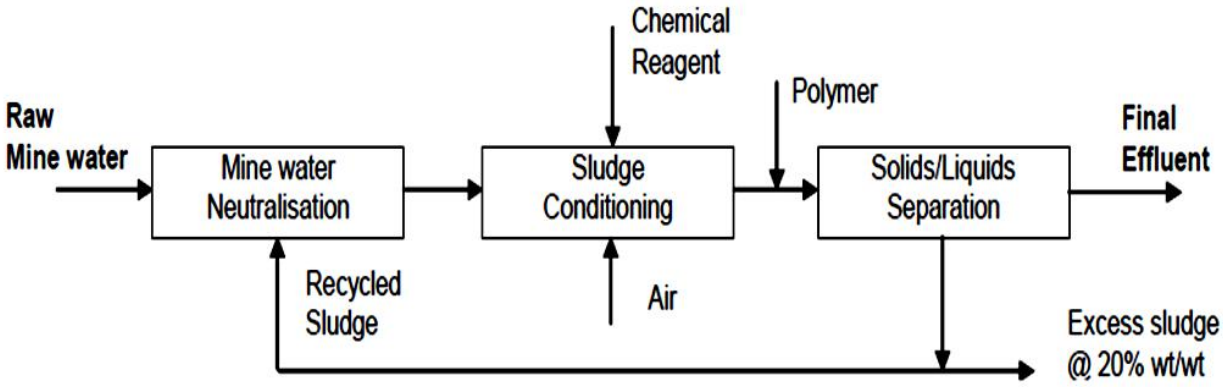


Figure 2.5: Alkali dosing plant conceptual outline (Rees et al, 2004)

This treatment process has been implemented in the Gauteng province, South Africa, as a short-term solution to the AMD problem (Fig. 2.6) (DWA, 2012).

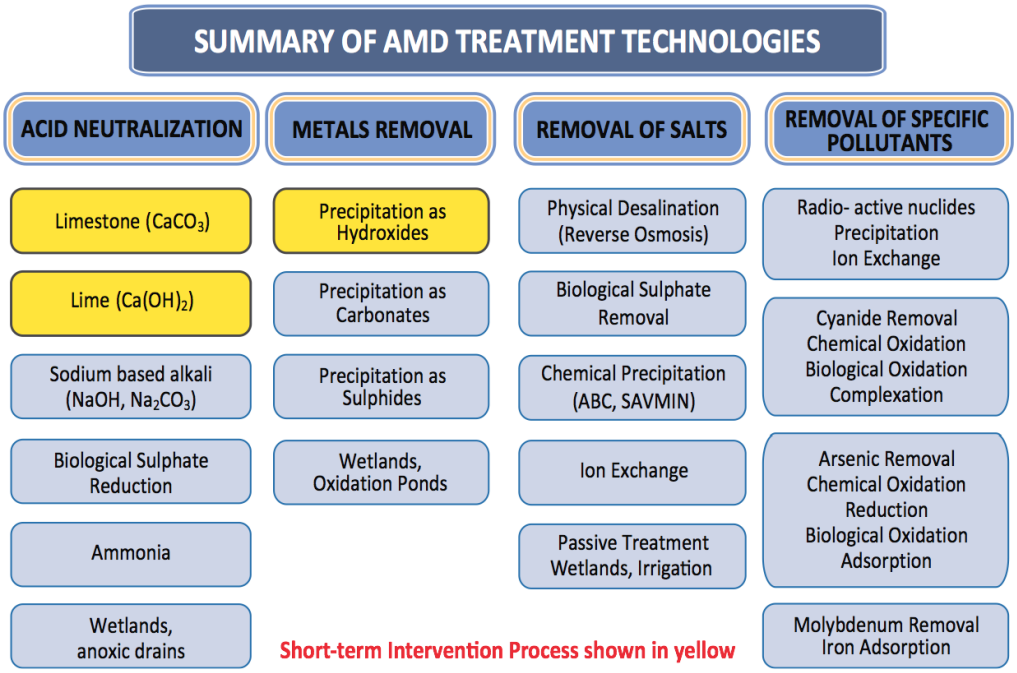


Figure 2.6: Short-term treatment processes (in yellow) used in Gauteng, South Africa (DWA, 2012)

The last treatment process under evaluation was the sulfide formation using bioreactors. Liquid based bioreactors are more commonly being used for the treatment of mine waters (Rees et al, 2004). "Liquid bioreactors are based on the same principle as RAPS; bacterial sulphate reduction (BSR) causes the formation of metal sulphides" (Rees et al, 2004. p. 10). The outline of the sulfide formation using bioreactors method can be seen in Fig. 2.7.

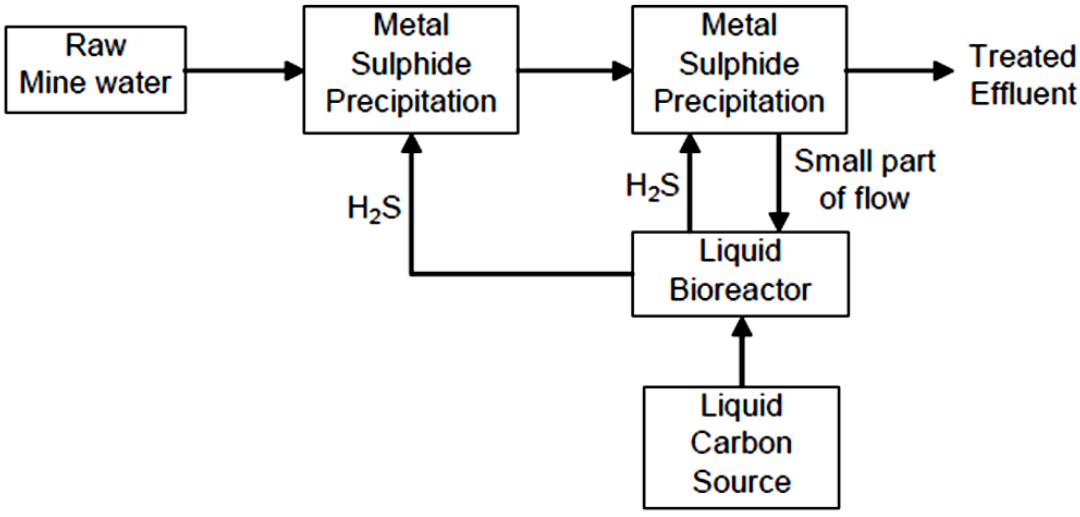


Figure 2.7: Sulphide formation using bioreactors conceptual outline (Rees et al, 2004)

An evaluation of each of the above treatment options was rendered, based on a ranking matrix and cost comparison, the passive treatment option was found to be the most viable for this mine site (Rees et al, 2004). From this treatment process the mine water was oxidized and the limestone dissolution would occur, which in turn would, encourage precipitation and accretion. According to Rees et al (2004) adit 6 was less polluted than adit 9. The system was therefore implemented in such a way so as to maximize the residence time of the mine water coming from adit 9.

From the above paper it is once again clear that the free surface flow interaction with the flow within the gabions was not analysed in sufficient detail. Rees et al (2004) did, however, consider the maximizing of the mine water's residence time. This was done by only partially treating the water from adit 6 so as to allow longer treatment time of the more polluted water produced from adit 9.

2.3.3 Hydraulic Studies

Samani et al (2004) produced a one-dimensional model to analyse the flow through rockfill dams. Since rockfill dams require the use of coarse particles, Darcy's law is no longer valid (Samani et al, 2004). This is because Darcy's law is based on laminar flow; however coarse particles produce turbulent flow within the pores due to the increased pore sizes and subsequent increase in Reynolds number (Re). Samani et al's (2004) model incorporates the Reynolds number (Re) and the Darcy-Weisbach coefficient *(f)*. This model can be used to determine the water level both upstream and downstream of the rockfill dam. The outflow hydrograph can then be produced, yielding the flow rate through the rockfill dam. Samani et al (2004) optimized the f – relationship for a rock size range of 25-130 mm in diameter.

The above paper helps understand the flow through rockfill; however, it is limited to one-dimensional flow. When attempting to treat AMD it is important to optimize the material used in the gabions. This would require understanding the behaviour of flow in at least two dimensions.

There have been many studies conducted on flow through porous media. The aforementioned method has focused on analysing the Reynolds number and Darcy-Weisbach coefficient *(f)*. Mulqueen (2005) has chosen to analyse hydraulic conductivity (*K*). Hydraulic conductivity (*K*) is a proportionality constant which is commonly used to analyse the flow of fluid through porous media. In order to use Darcy's Law, as previously stated, there must be laminar flow (Mulqueen, 2005), which does not apply in high velocity flows through gravel and drains. Darcy's Law only applies to one-dimensional flow and is used worldwide to model flow through porous media. Mulqueen (2005) reviewed the applicability of the use of Darcy's one-dimensional law. This was done by analysing flow tests in a laboratory on a range of gravel diameter sizes. Mulqueen (2005) found that for finer aggregates, laminar flow occurs and Darcy's law can be used without significant error; however, for coarser aggregates it was noticed that the flow characteristics resembled the flow of rough walled pipes.

The flow within a gabion is still not fully understood and requires more attention. Mulqueen (2005) agrees with Samani et al's (2004) use of the *f*- relationship. This is evident as rough walled pipes (the behaviour suggested by Mulqueen (2005)) are conventionally analysed using the Darcy-Weisbach equation. The Darcy-Weisbach friction factor tends towards a constant value as the Reynolds number increases for a particular pipe wall's relative roughness.

Michioku et al (2005) investigated the flow through a rubble mound weir. Their investigation was done to allow for the migration of aquatic life and the transportation of physical and chemical substances in water. Conventional weirs comprise an impermeable body. This impermeable body, however, negatively impacts the river environment as the aforementioned substances and aquatic life cannot pass through. They formulated the discharge as a function of the water depth, porosity and grain diameter and geometrical dimension of the structure (Michioku et al, 2005). The experiment consisted of a rectangular weir and was conducted in an open channel flume (Fig. 2.8).

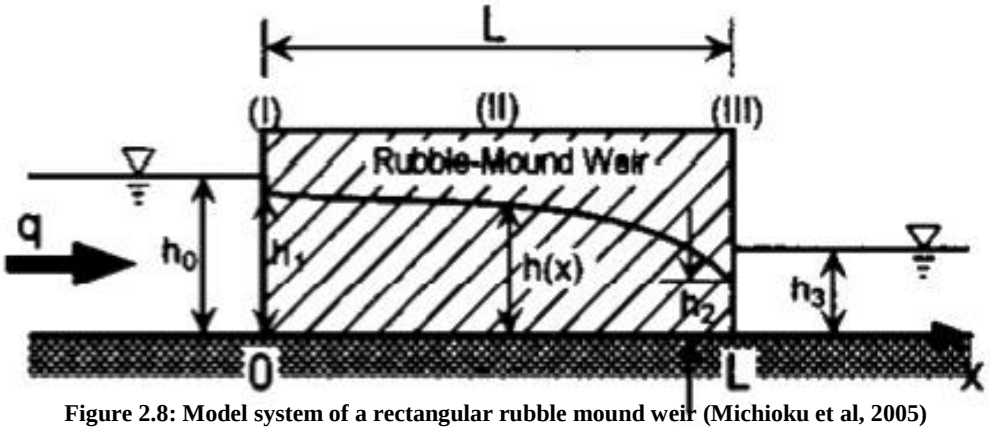


Figure 2.8: Model system of a rectangular rubble mound weir (Michioku et al, 2005)

Michioku et al (2005) focussed on the ordinary flow conditions, where the water surface was below the top of the weir. The rubble mound weir was assumed to be rectangular. The model was divided into three regions (Fig. 2.8): (I), (II) and (III). Region (I) is the cross-section at x = 0 where the flow suddenly converges from the open channel to the porous body i.e. the rubble mound weir. Region (II) is the reach between x = 0 and x = L where the flow is gradually varied in the porous body. Region (III) is the cross-section at the downstream end of the weir x = L where flow rapidly diverges from the porous body to the open channel. In this model, L is the weir length. Momentum principles were used to analyse each region.

Momentum balance for region (I):

Due to the sudden contraction of flow, the momentum and continuity equations are written in the same way as a conventional analysis of a suddenly contracting open channel (Michioku et al, 2005). The momentum equation is shown in (2.4) and the continuity equation is shown in (2.5).

$$\rho q(\delta_1 U_1 - \delta_0 U_0) = \rho g B_0 \frac{h_0^2}{2} - \rho g (B_0 - B_1) \frac{h'^2}{2} - \rho g B_1 \frac{h_1^2}{2} \qquad (2.4)$$

$$q = U_0 B_0 h_0 = U_1 B_1 h_1 \qquad (2.5)$$

where: B is the channel width,

q is the volumetric flow rate,

δ is the velocity correction factor and

h is the flow depth

h' is the transition water depth across the cross-section

The subscripts 0 and 1 refer to the variables just upstream and downstream sides of the cross-section, respectively (Michioku et al, 2005).

Momentum balance for region (III):

The stream suddenly diverges from the porous body in this region. Depending on the downstream flow conditions, one of two situations may arise (Michioku et al, 2005):

1. A flow regime whereby the discharge is controlled at the downstream edge of the weir and the flow on the downstream side is supercritical.
2. A flow regime in which the flow remains subcritical throughout the entire reach. If the downstream side of the weir is supercritical then the flow dams up from downstream. Conservations of momentum (2.6) and mass (2.7) are formulated in the same way as in region (I).

$$\rho q(\delta_3 U_3 - \delta_2 U_2) = \rho g B_1 \frac{h_2^2}{2} + \rho g (B_0 - B_1) \frac{h''^2}{2} - \rho g B_0 \frac{h_3^2}{2} \qquad (2.6)$$

$$q = U_2 B_1 h_2 = U_3 B_0 h_3 \qquad (2.7)$$

where: h'' is the transition water depth across the cross-section,

Subscripts 2 and 3 refer to variables of the upstream and downstream side of the cross-section, respectively.

The governing parameters used to determine the discharge were: Reynolds number (*Re*), mound porosity (*n*), the rubble grain diameter in dimensionless form (d_m/h_o), upstream and downstream water depths (h_o and h_3 respectively), weir length (*L*) and the bed slope of the channel (*i*) (Michioku et al, 2005).

Michioku et al (2005) found that the laminar flow component within the mound had little effect on the discharge and could therefore be neglected. The experiment was also based on one-dimensional flow which does not account for the lateral flow within the mound due to pressure differences and flow impact on the grains.

The flow around the boundary of porous media is of importance when considering the use of gabions for AMD treatment. Gupte and Advani (1997) investigated this flow interaction by making use of Laser Doppler Anemometry (LDA). The porous media used was a network of continuous glass strands. A Hele-Shaw cell was used to simulate the open channel flow near the Darcy flow within the porous media. They traversed across the cell (perpendicular to the flow) to measure the steady state velocity profiles using the LDA. From this experimentation it was found that the boundary layer depth was approximately equal to the channel depth.

Gupte and Advani (1997) analysed the flow interaction between open flow and porous media flow. The analysis helps understand how the flow behaves at the boundary. It is, however, limited in its ability to analyse boundary layer flow near porous media with large grain sizes whereby turbulent flow within the pores occurs.

Stephenson (1979) has significantly contributed to the theory behind flow through rockfill. He presented a flume experiment whereby the flow through a rock-filled gabion was investigated. Velocity results through the rockfill were accurate up to a maximum of 0.5 m/s (which corresponded to a maximum Reynolds number of 10^5); however, these results could only be obtained by lining the side of the flume with 25 mm thick foam rubber (Stephenson, 1979). Stephenson (1979) suggests a differential equation which accounts for flow in three directions. This equation does, however, require solution by finite element analysis due to its complexity.

The differential equation given by Stephenson (1979) is derived from Darcy's Law. This then introduces the previously stated limitation to laminar flow. Once pore sizes increase to a point where turbulent flow is induced the three dimensional equation of analysis is no longer valid.

Based on the discussed literature it is evident that a better understanding of turbulent flow through rockfill is required in order to fully understand how the gabions interact with the river flow. This requirement is in agreement with the proposed work to be done for AMD treatment. The proposed treatment is based on the use of Blast Furnace Slag filled gabions. These gabions will be strategically placed into the affected rivers. The slag is thought to be sufficiently alkaline to raise the pH of the acidic water to an acceptable level. When testing the effects of gabions in a river the residence time distribution will give an indication of the flow interaction which is occurring. The flow could be modelled and results compared to those obtained in the experiments. Once this is understood the treatment process can be better analysed and optimized.

3 EXPERIMENTAL METHODOLOGY

The gabions were strategically placed in the flume and FWT Red dye was injected into the flume to simulate the AMD. Water samples at the outflow of the flume were taken and the concentration of each sample was determined, in a spectrophotometer, in order to establish the residence time distribution for each experiment. All experiments were conducted using 26 mm size gravel in the gabions and four 20 ml syringes were used to inject the FWT Red dye into the system. The experimental methodology is explained, in detail, below.

3.1 Spectrophotometer Calibration

A spectrophotometer makes use of light waves to determine the concentration of a given sample. The wavelength of the light used could be adjusted depending on the sensitivity required.

The spectrophotometer needed to be calibrated in order for sample readings to be obtained from it. Varying concentrations (0.1, 1, 10, 25 and 50 mg/l) of the FWT Red dye was mixed and each concentration was analysed in a spectrophotometer. The tracer concentrations were individually placed in a spectrophotometer. The mixed concentration values were manually entered into the spectrophotometer while the absorbency values were measured by making use of the set 550 nm light wavelength. The results of the absorbency values were plotted against the actual mixed concentration values to produce a calibration curve (Appendix A) and was saved as a parameter (Params) from which future sample concentrations could be read. The spectrophotometer and the calibration concentration samples are shown in Fig. 3.1.

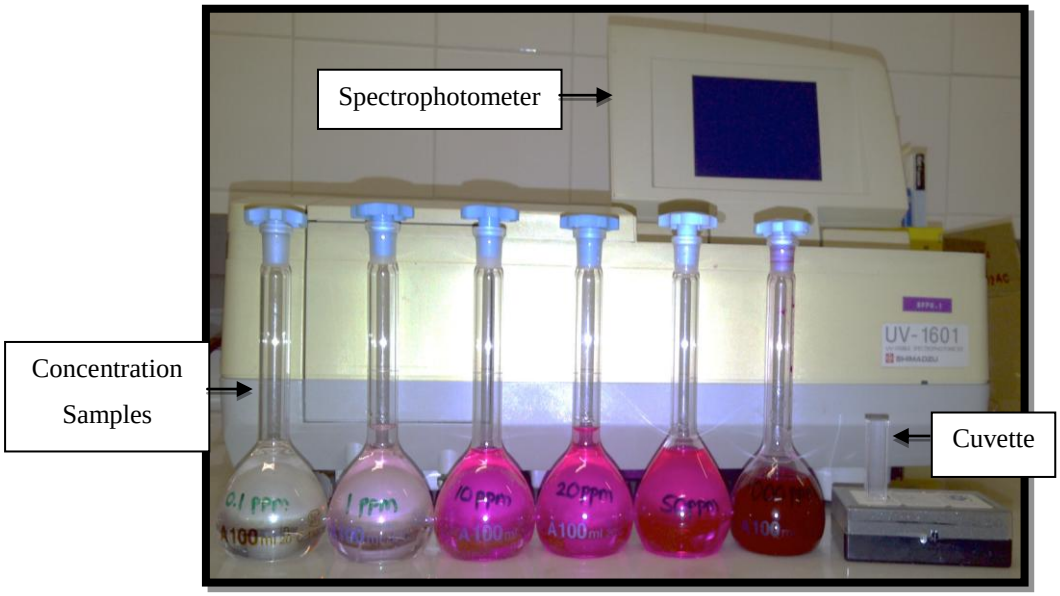


Figure 3.1: Spectrophotometer and calibration concentration samples

3.2 Gabion Construction and Arrangements

3.2.1 General

The analysis of the flow through the gabions was conducted in a flume with a width of 0.92 m. FWT Red dye was used to indicate the flow of the water in the flume which simulated hypothetical AMD flow in a river. The dye used had a similar density to water, which ensured that settlement or floating of the dye did not occur i.e. the dye mixed with the flow in the flume. The flume was supplied by a constant head tank, which recirculated the water flowing through the system. The reintroduction of trace amounts of tracer was accounted for and is described in Chapter 3.3.2. All experiments were conducted with the same flow rate and the inlet valve to the flume was used to control the flow rate. The valve was opened and the flow rate monitored on the flow meter. Once the flow rate remained constant the valve was adjusted until the flow rate remained at 9.92 l/s. The weir at the end of the flume was used to change the flow conditions for the appropriate experiments i.e. the weir was raised to increase the flow depth or lowered to decrease it.

The gabions that were used in the experiments were of dimensions (length x breadth x height) 0.29 m x 0.29 m x 0.175 m. All of the gabions were filled with 26 mm size gravel (Fig. 3.2).

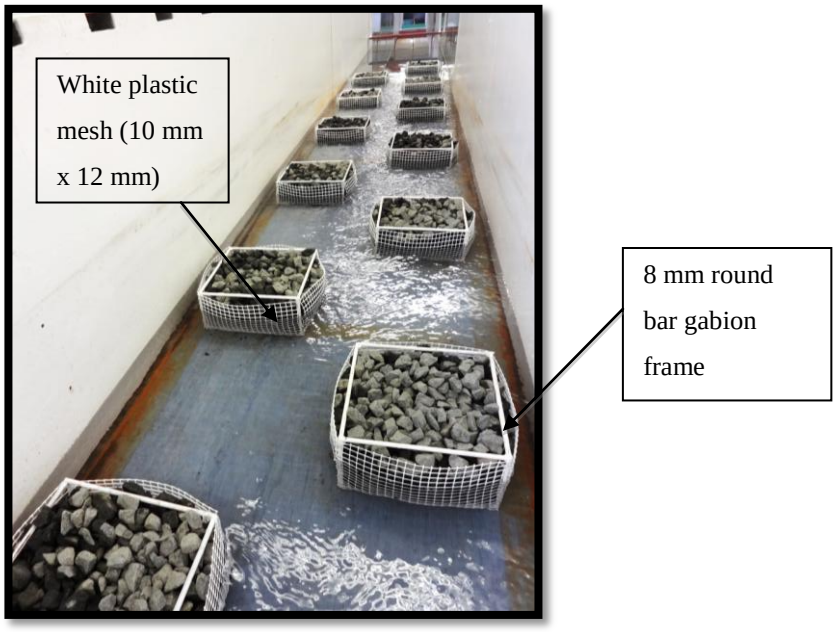


Figure 3.2: Gabions (0.29 m x 0.29 m x 0.175 m) filled with 26 mm stone

The gabion frames were constructed by welding 8 mm round bar together to the required dimensions. Once the frames were primed and painted white, the white plastic mesh (10 mm x 12 mm) was cut into the correct sized panels and attached to the steel frame using cable ties of dimensions (length x breadth) 100 mm x 2.65 mm. One additional gabion of dimensions (length x breadth x height) 0.62 m x 0.62 m x 0.38 m was also constructed, as previously mentioned, so that the flow pattern of a large single gabion could be assessed.

3.2.2 Gabion Arrangements

Three different gabion arrangements were analysed. Each arrangement was tested so that the total submerged volume remained the same. These arrangements are as follows:

- A single gabion of dimensions (length x breadth x height) 0.62 m x 0.62 m x 0.38 m.

- Four gabions positioned in a staggered pattern (arrangement 1). These four gabions represent a ‘slice’ of a more extensive distribution that would be used in a stream. This extensive distribution, containing more than four gabions, is shown in Fig. 3.3, whereby the dashed lines denote the hypothetical river boundary with hypothetically positioned gabions and the solid lines denote the flume boundary with gabions placed in a staggered pattern.

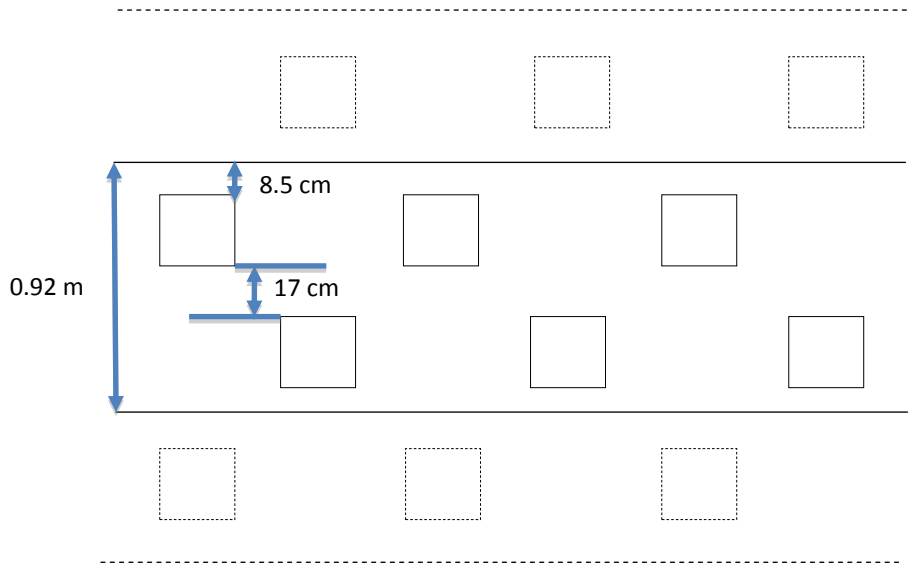


Figure 3.3: Plan view of arrangement 1

- Four gabions positioned in an aligned pattern (arrangement 2). These four gabions also represent a ‘slice’ of a more extensive distribution that would be used in a stream. This extensive distribution, containing more than four gabions, is shown in Fig. 3.4, where the dashed lines denote the hypothetical river boundary with hypothetically positioned gabions and the solid lines denote the flume boundary with gabions placed in an aligned pattern.

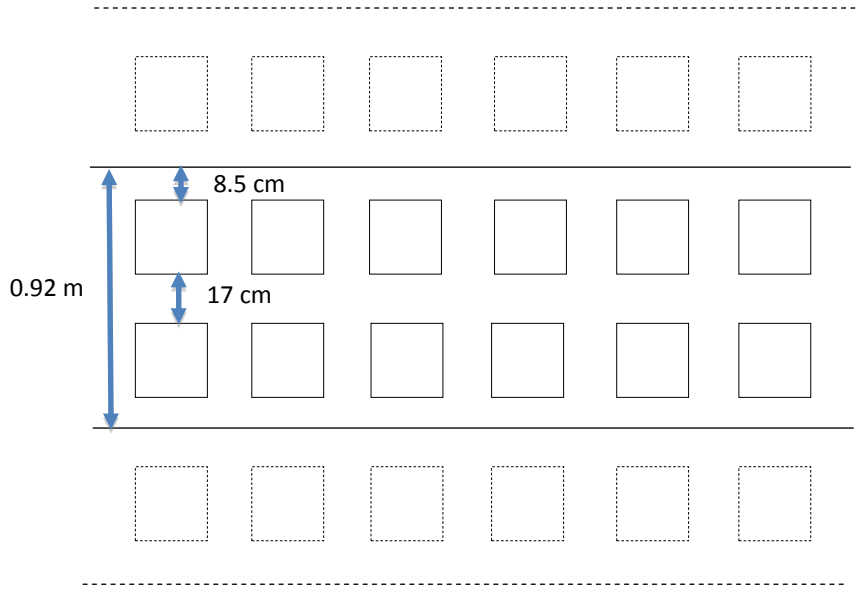


Figure 3.4: Plan view of arrangement 2

3.2.3 Change of Flow Depth

Changing the flow depth in the flume allowed for the change in submerged volume to be tested without the flow pattern changing. This would ensure that only the change in submerged volume was being tested. The weir gate at the end of the flume controlled the flow depth (Fig. 3.5). Once the weir gate was adjusted, the flow was given sufficient time to regulate to the adjustment before the flow depth was measured and set to the specified depth.



Figure 3.5: Weir gate control at flume end

3.2.4 Experimental Layout

A total of nine experiments were run. All experiments were injected with four 20 ml syringes filled with 25 000 ppm concentration of the FWT Red dye. These syringes were injected at the positions indicated by the dowel rods (Fig. 3.13). Table 1 shows the layout and configuration of each experiment. Figs 3.6-3.12 are schematic diagrams of the experimental layout for each experiment and have not been drawn to scale. In these figures the variables x and L_e are the lengths of the gabions and the distance from the injection point to the weir, respectively.

Table 3.1: Experimental layout and configuration

	Arrangement Pattern	Flow Depth (m)	Number of Gabions	Length of Gabions, x (m)	Distance of Dye Injection from first Gabion (m)	Distance from last Gabion to Weir (m)	Distance from Injection Point to Weir, L_e (m)	Flow Rate (l/s)	Comments
Experiment 1	None	0.13	0	N/A	N/A	N/A	9.79	9.92	Control experiment
Experiment 2	1	0.16	8	3.51	1.8	0.8	6.11	9.92	These experiments were used to test the effect of changing the flow depth
Experiment 3	1	0.13	8	3.51	1.8	0.8	6.11	9.92	
Experiment 4	1	0.10	8	3.51	1.8	0.8	6.11	9.92	
Experiment 5	1	0.13	4	1.67	1.8	0.8	4.27	9.92	These experiments were used to assess the effects of changing the gabion arrangements
Experiment 6	2	0.13	4	0.75	1.8	1.72	4.27	9.92	
Experiment 7	Single Gabion	0.112	1	0.62	1.8	1.84	4.27	9.92	
Experiment 8	1	0.13	12	5.35	1.8	0.8	7.95	9.92	Together with experiments 3 and 5, these experiments were used to assess the effect of increasing the number of gabions
Experiment 9	1	0.13	16	7.19	1.8	0.8	9.79	9.92	

The diagrams to follow are schematics and not drawn to scale. All gabions were of dimensions (length x breadth x height) 0.29 m x 0.29 m x 0.175 m except for the single gabion which was of dimensions 0.62 m x 0.62 m x 0.38 m.

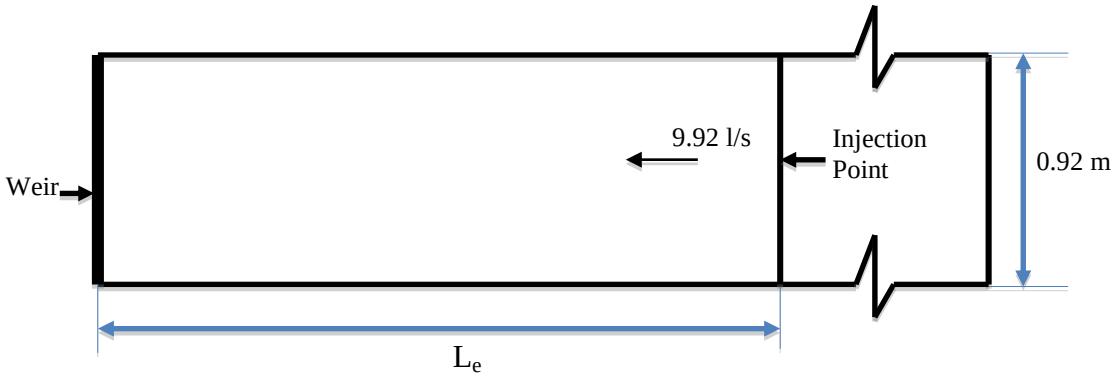


Figure 3.6: Plan view of the experimental layout for experiment 1 - empty flume

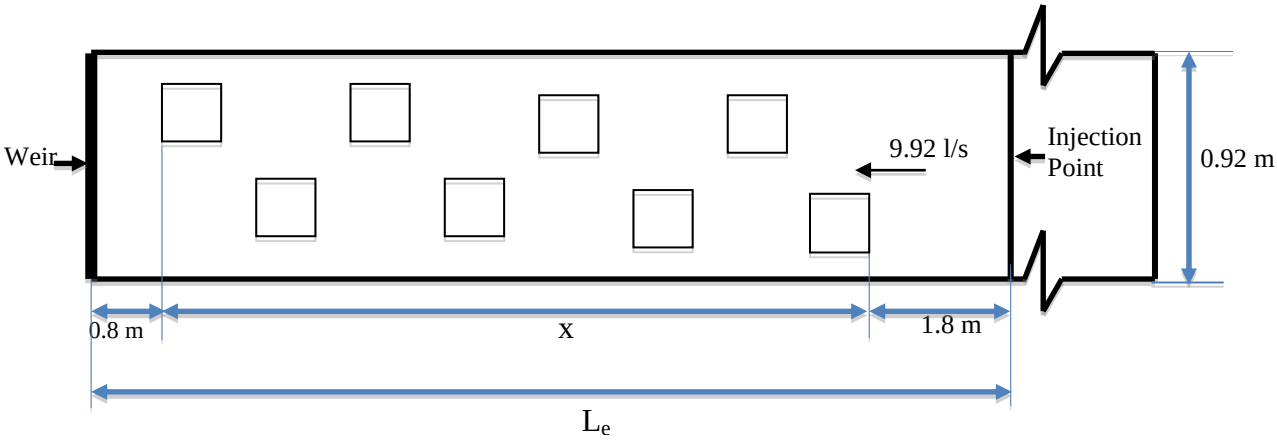


Figure 3.7: Plan view of the experimental layout for experiments 2, 3 and 4 - change in flow depth assessment

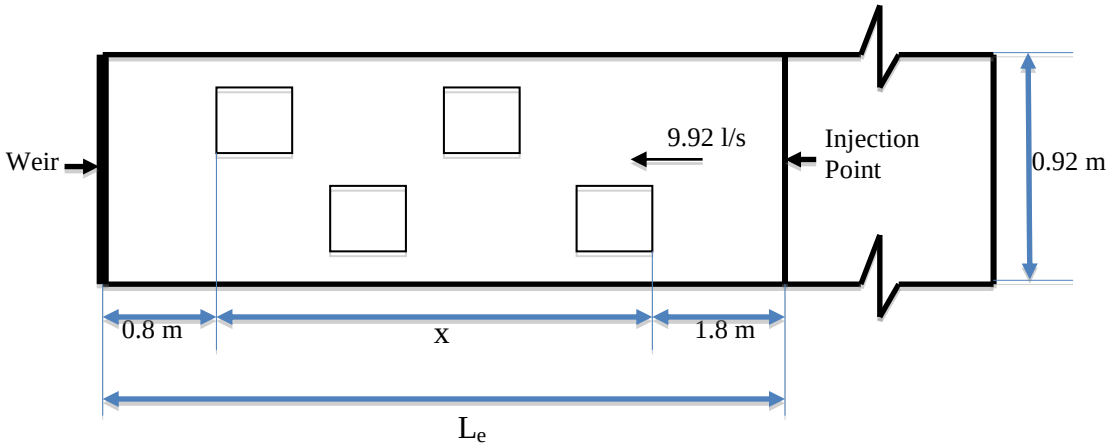


Figure 3.8: Plan view of the experimental layout for experiment 5 - change in flow pattern assessment

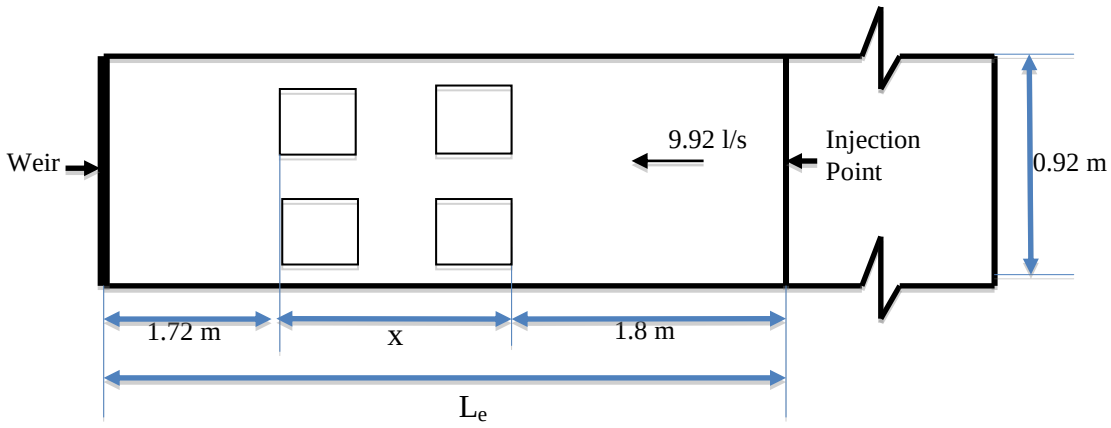


Figure 3.9: Plan view of the experimental layout for experiment 6 - change in flow pattern assessment

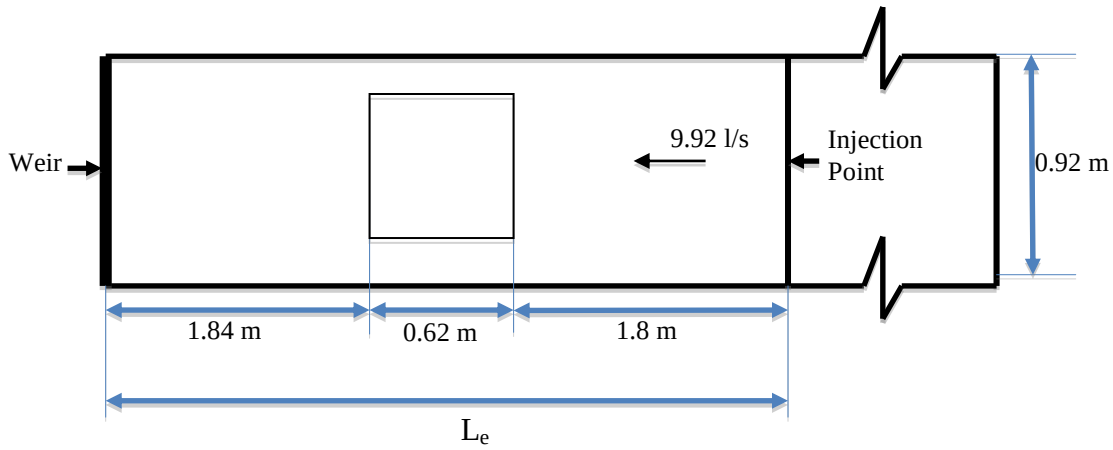


Figure 3.10: Plan view of the experimental layout for experiment 7 - change in flow pattern assessment

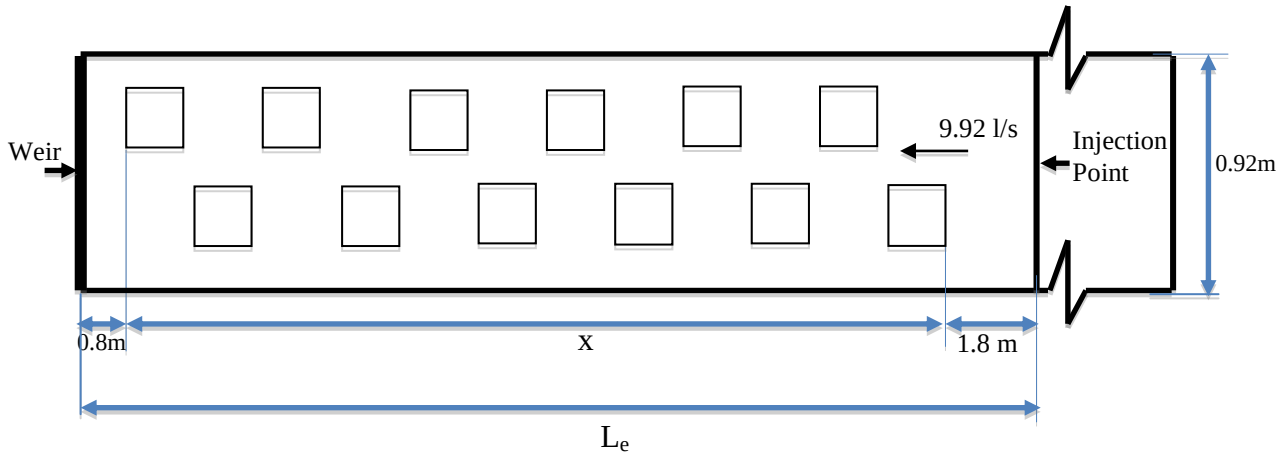


Figure 3.11: Plan view of the experimental layout for experiment 8 - change in the number of gabions assessment (together with experiments 3 and 5)

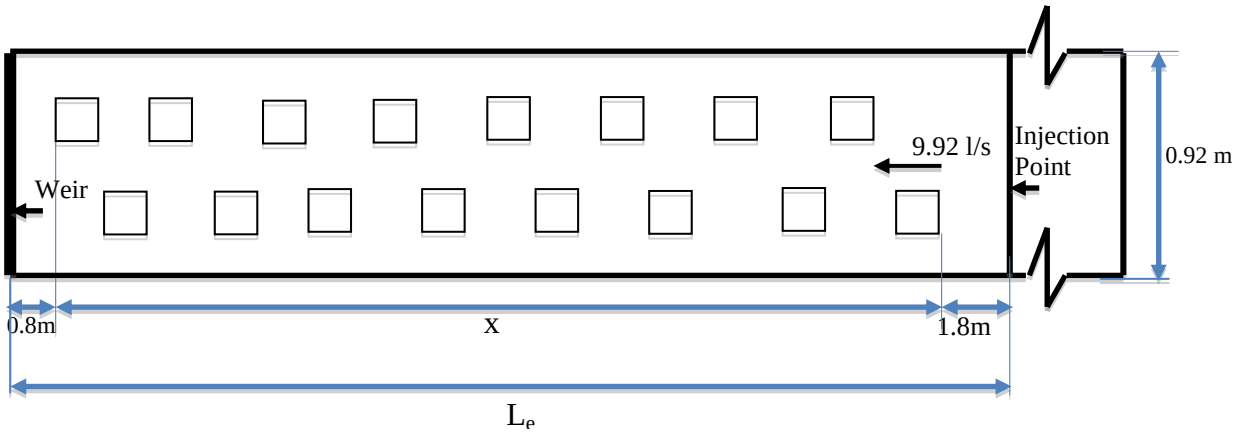


Figure 3.12: Plan view of the experimental layout for experiment 9 - change in the number of gabions assessment (together with experiments 3 and 5)

3.3 Data Collection

3.3.1 Injection Scheme

The injection points for the FWT Red Dye were chosen to ensure that the dye mixed fully both across the width of the flume and vertically before reaching the next section. Using four injection points evenly spaced across the width of the flume and positioned at half the flow depth for each experiment ensured this. At each injection point a 20 ml syringe was used to inject the dye into the flume. All four syringes were injected into the system at the same time over a 3 second period. This was done so as to simulate an impulse of dye being injected into the system. The injection scheme is seen in Fig. 3.13 while Fig. 3.14 indicates the mixing which occurred prior to the dye reaching the gabions.

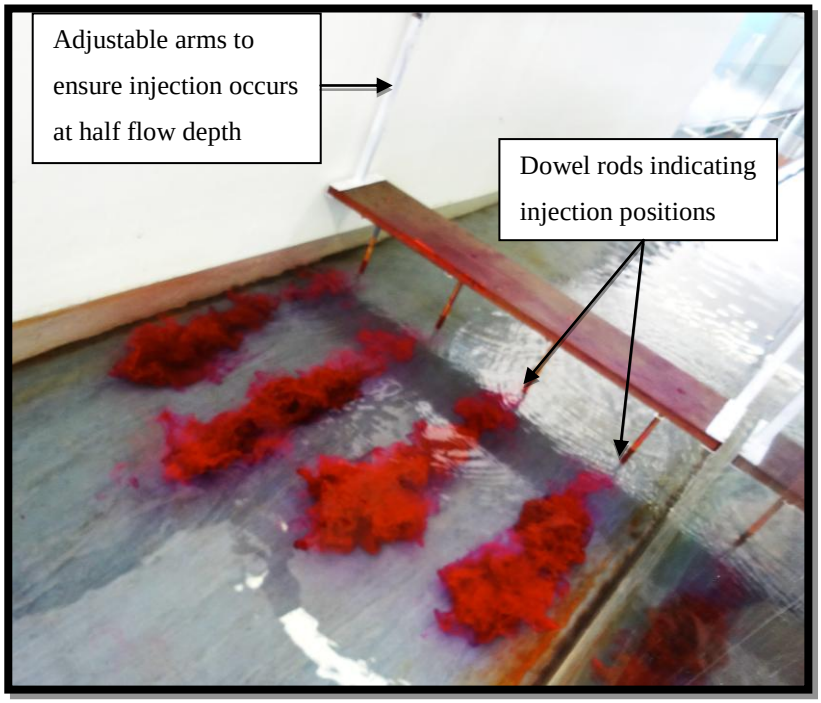


Figure 3.13: Adjustable injection scheme

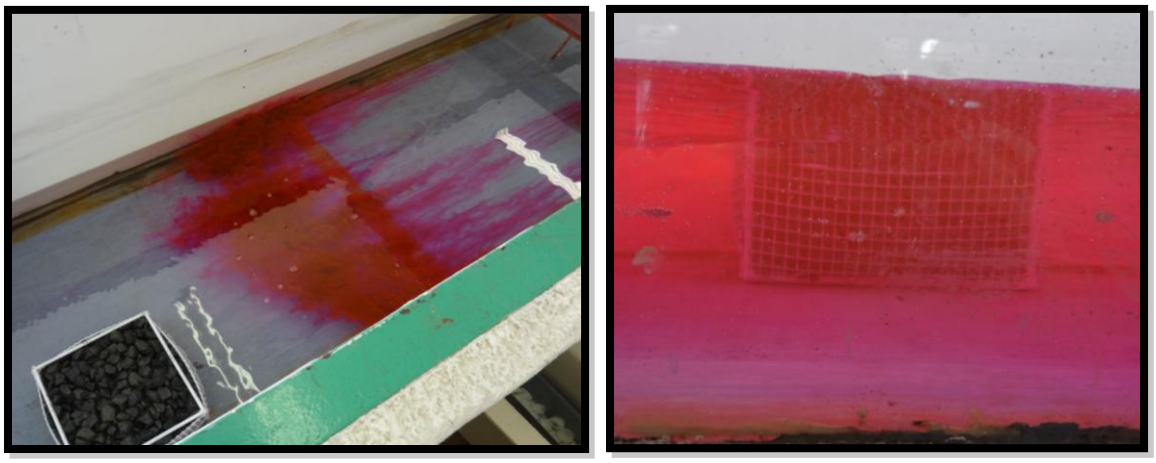


Figure 3.14: Indication of horizontal (left) and vertical (right) mixing

3.3.2 Collection Scheme

In order to obtain and analyse data accurately it was imperative to ensure that the flow across the full width of the flume was collected and mixed before a sample was taken at each time interval. A collection trough was constructed and placed on wheels and a guided track so as to ensure ease of flow collection. A steel sheet

was riveted, at an inclination towards the flume, onto the front end of the trough so as to guide the water into the trough while minimizing any splashing which could cause loss of quality of data and subsequently lead to inaccurate results. The collection scheme, in and out of use, is shown in Fig. 3.15. The steel sheet and trough ensured mixing in the direction of flow, which was why samples had to be taken across the length of the trough using the polytop sample containers. The sample containers were numbered so as not to confuse which time they were taken.

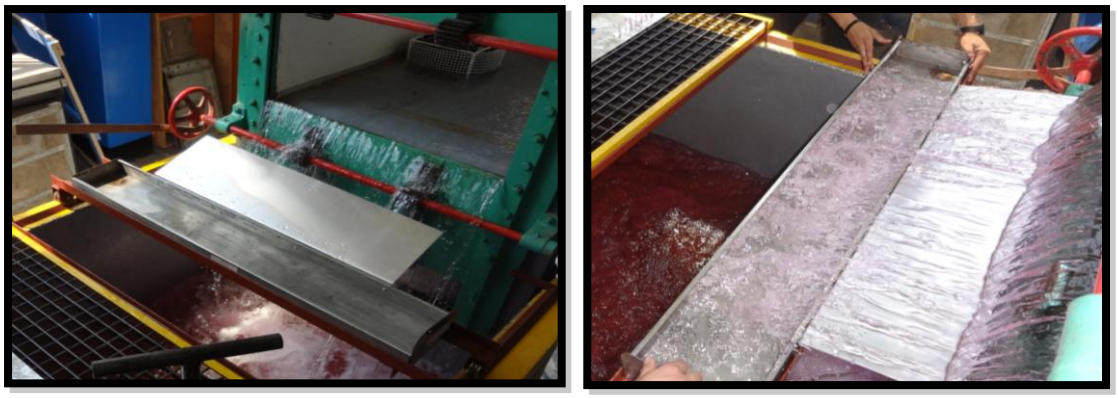


Figure 3.15: Collection scheme in and out of use

A base sample was taken before experimentation occurred because the flume used had a recirculating water tank. A base sample is an initial sample, which is taken prior to any dye entering the system. The base samples were used to determine if the dye from previous experiments were affecting the results of the current experiment. If the base sample did not read zero concentration in the spectrophotometer then all subsequent samples, for that particular experiment, were adjusted by subtracting the base sample reading from each sample throughout the experiment. The laboratory water tank was emptied, cleaned out and refilled with fresh water after approximately three experiments to limit the effects of the dye from previous experiments. Base samples were taken for every experiment, regardless of when the water tank was cleaned out and refilled.

3.4 Test Procedure

For all experiments the gabions were filled with gravel, which had an average diameter of 26 mm. Four syringes, each containing 20 ml of the 25 000 ppm concentration FWT Red Dye was injected at the positions indicated by the dowel rods.

3.4.1 Residence Time Distribution of the Empty Flume: Control

The experiments discussed in Chapters 5, 6 and 7 were all conducted to assess the effects that the gabion(s) had on the residence time distribution. This effect can only be understood by comparing the results to those obtained when the residence time distribution was analysed for the flume functioning with no gabions in it.

The flume was set up by positioning the injection scheme 9.79 m upstream of the weir gate (Fig. 3.6). The flow depth was set at 13 cm and samples were timed and taken to a point where all the dye had left the system. The flow rate remained at 9.92 l/s.

3.4.2 Changing the Flow Depth

The flow depth was changed to investigate the effect that the change in submerged volume of the gravel had on the mean residence time and the RTD. This was only done for gabion pattern 1. The gabion size could have also caused a change in submerged volume; however, this would also change the flow pattern that occurred around the gabions and it would not be clear whether the change in submerged volume or the change in flow pattern produced the change in the residence time distribution.

The flume was prepared for experimentation by setting up eight gabions as shown in Chapter 3.2.4 (Fig. 3.7). The gabions were filled with gravel, which had an average diameter of 26 mm. The injection scheme was positioned 1.8 m away from the first gabion encountered (Fig. 3.7).

Values x and L_e varied for every experiment as they depended on the number of gabions used (Table 3.1). When changing the flow depth these values were kept constant at 3.51 m and 6.11 m respectively. Four syringes, each containing 20 ml of the 25 000 ppm concentration FWT Red Dye were injected at the positions indicated by the dowel rods. Samples were timed and taken up until a point where all the dye had left the system.

The flow depths chosen to investigate were 16 cm, 13 cm and 10 cm. Since the gabions' height was 17.5 cm it was decided to start the testing at 16 cm so that no water washed over the gabions. The 10 cm flow depth was chosen based on the limitations of the weir gate at the flume end. In order to maintain the flow rate at 9.92 l/s and ensure that the flow depth was the same at the upstream and downstream face of the gabions, the minimum flow depth was kept at 10 cm. The 13 cm flow depth was chosen as it was the midpoint between the maximum and minimum flow depth investigated. For all flow depths the flow rate was kept constant at 9.92 l/s.

3.4.3 Changing the Gabion Arrangement

The gabion arrangement was changed to investigate the effect that the change in pattern of the gabions had on the mean residence time and its distribution. The flow depths were adjusted to ensure that for each arrangement the submerged volume remained the same. Three gabion arrangements were tested: arrangement 1 (Fig. 3.8), arrangement 2 (Fig. 3.9) and a single gabion of dimensions (length x breadth x height) 0.62 m x 0.62 m x 0.38 m (Fig. 3.10).

The flume was prepared for experimentation by setting up four gabions in the arrangement 1 pattern (Fig. 3.8), followed by the arrangement 2 pattern (Fig. 3.9) and lastly the single gabion (Fig. 3.10). The injection scheme was positioned 1.8 m away from the first gabion encountered.

As shown in Table 3.1, when using arrangement 1 the values for x and L_e were 1.67 m and 4.27 m respectively. When using arrangement 2 the values for x and

L_e were 0.75 m and 4.27 m respectively. When using the single gabion the values for x and L_e were 0.62 m and 4.27 m respectively.

The length of the experiment, from injection point to weir gate, was kept constant so that the results could be compared. The distance from the first gabion encountered was also kept constant so that the mixing conditions, of the dye before gabion interaction occurs, were consistent i.e. mixing occurred both laterally and vertically (Fig. 3.14).

The flow depth was kept at 13 cm for arrangement 1 and arrangement 2; however, the flow depth had to be lowered to 11.2 cm for the single gabion to ensure that the submerged volume was the same for all three experiments. Once again the flow rate was kept at 9.92 l/s.

3.4.4 Changing the Number of Gabions

The number of gabions used was changed to investigate this effect on the mean residence time and its distribution. Four configurations were compared: four, eight, twelve and sixteen gabions. All four experiments were run using only arrangement 1 (Figs 3.7, 3.8, 3.11 and 3.12).

The experiments for four and eight gabions were set up and run in Experiments 5 and 3, respectively. The flume, therefore, only had to be set up with twelve and sixteen gabions. The injection scheme was positioned 1.8 m away from the first gabion encountered (Figs 3.11 and 3.12).

The values for x and L_e for four and eight gabions were as stated in Table 3.1. When using twelve gabions the values for x and L_e were 5.35 m and 7.95 m respectively. When using sixteen gabions the values for x and L_e were 7.19 m and 9.79 m respectively.

The flow depth was kept at 13 cm for all four experiments to ensure experimental consistency. Once again the flow rate was kept at 9.92 l/s.

3.5 Residence-Time Distribution (RTD) Analysis

3.5.1 Introduction

The theory used to analyse the results is based on statistical modelling used to describe chemical reactors. A chemical reactor is a device that is used to contain controlled chemical reactions. These reactions occur in a reactor under conditions which can be monitored and controlled to ensure safety and efficiency. This theory characterizes non-ideal reactors. A non-ideal reactor is one which does not behave in an ideal manner i.e. the dye which is input into the system, at time zero, does not all exit the system at the specified time t_i. This is due to flow characteristics such as short-circuiting, dead zones and diffusion from the concentration gradient. Short-circuiting is where the dye does not interact with the system; it simply flows through the path of least resistance, bypasses and exits the system a short time after the dye has been input into it. Dead zones are characterised by a lack of flow i.e. the velocity in these regions are very low and the dye is trapped there and is only able to diffuse into the surrounding flow paths, which experience a faster flow velocity. Dead volumes decrease the available flow for reaction. The statistical modelling used to describe a chemical reactor is done by making use of the following functions: the residence time distribution function E(t), the mean residence time τ_m and the variance σ^2. The residence time distribution function describes, in a quantitative manner, how much time each fluid element has spent in the reactor; whereas the mean residence time quantifies the average time that all fluid elements have spent in the reactor. The variance describes how far off, from the norm, the reactor is compared to that of an ideal reactor (Fogler, 2006).

For investigating non-ideal reactors one can consider modelling the flow patterns using two models: continuous-stirred-reactors (CSTRs) or plug-flow-reactors (PFRs). A CSTR is a reactor which has a continuous input of dye, whereas a PFR has an instantaneous input of dye at the start of the experiment. These models, however, do not account for the non-idealistic behaviour of the system. This now introduces the use of a second, higher level, approximation which uses macromixing/(RTD) information. The third approximation uses micromixing

information to make predictions about the conversions in non-ideal reactors (Fogler, 2006).

In an ideal plug-flow-reactor, the atoms that flow through the reactor would all leave at the same time, provided that they entered at the same time. This time spent in the reactor is known as the ideal residence time of the atoms. In CSTRs, however, this does not occur. The atoms leave the reactor at varying times. This produces a distribution of residence times for the material in the reactor as some atoms will leave the system almost immediately (i.e. short-circuiting) while most of the atoms will only leave after spending, approximately the mean residence time (τ_m) in the reactor (Fogler, 2006). For example if ten atoms enter the system in a CSTR, these atoms may leave or be in the reactor for different periods of time. Thus producing a varying distribution of times.

The residence time distribution (RTD) describes the mixing which occurs in a chemical reactor (Fogler, 2006). As there is no mixing in an ideal PFR, the RTD will be different than in a CSTR. The RTD displayed by a given reactor will produce distinctive clues to the type of mixing which occurs within it (Fogler, 2006).

The reactor type which was used as a model for our system, the gabions in the flume, is known as a packed-bed reactor. Due to the material packing and the variable resistances induced into the reactor, the fluid flowing through the system does not flow uniformly. A large proportion of the fluid will flow through the part of the channel which contains the least resistance. Due to the variable resistances in the reactor, certain molecules of fluid will take longer to be expelled from the system. This means that certain molecules will have more contact with the material than others.

3.5.2 Measuring the Moments of the RTD for Pulse Input Experiments:

The following theory has been largely adapted from Levenspiel (1999). pg 257 – 282, 293 – 304 & 321 – 325

In order to assess the residence time distribution from the concentration samples obtained from the experiments, graphs of Concentration vs. Time [C(t) graphs] need to be plotted. Once these graphs have been produced they are converted into E(t) graphs.

This is done by first calculating Q (the area under the C(t) graph) as follows:

$$Q = \sum_{i=0}^{n} C_i \Delta t \qquad (3.1)$$

Where: C_i is the concentration (mg/l) of sample i taken at time t_i (min) and
Δt is the time interval for the given C_i value

A corresponding E_i value can be determined for every C_i value as follows:

$$E_i = \frac{C_i}{Q} \qquad (3.2)$$

Where: E_i is the residence time distribution function for sample i

The following parameters are then calculated in order to determine the moments of the E(t) distribution:

a. $t_i \,.\, E_i \,.\, (t_i - t_{i-1})$ (3.3)

b. $t_i^2 \,.\, E_i \,.\, (t_i - t_{i-1})$ (3.4)

The first moment of the distribution (mean residence time) is defined as:

$$\tau_m = \sum_{i=1}^{n} t_i \,.\, E_i \,.\, (t_i - t_{i-1}) \tag{3.5}$$

The residence time for an ideal reactor is defined as:

$$\tau_{Ideal} = \frac{V \,.\, \varepsilon}{F} \tag{3.6}$$

Where: ε is the porosity/void fraction of the packed material and is defined as:

$$\varepsilon = \frac{V_V}{V} \tag{3.7}$$

V_V is the volume of the voids in the material

V is the volume of the system

F is the volumetric flow rate of the system

In chemical engineering ε is known as the 'void fraction', whereas in civil engineering it is known as the 'porosity' (Bird et al, 1960).

The second moment (σ^2) describes the degree of dispersion and is defined as:

$$\sigma^2 = \left(\sum_{i=1}^{n} t_i^2 \,.\, E_i \,.\, (t_i - t_{i-1}) \right) - \tau_m^2 \tag{3.8}$$

The second moment has to be normalized so that the dispersion number, D, can be found. The normalized second moment (σ_θ^2) is defined as:

$$\sigma_\theta^2 = \frac{\sigma^2}{\tau_m^2} \tag{3.9}$$

The dispersion number, D, can be solved for iteratively using the following equation:

$$\sigma_\theta^2 = 2\,.\,D - 2\,.\,D^2\,.\left(1 - e^{-1/D}\right) \tag{3.10}$$

Because an ideal PFR can be simulated using an infinite number of CSTRs in series, it may be required to calculate the number of tanks, N, that is required to simulate a given PFR model. N is defined as:

$$N = \frac{1}{\sigma_\theta^2} \tag{3.11}$$

The effective volume is a parameter which is used to determine the efficiency of the system. It describes the ratio of the systems volume that is active (i.e. what volume is not dead). The effective volume is defined as:

$$V_{eff} = {}^{\tau_m}/_{\tau_{Ideal}} \tag{3.12}$$

The hydraulic efficiency is a parameter which may be useful when a comparison between different system designs is required. This is defined as (Persson and Wittgren, 2003):

$$\lambda = V_{eff}\,.\left(1 - \frac{1}{N}\right) \tag{3.13}$$

The above-defined parameters are used to determine the degree of non-ideality within the reactor i.e. the gabion filled flume.

The residence time distribution analysis was run for each experiment to determine the effect a change in gabion arrangement, submerged volume and number of gabions used would have on the residence time distribution.

3.5.3 Residence-Time Distribution (RTD) Analysis Example

Considering the data below the residence time distribution can be determined. This hypothetical set of data is for a set of eight gabions positioned in the flume in a staggered pattern.

Table 3.2: Hypothetical set of data representative of eight gabions in a flume

Column 1	Column 2	Column 3	Column 4	Column 5 Eq (3.1)	Column 6 Eq (3.2)	Column 7 Eq (3.3)	Column 8 Eq (3.4)
Container	**Time (min)**	**ABS**	**Concentration, C_i (mg/l)**	**Q_i (mg.hr/l)**	**E_i**	**$t_i.E_i.\Delta t$**	**$t_i^2.E_i.\Delta t$**
0	0	0	0	0	0	0	0
1	0.50	0.09	0.60	5.00E-03	1.26	0.000	7.34E-07
2	1.00	0.27	7.00	5.83E-02	14.80	0.002	3.42E-05
3	1.50	0.42	13.00	1.08E-01	27.48	0.006	1.43E-04
4	2.00	0.39	11.50	9.58E-02	24.31	0.007	2.25E-04
5	2.50	0.24	6.00	5.00E-02	12.68	0.004	1.83E-04
6	3.00	0.20	4.50	3.75E-02	9.51	0.004	1.98E-04
7	3.50	0.14	2.50	2.08E-02	5.28	0.003	1.49E-04
8	4.00	0.11	1.50	1.25E-02	3.17	0.002	1.17E-04
9	4.50	0.18	4.00	3.33E-02	8.45	0.005	3.96E-04
10	5.00	0.08	0.30	2.50E-03	0.63	0.000	3.67E-05
11	5.50	0.09	0.55	4.58E-03	1.16	0.001	8.14E-05
12	6.00	0.09	0.60	5.00E-03	1.26	0.001	1.05E-04
13	7.00	0.12	2.00	3.33E-02	4.22	0.008	9.59E-04
14	8.00	0.08	0.15	2.50E-03	0.31	0.001	9.39E-05
15	9.00	0.08	0.20	3.33E-03	0.42	0.001	1.58E-04
16	10.00	0.07	0.00	0.0E+00	0.00	0.000	0.00E+00

Column 1 indicates the label given to each polytop sample container used during the experiment. Column 3 shows the absorbancy values obtained from the spectrophotometer. These absorbancy values were used by the spectrophotometer to determine the concentration readings for each sample from the calibration curve obtained in Chapter 3.1. From equation (3.1) the area under the C(t) graph of the dye for each sample (Q_i), column 5, was determined; and subsequently the total area Q (the sum of all Q_i's which also equates to the area under the C(t)

graph). The residence time distribution function for each sample (E_i), column 6, was then determined using equation (3.2). In order to determine the residence time distribution function for the whole system the parameters listed in equations (3.3) and (3.4) were determined. These parameters are located in columns 7 and 8, respectively. In Table 3.2, Δt is the time interval between samples i.e. $\Delta t = t_i - t_{i-1}$. The first moment/mean residence time (τ_m) was determined by summing column 7 as indicated in equation (3.5). The second moment/variance (σ^2) was determined by summing column 8 and then subtracting τ_m^2 from that summation, as shown in equation (3.8). The normalised second moment (σ_θ^2) was then determined using equation (3.9). From this the dispersion number, D, was found using equation (3.10).

In order to assess the degree of non-ideality the ideal residence time must be determined. This was done using equation (3.6) where the void fraction was defined by equation (3.7). Because this system is not entirely filled with the packed material (gravel), as is with constructed wetlands, the void ratio cannot be used alone. The ideal residence time is a ratio of the volume of the voids to the volumetric flow rate i.e. the volume of voids is determined by subtracting the volume of the gabions from the volume of the flume. For example, the flume volume was 0.7308 m^3, the volume of the gabions was determined by multiplying the submerged volume by (1-void fraction) i.e. in this example the submerged volume of gabions was 0.047 m^3: 8 x 0.29 m x 0.29 m x 0.13 m x (1-0.459) (eight gabions with plan area of 0.29 m x 0.29 m and flow depth of 0.13 m and void ratio of 0.459). The volume of the voids is then found by subtracting the submerged volume of gabions from the total flume volume: V_{voids} = 0.7308 – 0.047 = 0.6835 m^3. It was this value which was used to determine the ideal residence time (τ_{Ideal}) using equation (3.6). The effective volume was then found using equation (3.12). The equivalent number (N) of CSTRs to replicate these results was found using equation (3.11) and the hydraulic efficiency was then found using equation (3.13).

The results of this example are shown in Fig. 3.16 and Table 3.3

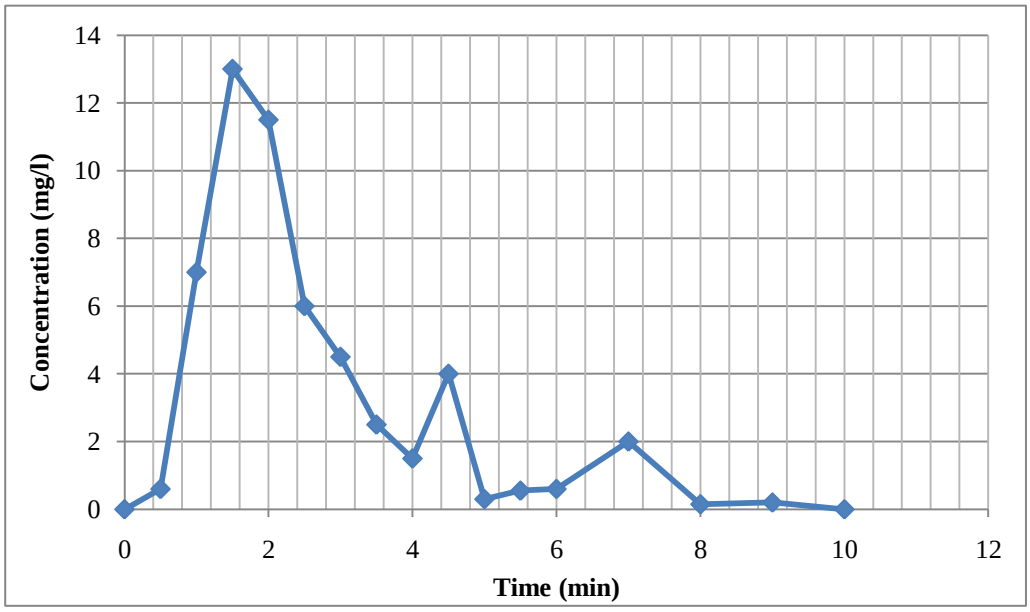


Figure 3.16: Concentration vs. time graph (C(t))

Table 3.3: Example results

ΣQ_i (mg.hr/l)	0.473
τ_m (hr)	0.045
τ_{Ideal}	0.019
V_{eff}	2.350
σ^2	8.611E-04
σ_θ^2	0.426
D	0.282
λ	1.350
N	2.350

For this investigation it was required to determine the effect of the gabions. In order to do this the flow interaction with the gabions needed to be found. This was possible by assuming that all peaks, in the C(t) graph, which appeared after the first peak (which represents system bypass) represented the flow interaction of the gabions. The RTD analysis was then run again, however, this time the peaks of interest were isolated. This also allowed for the proportions of bypass flow (Fig. 3.17 and Table 3.4) and the flow interaction with the gabions (Fig. 3.18 and Table 3.5) to total flow to be determined.

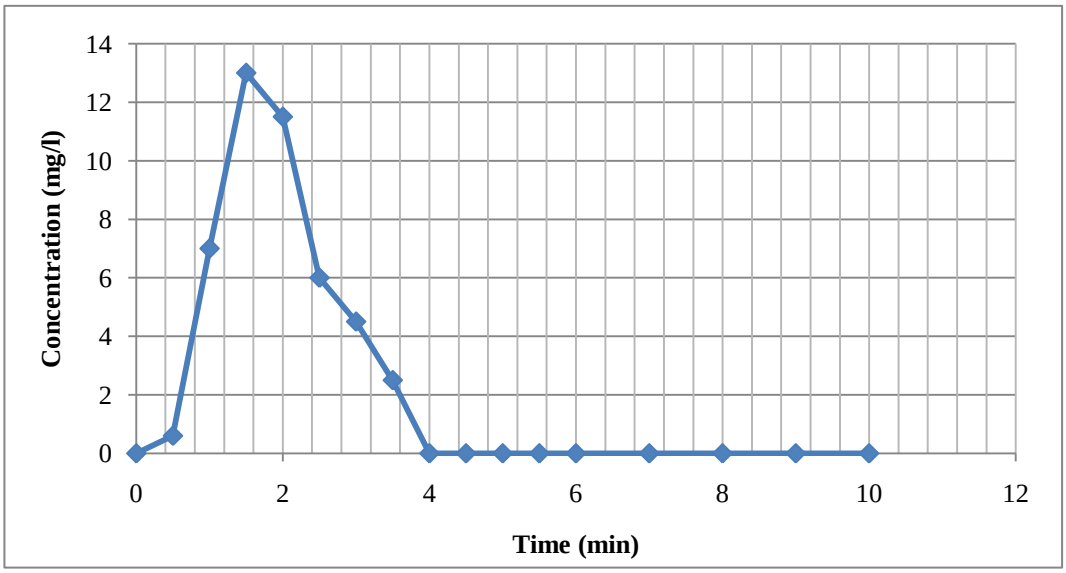


Figure 3.17: Concentration vs. time (C(t)) graph for the bypass peak

Table 3.4: Bypass peak analysis

Container	Time (min)	ABS	Concentration (mg/l)	Q_i (mg.hr/l)	E_i	$t_i.E_i.\Delta t$	$t_i^2.E_i.\Delta t$
0	0	0	0	0	0	0	0
1	0.50	0.09	0.60	5.00E-03	1.59	0.000	9.23E-07
2	1.00	0.27	7.00	5.83E-02	18.62	0.003	4.31E-05
3	1.50	0.42	13.00	1.08E-01	34.59	0.007	1.80E-04
4	2.00	0.39	11.50	9.58E-02	30.59	0.008	2.83E-04
5	2.50	0.24	6.00	5.00E-02	15.96	0.006	2.31E-04
6	3.00	0.20	4.50	3.75E-02	11.97	0.005	2.49E-04
7	3.50	0.14	2.50	2.08E-02	6.65	0.003	1.88E-04
8	4.00	0.11	1.50	1.25E-02	3.17	0.002	1.17E-04
9	4.50	0.00	0.00	0.00E+0	0.00	0.000	0.00E+00
10	5.00	0.00	0.00	0.00E+0	0.00	0.000	0.00E+00
11	5.50	0.00	0.00	0.00E+0	0.00	0.000	0.00E+00
12	6.00	0.00	0.00	0.00E+0	0.00	0.000	0.00E+00
13	7.00	0.00	0.00	0.00E+0	0.00	0.000	0.00E+00
14	8.00	0.00	0.00	0.00E+0	0.00	0.000	0.00E+00
15	9.00	0.00	0.00	0.00E+0	0.00	0.000	0.00E+00
16	10.00	0.00	0.00	0.00E+0	0.00	0.000	0.00E+00

The bypass area under the C(t) graph of the dye was found to be 0.376 mg.hr/l, therefore the percentage bypass was: (0.376/0.473)x100 = 79.5%

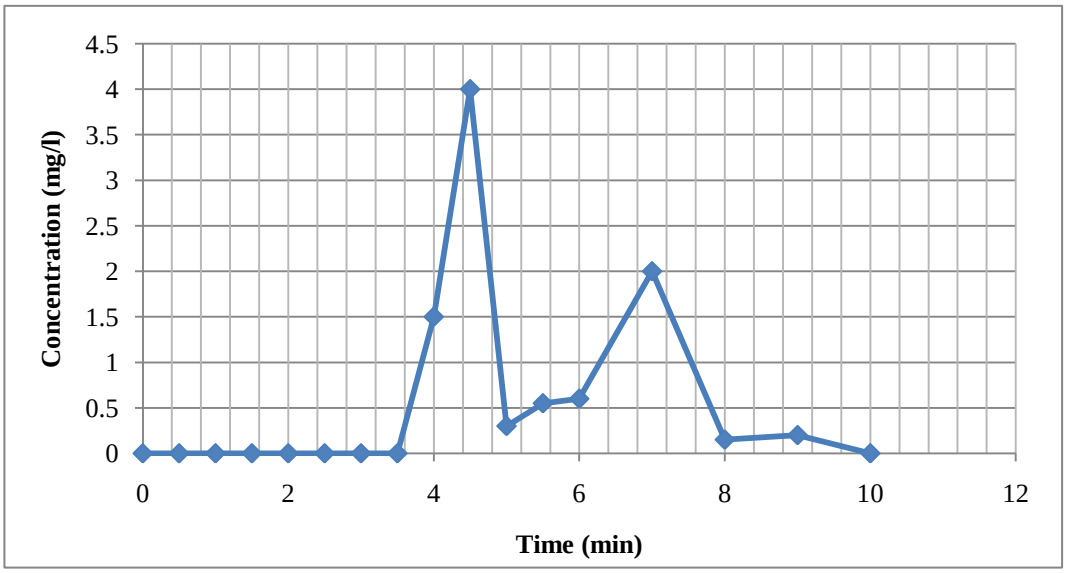


Figure 3.18: Concentration vs. time C(t) graph for the flow interaction with gabions peaks

Table 3.5: Flow interaction with gabions peak analysis

Container	Time (min)	ABS	Concentration (mg/l)	Q_i (mg.hr/l)	E_i	$t_i.E_i.\Delta t$	$t_i^2.E_i.\Delta t$
0	0	0	0	0	0	0	0
1	0.50	0.00	0.00	0.00E+00	0.000	0.000	0.000E+00
2	1.00	0.00	0.00	0.00E+00	0.000	0.000	0.000E+00
3	1.50	0.00	0.00	0.00E+00	0.000	0.000	0.000E+00
4	2.00	0.00	0.00	0.00E+00	0.000	0.000	0.000E+00
5	2.50	0.00	0.00	0.00E+00	0.000	0.000	0.000E+00
6	3.00	0.00	0.00	0.00E+00	0.000	0.000	0.000E+00
7	3.50	0.00	0.00	0.00E+00	0.000	0.000	0.000E+00
8	4.00	0.11	1.50	1.25E-02	15.45	0.009	5.72E-04
9	4.50	0.18	4.00	3.33E-02	41.20	0.026	1.93E-03
10	5.00	0.08	0.30	2.50E-03	3.09	0.002	1.78E-04
11	5.50	0.09	0.55	4.58E-03	5.66	0.004	3.96E-04
12	6.00	0.09	0.60	5.00E-03	6.18	0.005	5.15E-04
13	7.00	0.12	2.00	3.33E-02	20.60	0.040	4.67E-03
14	8.00	0.08	0.15	2.50E-03	1.54	0.003	4.57E-04
15	9.00	0.08	0.20	3.33E-03	2.06	0.005	7.72E-04
16	10.00	0.07	0.00	0.00E+00	0.00	0.000	0.00E+00

The area under the C(t) graph of the dye which interacted with the gabions was found to be 0.097 mg.hr/l, therefore the percentage gabion interaction was: (0.097/0.473)x100 = 20.5%

4 RESULTS AND DISCUSSION

All residence time distribution analysis spreadsheets are shown in Appendix B.

4.1 Residence Time Distribution of the Empty Flume: Control

The experiments were run and the samples analysed using the spectrophotometer. The concentration readings were then used to determine the residence time distribution for the experiment. Fig. 4.1 shows the residence time distribution obtained.

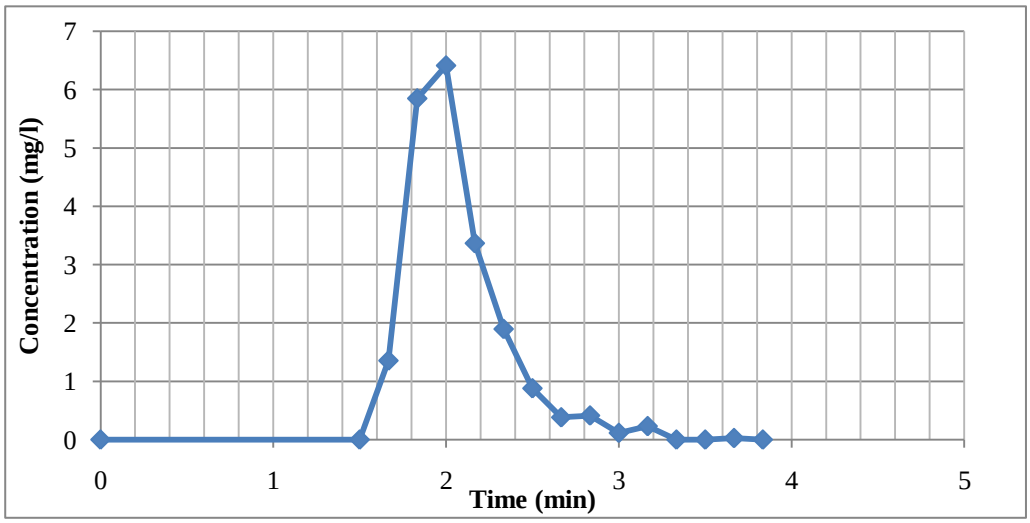


Figure 4.1: Residence time distribution for experiment 1: empty flume

The empty flume experiment shows a longer mean residence time (2.04 min) (Eq 3.5) when compared to the other eight experiments (discussed below). This must be attributed to absence of gabions. When the gabions were present they reduced the cross sectional area of the flume which is available to flow. Due to the constant flow rate, the reduced cross sectional area resulted in an increased flow velocity in that flow path. Thereby decreasing the mean residence time obtained. The empty flume does not experience a reduction in cross sectional area and therefore the velocity is slower than if gabions were present. It was noted, however, that as the dye moved down the length of the flume the dye at centre of the flume moved slightly faster than the dye nearest to the sidewalls of the flume (Fig. 4.2).

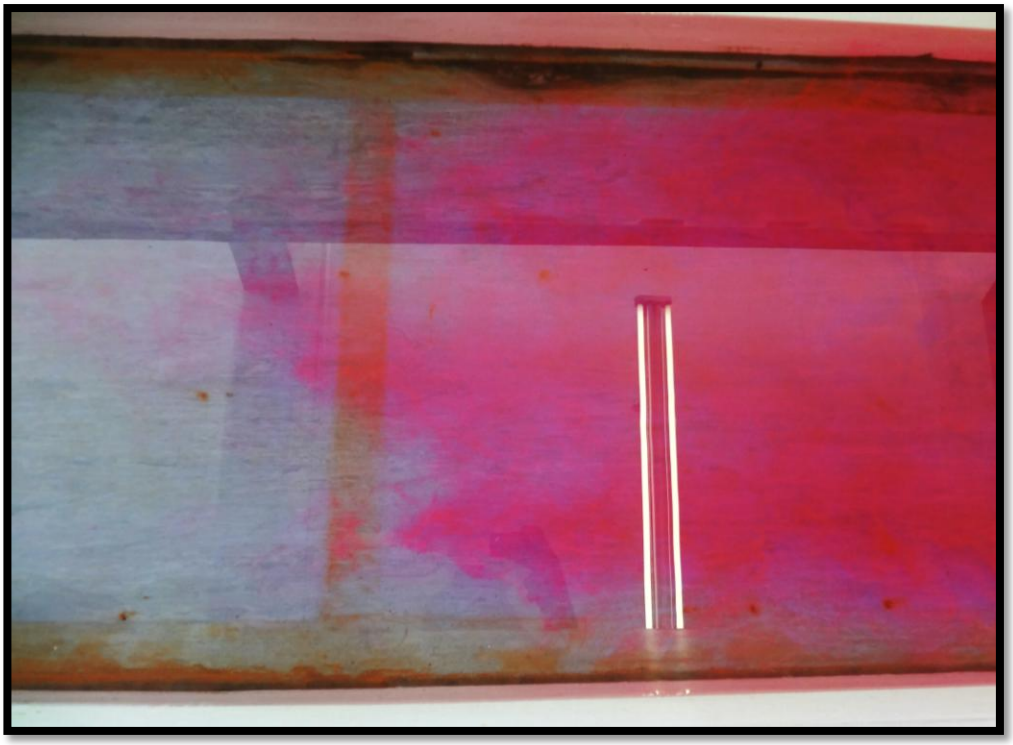


Figure 4.2: Plan view of dye flowing in the empty flume experiment

In Fig 4.2 the flow of the tracer flows faster in the centre of the channel as opposed to the flow at the walls of the channel. This produces the 'boat-like' flow pattern shown. This flow pattern is attributed to the no-slip condition which assumes a Newtonian fluid. This condition states that the flow distribution tends to zero as it approaches a boundary. This condition was prominent in all of the experiments; however, it was considered to have a negligible effect due to the large amount of fresh water compared to the dye caught at the boundary. Fig. 4.3 shows no-slip condition at the injection scheme during experimentation. The spectrophotometer was also not sensitive enough to analyse such small concentrations.

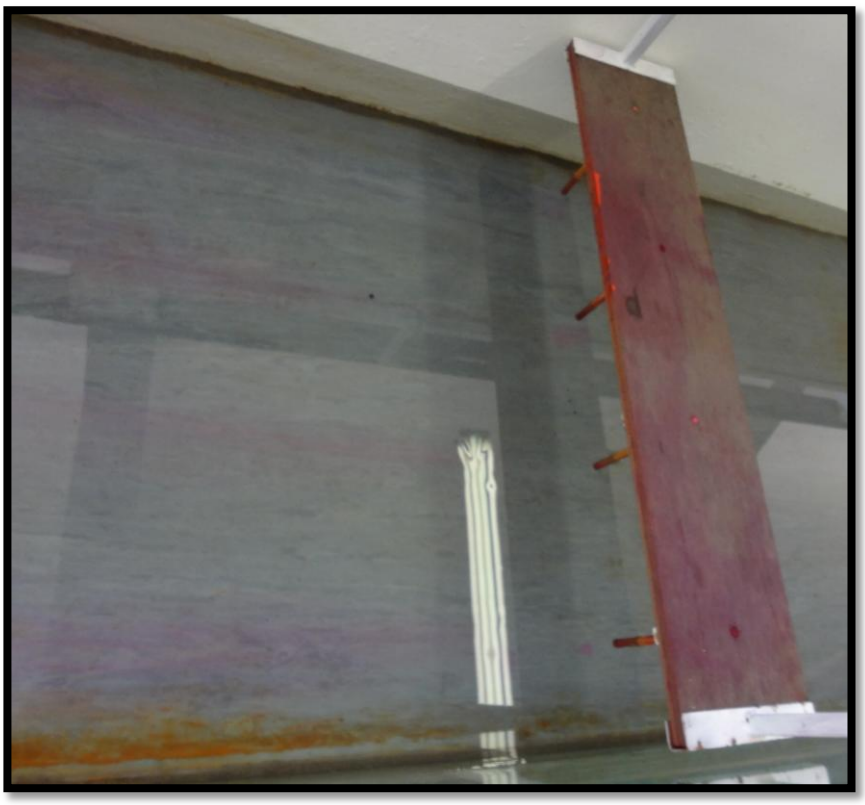


Figure 4.3: No-slip condition observed during experimentation

The dye, caught in the no-slip condition, at the boundary will slowly diffuse up into a faster flow path. This diffusion occurs so slowly that it can be considered negligible with regards to sample analysis.

4.2 Changing the Flow Depth

The experiments 2, 3 and 4 were run and the samples analysed using the spectrophotometer. The concentration readings were then used to determine the residence time distribution for each experiment. Figs 4.4 through 4.6 are the residence time distributions for the three different flow depths.

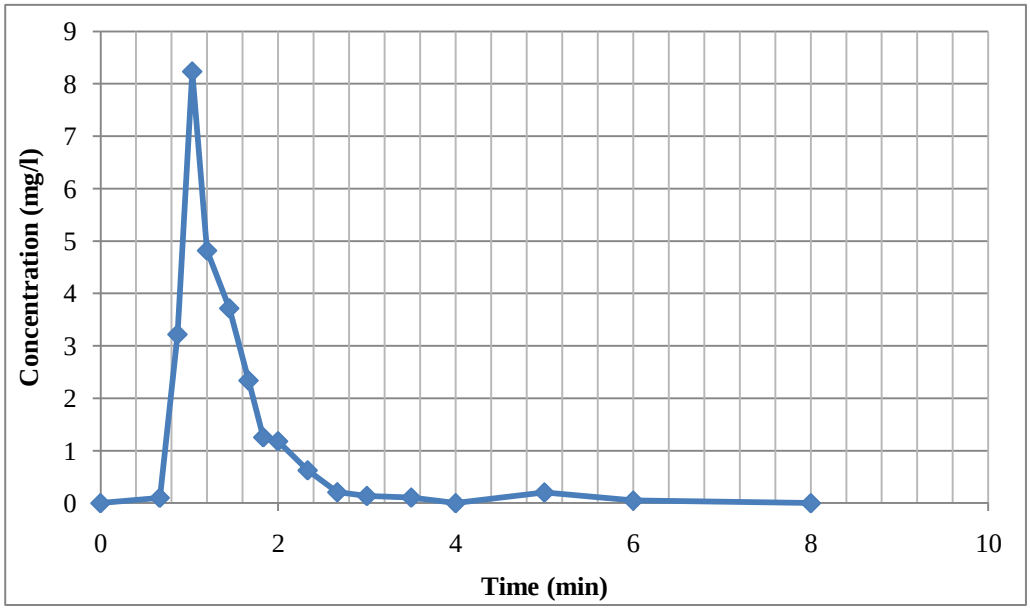


Figure 4.4: Residence time distribution for experiment 2: 16 cm flow depth

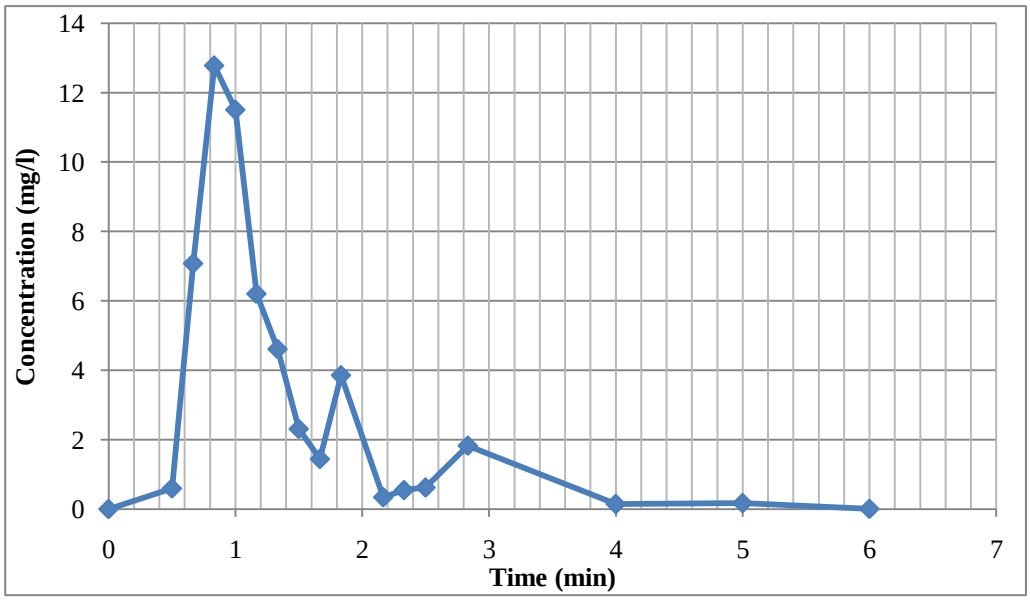


Figure 4.5: Residence time distribution for experiment 3: 13 cm flow depth

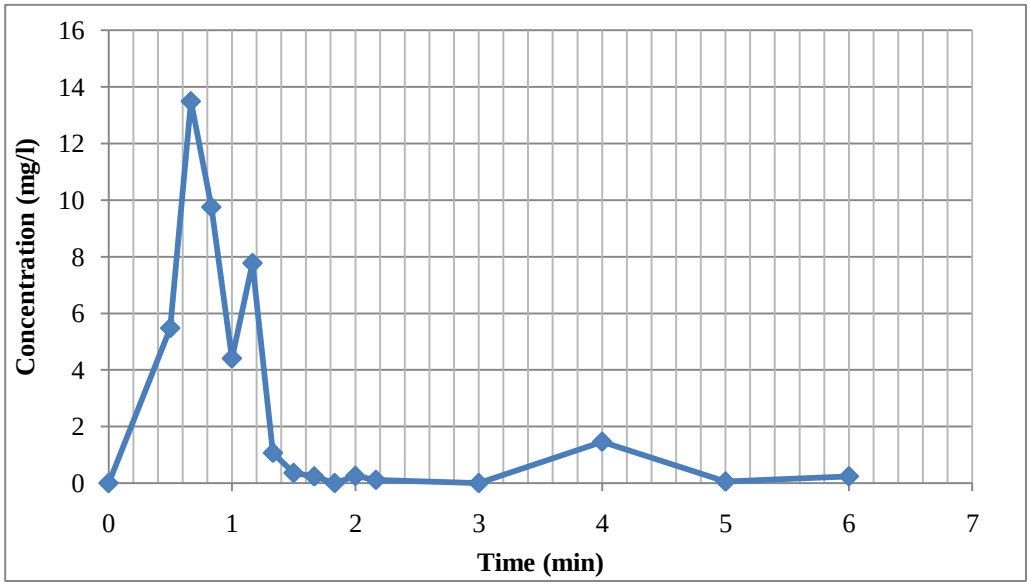


Figure 4.6: Residence time distribution for experiment 4: 10 cm flow depth

From the above figures it was clear that there was a significant effect on the RTD caused by the change of submerged volume. Logically one would assume that an increased submerged volume would produce results indicative of increased flow through the gabions but this has not occurred. In order to determine and compare the effects one cannot just look at the increase or decrease in the peak values. Due to the varying flow depths the dye diluted differently which was why the values off the curves cannot be compared and, if compared, would lead to incorrect conclusions.

We can compare the proportion of each peak's area under the C(t) graph to total area under the C(t) graph. Isolating each peak (see page 41) and then running the residence time distribution analysis would achieve this. When comparing the proportion of flow in each peak it was important to understand what each peak represented. It was assumed that the initial peak represented the total system bypass and all other peaks represented some form of gabion interaction. This comparison is seen in Table 4.1.

Table 4.1: Flow proportion distribution comparison when changing the flow depth

		Percentage of Flow Interaction with Gabions	Percentage of Bypass Flow	Mean Residence Time (min)
Arrangement 1	**16cm Flow Depth**	4.72	95.28	1.54
	13cm Flow Depth	19.36	80.64	1.32
	10cm Flow Depth	38.43	61.57	1.35

Table 4.1 gives a clear indication of the effect that a change in the submerged volume had on the gabion performance. As the flow depth decreased the flow proportion which has some form of gabion interaction improved significantly. It is still unclear how the flow interacts exactly with the gabions; however, it is thought that the low interaction of flow with the gabions, at a flow depth of 16 cm, was due to the flow depth being similar to the gabion height. It was thought that the flow would tend to the top of the gabion as it sought the path of least resistance. This would cause most of the flow to pass through the top layer of the gravel, which would in turn decrease the interaction with the gravel. At a flow depth of 13 cm the interaction improved significantly, however, a flow depth of 10 cm proved to produce the most flow interaction with the gabions. The increased distance to the top of the gabion would increase the resistance to the flow and would decrease the amount of flow which would tend to the top, thereby enhancing the interaction of flow and subsequently decreasing the bypass flow. The decrease in flow depth would also increase the flow velocity which could impact on the recirculation of dead zones; thereby also improving retention time.

The mean residence time calculation produced an interesting trend. As the flow depth decreased the mean residence time appeared to decrease. As explained with the control experiment this is due to the increased velocity at certain sections due to the presence of the gabions. The mean residence time at a flow depth of 10 cm is very similar to the mean residence time in experiment 3, despite the increased velocity in experiment 4 caused by the decrease in flow depth. This also indicated the increased flow interaction with the gabions.

When compared to experiment 1 (empty flume: control) it was apparent that the presence of the gabions affected the residence time distribution. In experiments 2-4 the mean residence time was shorter than that obtained in experiment 1. The effect of the residence time distribution is evident in the shape of the C(t) graphs i.e. the additional peaks and shape of the bypass peak which occurred.

4.3 Changing the Gabion Arrangement

Figs 4.7 through 4.9 are the residence time distributions for the three different gabion arrangements tested in experiments 5, 6 and 7.

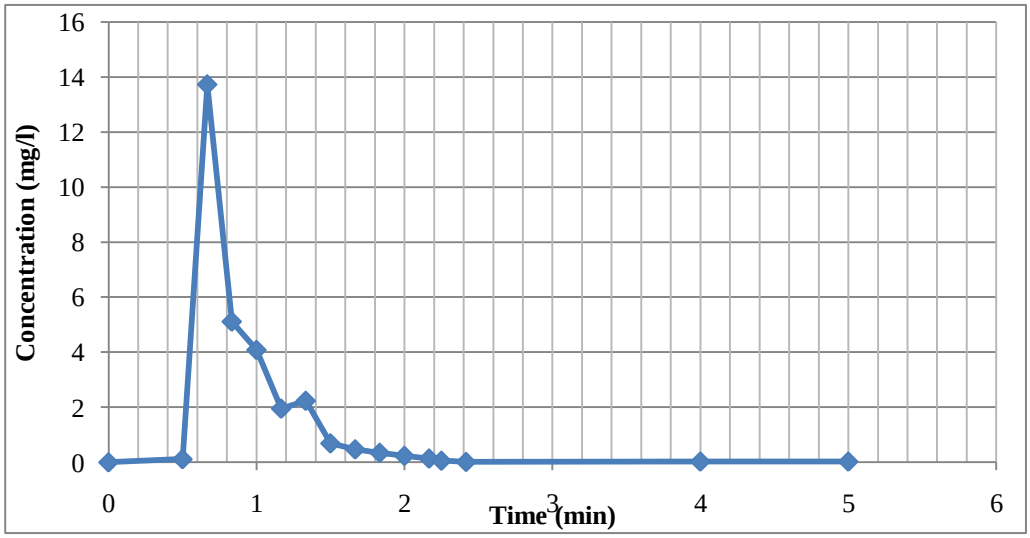


Figure 4.7: Residence time distribution for experiment 5: arrangement 1 using a flow depth of 13 cm

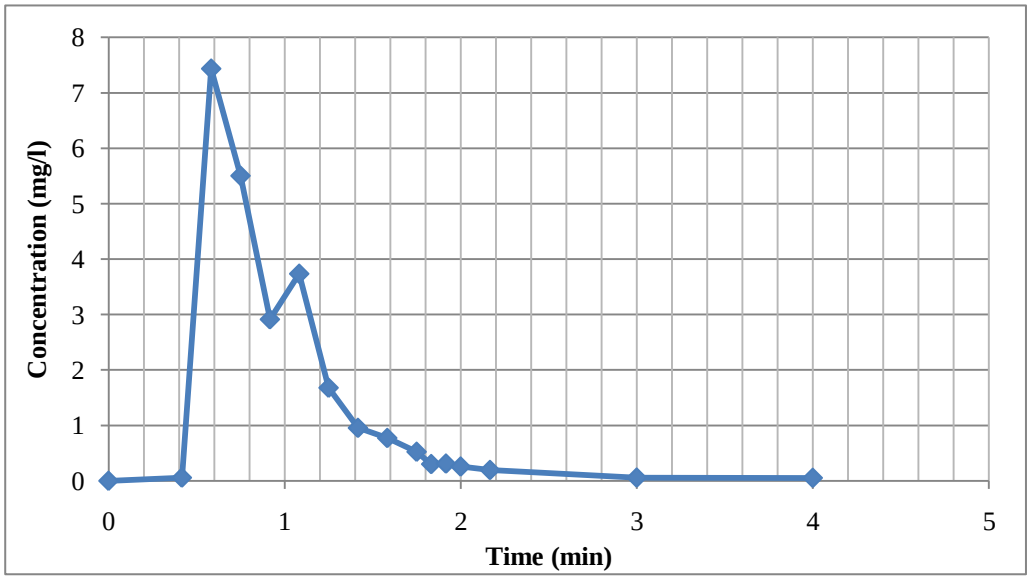


Figure 4.8: Residence time distribution for experiment 6: arrangement 2 using a flow depth of 13 cm

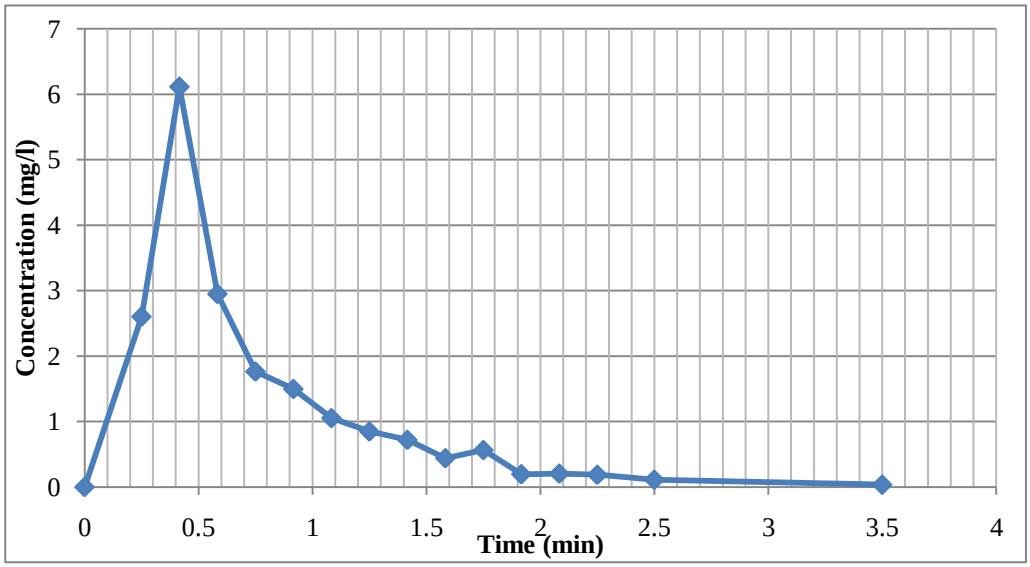


Figure 4.9: Residence time distribution for experiment 7: single gabion using a flow depth of 11.2 cm

From the above figures it was clear that there was a significant effect in the change of gabion arrangement. As stated previously the proportion of each peak's flow would be used to make comparisons to ensure consistency.

Once again it was assumed that the initial peak represented total system bypass and all the other peaks represented some form of gabion interaction. This comparison is seen in Table 4.2.

Table 4.2: Flow proportion distribution comparison when changing the gabion arrangement

	Percentage of Flow Interaction with Gabions	Percentage of Bypass Flow	Mean Residence Time (min)
Single Gabion: 0.62x0.62x0.38m	29.24	70.76	0.73
4 Gabions: Arrangement 1	15.32	84.68	0.94
4 Gabions: Arrangement 2	35.76	64.24	0.97

Table 4.2 gives a clear indication of the effect that a change in the gabion arrangement or flow pattern had on the gabion performance. Arrangement 1 and arrangement 2 produce similar mean residence times and are longer than that

produced for the single gabion. This means that the dye was in the system for a longer period of time, which potentially allows for more gabion interaction. Despite the shorter mean residence time, the single gabion appears to have a larger percentage of the flow interacting with the gabions when compared to arrangement 1. This could be attributed to the size of the single gabion which almost acted as a weir due to its wide dimensions. This forces more of the dye to pass through it and therefore decreases the percentage of bypass which occurs. Arrangement 1 had far larger paths whereby bypass could occur. Arrangement 2, however, proves to have the most gabion-flow interaction. Even though arrangement 2 had similar sized bypass paths as arrangement 1, the alignment of the gabions increased the delay time of the dye when passing from one gabion to the next. This is shown in Figs 4.10 through 4.12. These figures indicate the effect that the gabions have on the flow. On the left a portion of the tracer bypasses the gabions. The centre picture indicates the dead zones directly in front of each gabion. On the right the attenuation of flow is shown as the tracer was released from the gabions sometime later.

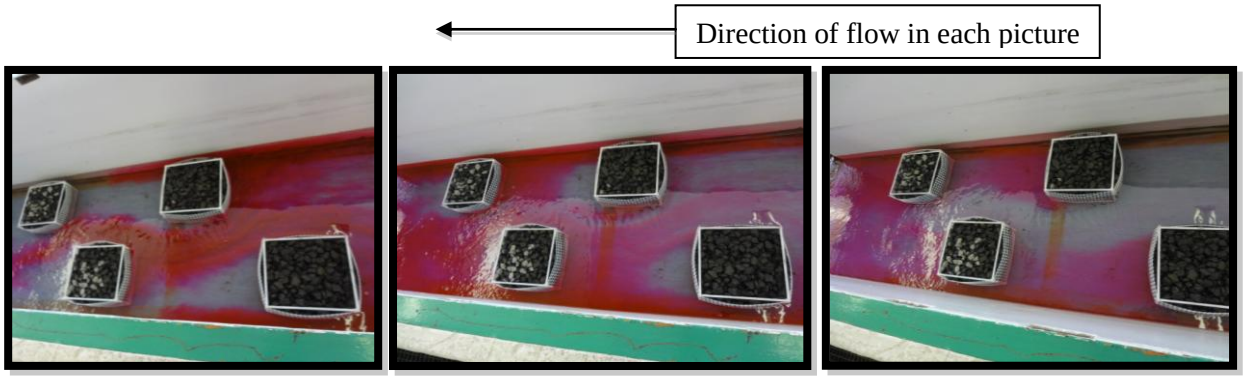


Figure 4.10: Flow pattern seen during experimentation – experiment 5: arrangement 1

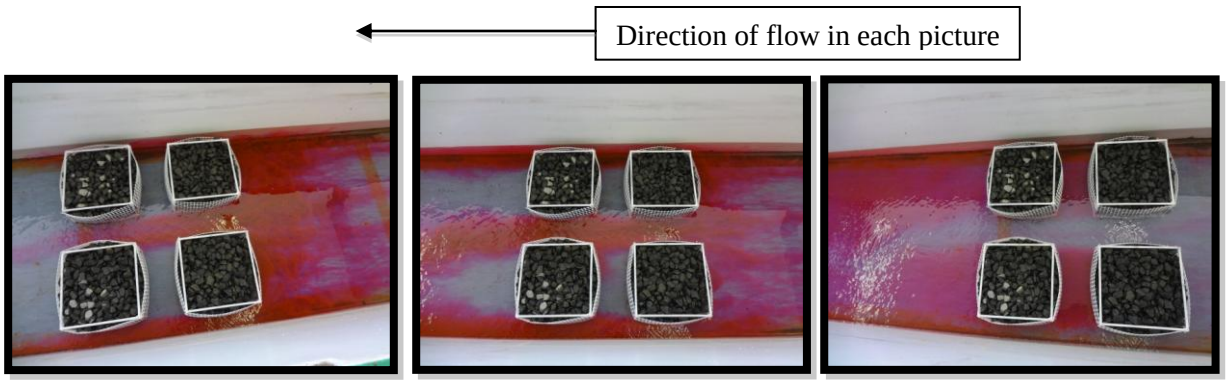


Figure 4.11: Flow pattern seen during experimentation – experiment 6: arrangement 2

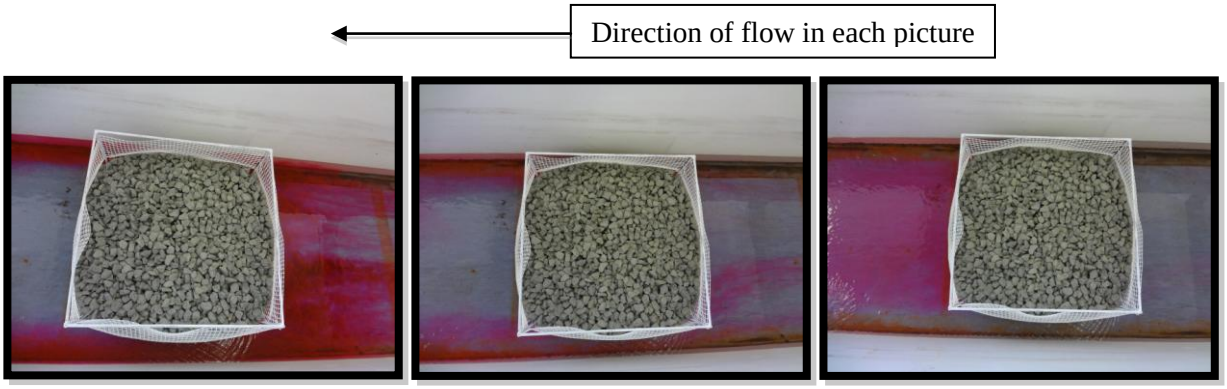


Figure 4.12: Flow pattern seen during experimentation – experiment 7: single gabion

When compared to the control experiment the most notable result was the significantly shorter mean residence time for each gabion arrangement (experiment 5, 6 and 7). This would indicate higher velocities in the regions surrounding the gabions, however, the flow interactions with the gabions are significant.

4.4 Changing the Number of Gabions

Figs 4.13 through 4.16 are the residence time distributions for experiments 5, 3, 8 and 9.

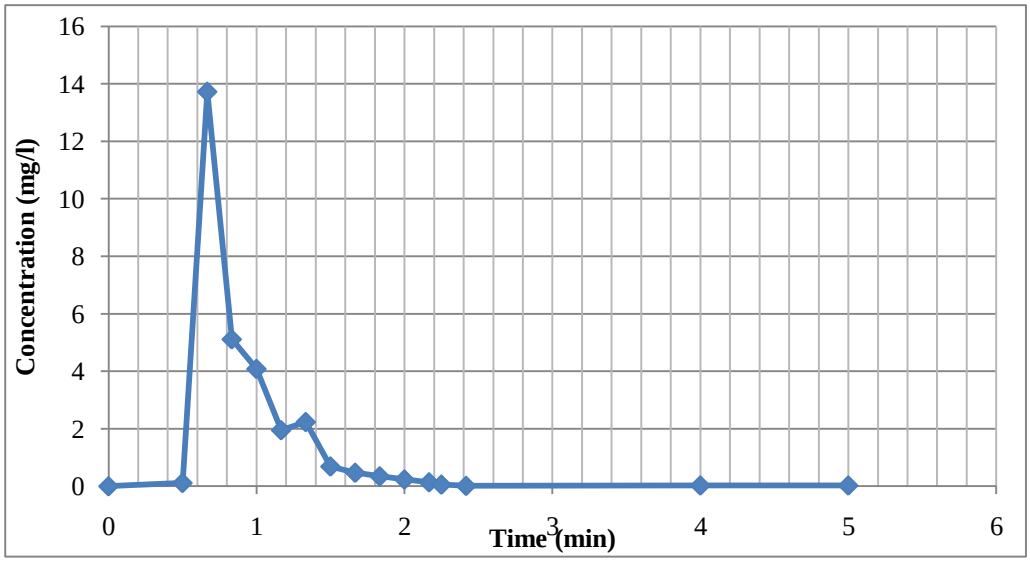


Figure 4.13: Residence time distribution for experiment 5: four gabions using arrangement 1

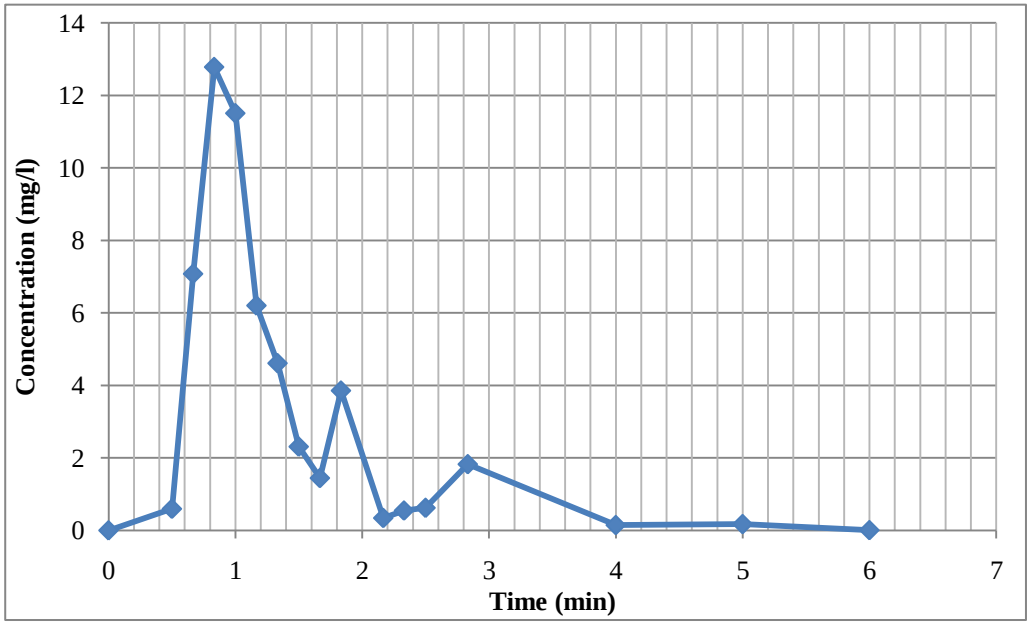


Figure 4.14: Residence time distribution for experiment 3: eight gabions using arrangement 1

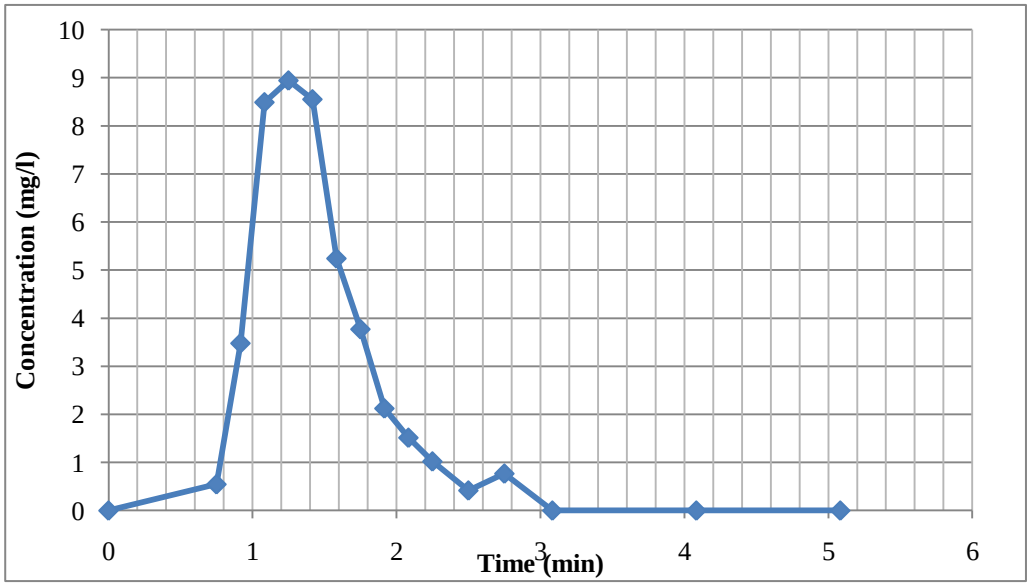


Figure 4.15: Residence time distribution for experiment 8: twelve gabions using arrangement 1

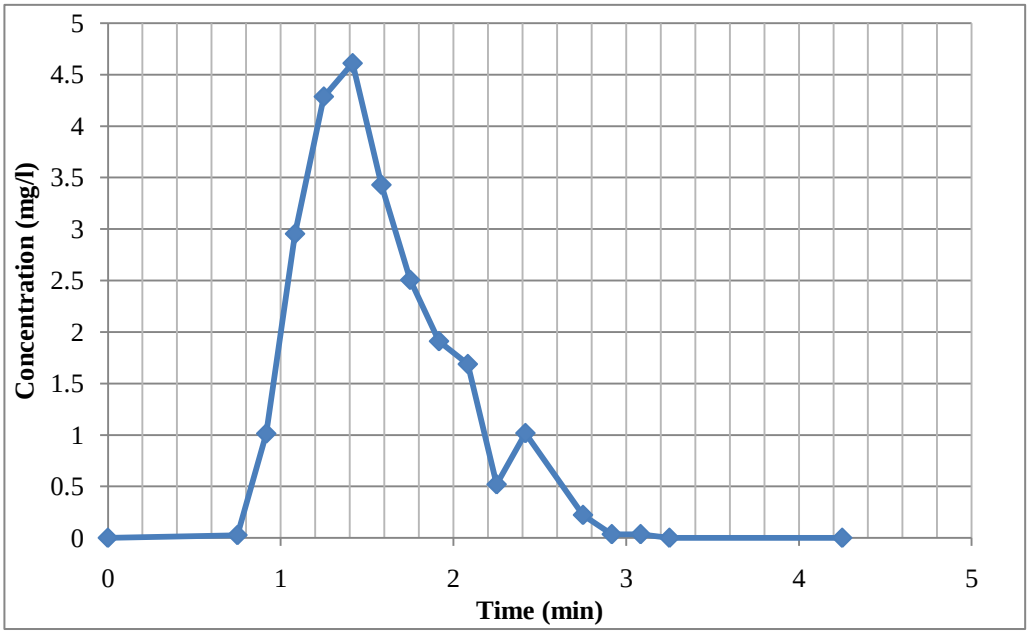


Figure 4.16: Residence time distribution for experiment 9: sixteen gabions using arrangement 1

From the above figures it was apparent that there was a significant effect in the mean residence time and its distribution as the number of gabions is increased. As stated previously the proportion of each peak's area under the C(t) graph would be used to make comparisons to ensure consistency. Due to the fact that the variables x and L_e (shown in Figs 3.7, 3.8, 3.11 and 3.12) varies for all four experiments the mean residence time was calculated and compared in terms of the mean residence time per unit length of gabions (x). This allows for comparison of the mean residence time for the four experiments.

When comparing the proportion of the area under the C(t) graphs for each peak it was important to understand what each peak represents. This was still unknown, however, a better understanding was obtained when using the dispersion model discussed in Chapter 5. It was therefore assumed that the initial peak represented total system bypass and all the other peaks represented some form of gabion interaction (Table 4.3).

Table 4.3: Flow proportion distribution comparison when changing the number of gabions

		Percentage of Flow Interaction with Gabions	Percentage of Bypass Flow	Mean Residence Time / Unit Length (min/m)
Arrangement 1	**4 Gabions**	15.32	84.68	0.56
	8 Gabions	19.36	80.64	0.38
	12 Gabions	2.43	97.57	0.26
	16 Gabions	15.22	84.78	0.22

In Table 4.3 we see the effect the change in the number of gabions used had on the mean residence time and its distribution. The flow interaction with gabions appeared to be increasing, however, there was a significant decrease when twelve gabions were tested. It appeared that an error had occurred during experimentation, however, these results proved to be consistent with those produced by the dispersion model which is discussed further in Chapter 5. The mean residence time per unit length of gabion decreased as the number of gabions increased (Fig. 4.17).

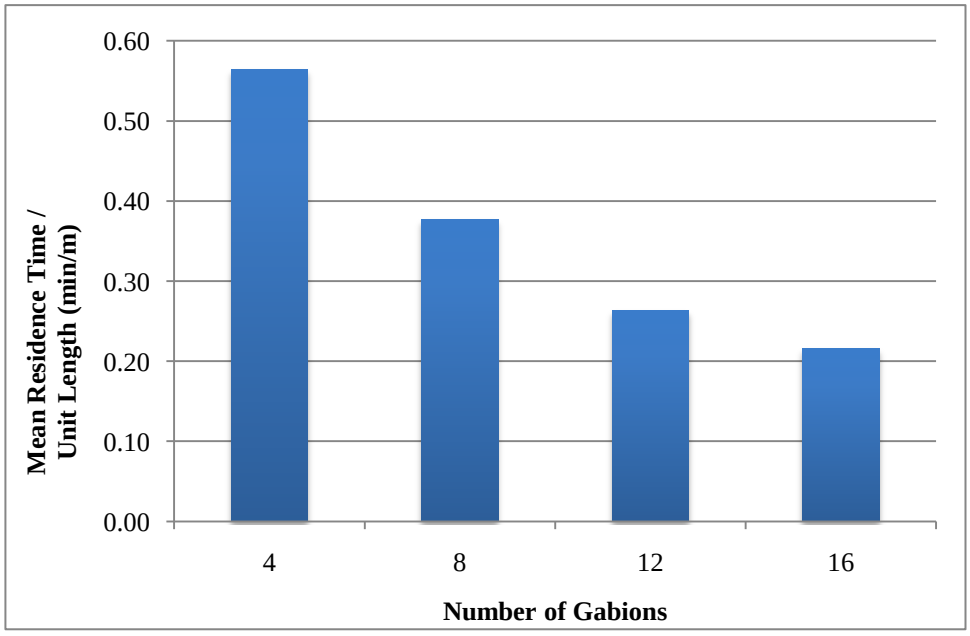


Figure 4.17: Comparison of the mean residence time per unit length for varying number of gabions

5 MODELLING THE CONCENTRATION DISPERSION IN A CHANNEL CONTAINING GABIONS

5.1 General

The dispersion of a contaminant through a channel reach containing gabions has been simulated using a modelling concept proposed by Professor C. S. James (pers.comm). The model enables the variation of relative concentration with time and distance along the channel to be described. The modelling procedure is explained in Chapter 5.2.

5.2 Model Design

The channel is divided longitudinally into successive zones, shown in Fig. 5.1.



Figure 5.1: Plan view of channel divided longitudinally into zones

The concentration is represented as a certain number of contaminated fluid 'particles', with C_0 being the number of fluid particles which are entering zone 1. If there are gabions present in a particular zone then there are a number of pathways that the fluid particles can follow through the zone. Each pathway will have a particular probability of occurrence and specified time to travel through the zone. Provisionally four pathways have been defined. This was based on the experiments and what appeared to be happening to the dye as it reached the gabions. The provisional pathways (Fig 5.2) are:

P_1: the particles do not encounter a gabion and pass, unaffected, through the zone i.e. complete system bypass

P_2: the particles encounter a gabion and are deflected from a straight path and therefore take longer to pass through the zone

P_3: the particles encounter a gabion and are delayed, e.g. by temporary

trapping upstream in the lee of the gabion, but then escape without passing through the gabion

P_4: the particles encounter a gabion and subsequently pass through it, taking significantly longer to pass through the zone

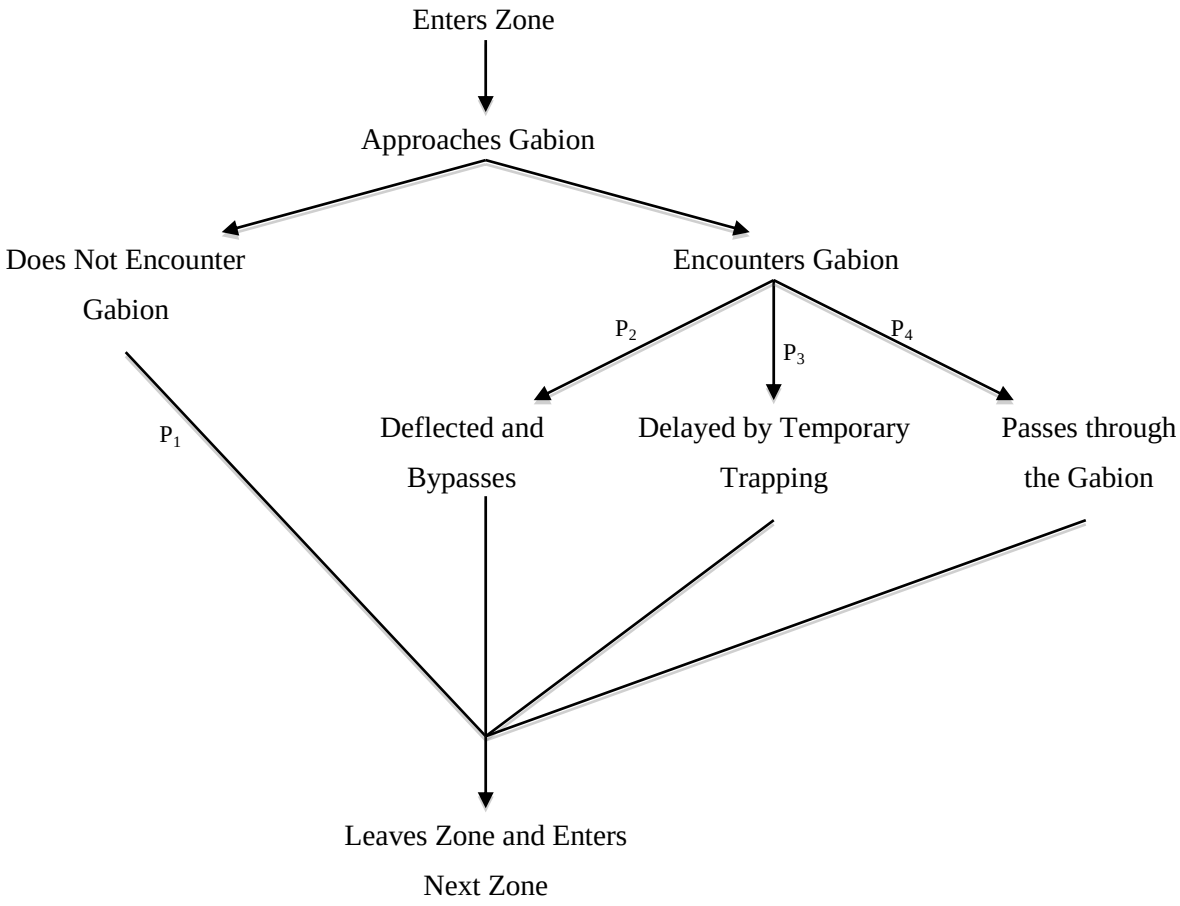


Figure 5.2: Flow of particles through zone

From Fig. 5.2 it is clear that the model is based on the assumption that complete mixing occurs at the end of each zone i.e. the dye leaving a zone is able to choose any of the four pathways as it enters the next zone.

Once the pathways are decided relative time scales are assigned to each pathway. Pathway P_1 is the quickest and is assigned a travel time, $T_1 = 1$. This means that the zone length (x) is defined by the unrestricted flow velocity (v) through it, x =

vT. The other time scales are specified as integer multiples of T_1. Probabilities are specified for each pathway: p_1, p_2, p_3, p_4. Where the sum of p_2, p_3 and p_4 must equal to p_1. In this model $p_1 = 1 - p_e$, where p_e is the probability of gabion encounter.

5.3 Model Simulation

The calculation procedure is illustrated for two channel zones in Fig. 5.3. C_0 is an arbitrary large number representing the impulse input into zone 1 at time zero. The number of particles exiting zone 1, along each pathway, are calculated and specified at the time of exit:

P_1: C_0 p_1 at T_1
P_2: C_0 p_2 at T_2
P_3: C_0 p_3 at T_3
P_4: C_0 p_4 at T_4

The above outputs of zone 1 are then considered to be the inputs to zone 2. The number exiting zone from each of the above pathways, along each pathway through zone 2, are then calculated and assigned to the corresponding times.

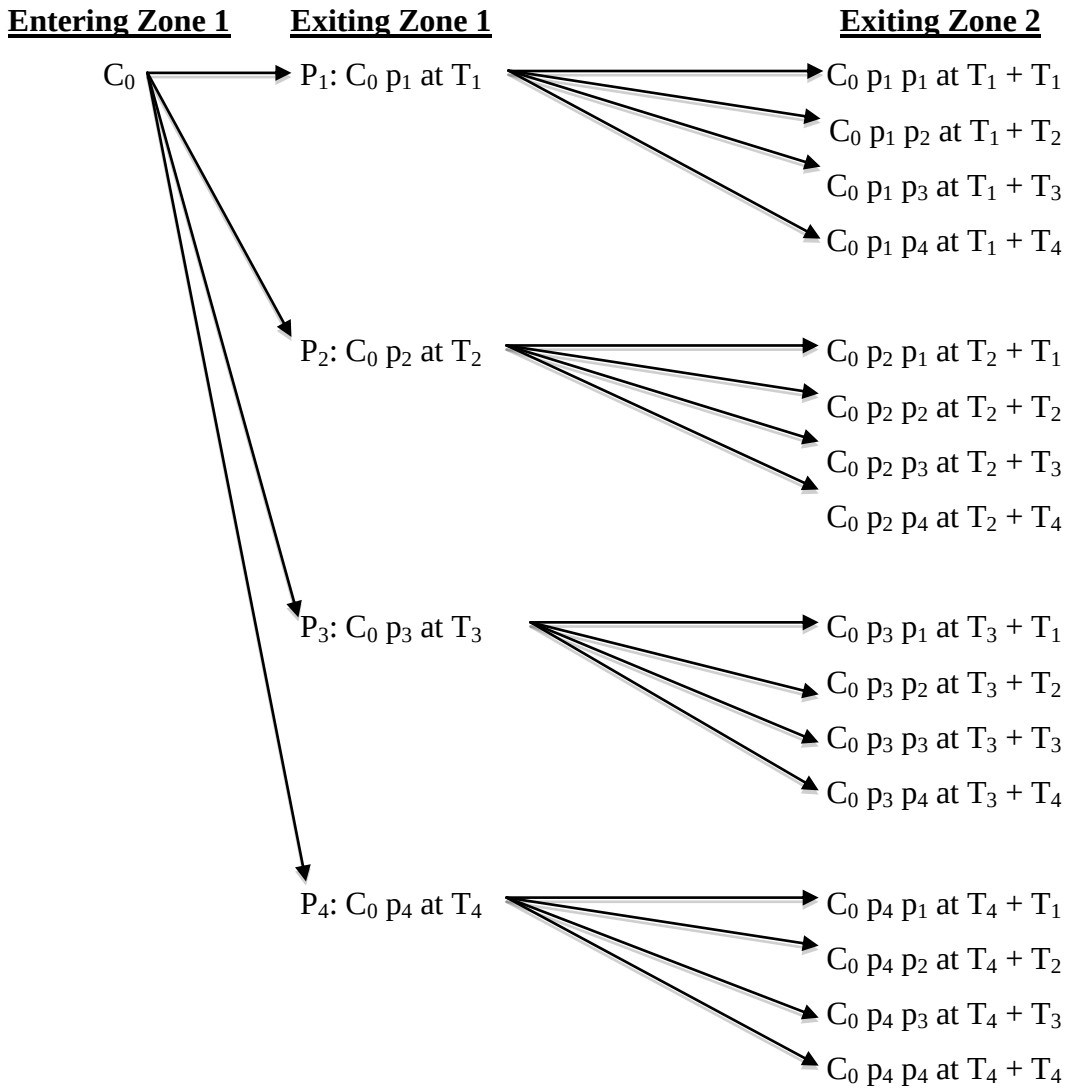


Figure 5.3: Simulation of relative concentration dispersion through two channel zones

The total number of particles exiting zone 2 and therefore entering zone 3 is obtained, at each time, by adding the contribution from all pathways. The total number of particles exiting zone 3 from each pathway is then calculated from the total number entering zone 3 at each time, as was done for zone 2. The procedure is continued in the same way for any number of additional zones.

Mrs L. Westraadt helped code the model in VBA (Appendix C) for application to these experimental conditions.

5.4 Use of the Model to Simulate Experimental Data

The model was used to simulate the experimental data obtained in experiments 5, 3, 8 and 9 i.e. varying the number of gabions (4, 8, 12 and 16 respectively) in a channel. Each set of four gabions represent a zone e.g. 8 gabions would represent the flow of the contaminated fluid 'particles' through two zones. This simulation was conducted to assess and understand what portion of flow was actually passing through the gabions. Once this was known it would allow for the optimisation of the gabion arrangements and subsequent treatment.

The results produced from this model agreed with the experimental data and residence time distribution analysis. The results from the model are shown in Figs 5.4 through 5.7 and Table 5.1. These results were obtained by fitting the data to match the experimental results.

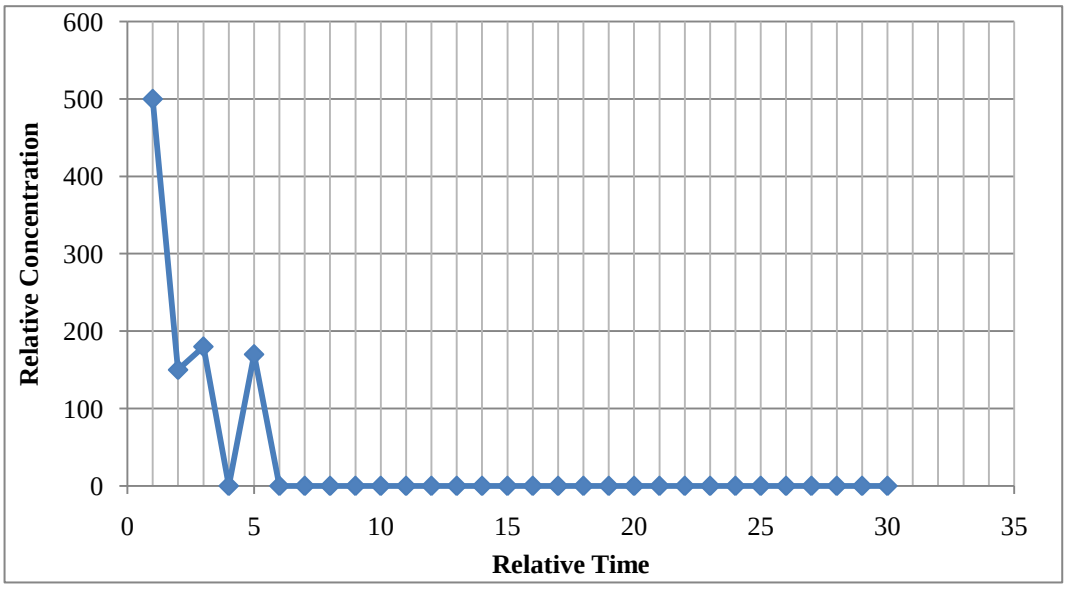


Figure 5.4: Simulated concentration vs. time (C(t)) graph for one zone – four gabions

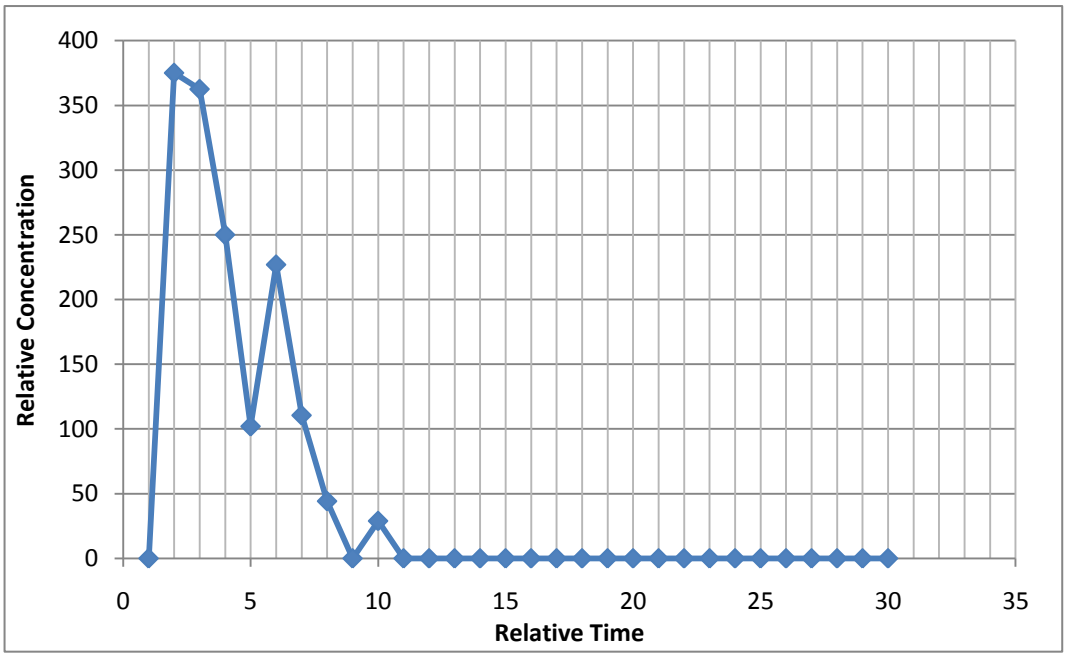


Figure 5.5: Simulated concentration vs. time (C(t)) graph for two zones – eight gabions

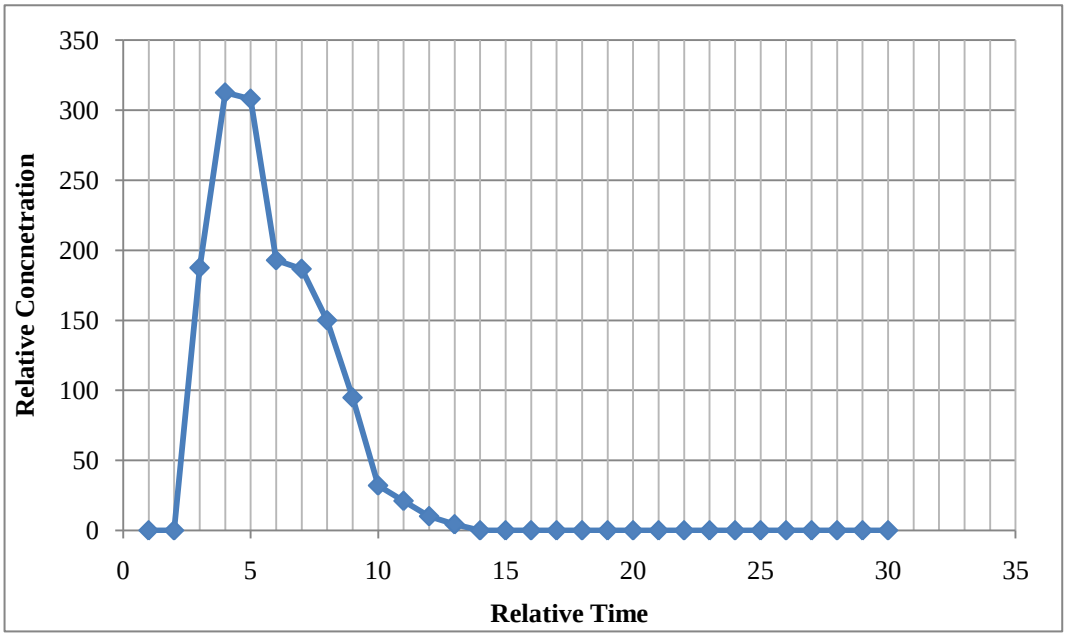


Figure 5.6: Simulated concentration vs. time (C(t)) graph for three zones – twelve gabions

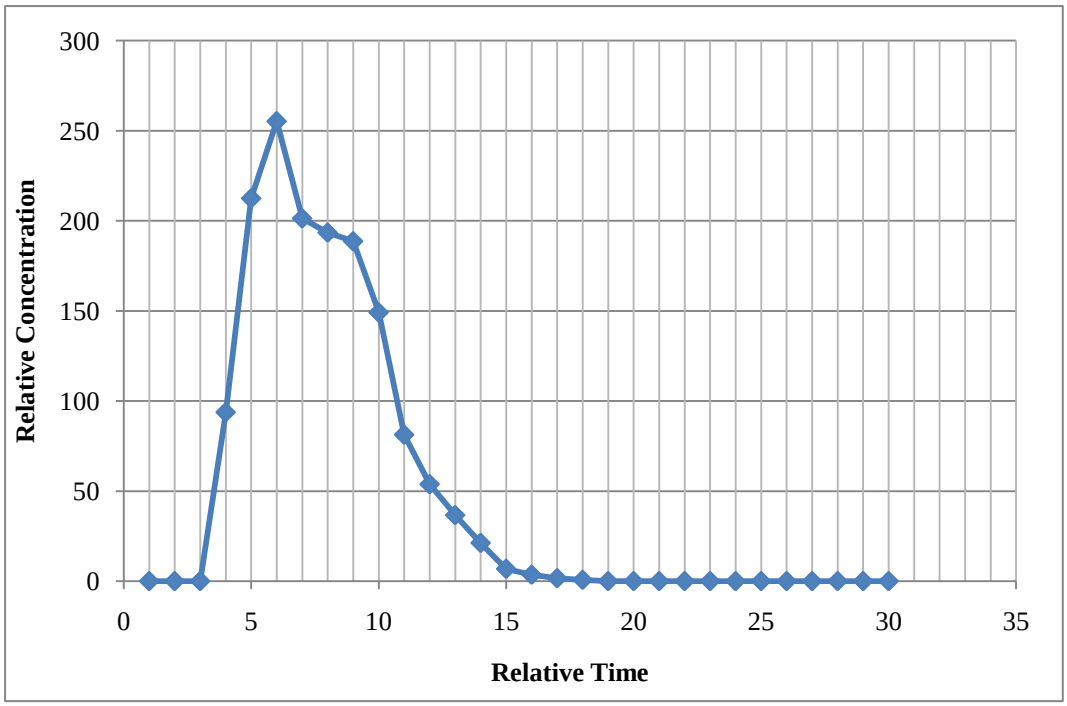


Figure 5.7: Simulated concentration vs. time (C(t)) graph for four zones – sixteen gabions

The above figures all display residence time distribution curves similar to those obtained during experimentation. There are slight discrepancies in their shape; however, this could be attributed to the simplified nature of the model. The model only accounts for four possible pathways which could be incorrect. The model also assumes that the particles exiting one zone are all available and able to choose any pathway when entering the next zone. Discrepancies could also arise due to the concept of non-ideal mixing, edge effects and boundary layer effects. The time and concentration values in Figs 5.4 through 5.7 cannot be compared to those obtained during experimentation. This was because the model does not account for the dilution (caused by the continuous fresh water supply) of the dye particles. During experimentation the dye injected into the system will dilute at different rates (depending on the level bypass) with the fresh water supply thereby producing different concentration readings. The model does not simulate this dilution. The model was used, however, to assess the assumptions made during the analysis of the experimental data. Namely, the assumption that the initial peak

represents total system bypass whereas all subsequent peaks represent some form of gabion interaction.

Table 5.1 shows the input into the model with regards to the proportion of flow in each pathway for each zone, which produced the above figures (5.4 to 5.7). The input values were obtained by fitting them to match the experimental results.

Table 5.1: Model input – proportion of flow in each pathway for each zone

		Zone				Time Units
		1	2	3	4	
Flow Path	P1: Total Bypass	0.5	0.75	0.5	0.5	1
	P2: Encounter and Deflect	0.15	0.5	0.35	0.3	2
	P3: Encounter, Delay and Deflect	0.18	0.08	0.15	0.04	3
	P4: Flow through Gabion	0.17	0.17	0	0.16	5

Table 5.1 confirms the results obtained in experiments 5, 3, 8 and 9. It also suggests the assumption made, when analysing the experimental results, incorrect. Table 5.1 indicates that the initial peak represents all forms of bypass and not just total system bypass i.e. pathway 1. This means that all subsequent peaks in the experimental data represent the flow through the gabions. This differs from the assumption made in the experimental analysis that all subsequent peaks represent any gabion interaction. The comparison of the experimental and modelled results is shown in Table 5.2.

Table 5.2: Comparison of the experimental and modelled results

	Zone 1: Four Gabions		Zone 2: Eight Gabions		Zone 3: Twelve Gabions		Zone 4: Sixteen Gabions	
	Experiment	Model	Experiment	Model	Experiment	Model	Experiment	Model
Proportion of Flow through the Gabions	0.153	0.17	0.194	0.17	0.024	0	0.152	0.16
Percentage Error	10.97		12.19		100		5.12	

The model appears to simulate the flow of the contaminated fluid ‘particles’ accurately. The error in zone three appears to be large, however, when viewed in context there is little difference between zero flow through the gabions and 2.4%. The errors observed could be attributed, as previously stated, to experimental error and the sensitivity limitations of the Spectrophotometer.

An interesting trend, which appeared in the results, was the sudden decrease in flow through the gabions when twelve gabions were used. It is assumed that the mixing at the start of zone three occurred in such a way that the bypass pathways were favoured. It is also possible that in the experimental analysis the peaks, which represented the gabion interaction flow merged with the bypass peak due to the interference that the gabions caused. The merging of these peaks would produce a bypass peak that was a lot wider than if additional peaks were present. This mergence would affect the data points chosen when isolating the bypass and subsequent peaks.

6 CONCLUSIONS AND RECOMMENDATIONS

6.1 Summary and Conclusions of the Present Study

Residence time distribution theory was used to assess the effects that strategically placed gabions had on the interaction of river flow. These experiments were conducted in a 0.92 m wide flume with the flow rate controlled to 9.92 l/s. Three variables were tested: the changing flow depth (submerged volume), the change in the gabion arrangement or pattern and the change in the number of gabions used. FWT Red Dye was used to simulate the water contaminant and was injected into the system as an impulse over three seconds. The samples were taken at particular time intervals at the flume end. These were then analysed in the spectrophotometer and subsequently analysed using residence time distribution theory.

When changing the flow depth it was apparent that the interaction of flow with the gabions improved as the flow depth was reduced. When changing the flow pattern arrangement 2 (the aligned pattern) and the single gabion improved the flow interaction the most when compared to arrangement 1 (the staggered pattern). It was thought that the single gabion produced these results because it was acting more as a weir and there were very small bypass sections. Arrangement 2, however, was thought to have produced these results because the dye was delayed for a longer period of time due to the alignment of the gabions, which increased the flow interaction. When changing the number of gabions (using arrangement 1) the flow interaction appeared to remain at a constant proportion of approximately 17% for all 4, 8 and 16 gabions. The flow interaction for twelve gabions produced a sudden decrease in flow interaction to approximately 2%. It was thought that this could be attributed to the mergence of the bypass peak with all subsequent peaks, thereby, producing a single peak that was wider than the bypass peaks seen in the other three experiments. It must also be noted that the isolation of peaks may have been slightly inaccurate. This is attributed to the lack of data points on the curve. The number of points collected were limited due to the flow rate of the dye and the ability to mix, collect a sample and empty the collection trough

quickly enough. The intervals used to take samples were optimised to ensure the maximum number of samples could be taken before the dye left the system.

Thus, if we were to create reactive gabions, based on this data we would recommend that 16 gabions positioned using arrangement 1 (staggered pattern) be used. Provided the flow depth is approximately 13 cm, this pattern would provide an average proportion of gabion-flow interaction of 17%. Thus potentially treating 17% of the AMD contamination. The level of AMD neutralisation will, however, be dependent on the blast furnace slag used in the gabions and the rate at which the slag reacts with the AMD.

6.2 Recommendations for Future River Flow Studies Related to Gabions

Recommendations for future studies include:

- Determining the optimum reaction rate required for the blast furnace slag to neutralise the AMD to predetermined acceptable standards,
- Optimising the model to include varying the arrangements of the gabions,
- Optimising the model to account for the continuous supply of fresh water, which would cause diluting of the contaminated fluid ‘particles’,
- Investigate the gabion-flow interaction in a more extensive distribution,
- Investigate the assumptions made in order to determine the flow through the gabions and subsequent flow regime,
- Model the flow velocity through the gabions in three directions

The above investigations would help better understand and subsequently predict the interaction of river flow with gabions, thus enabling this AMD treatment method to be optimised.

7 REFERENCES

Arnold DE, Skinner WD, Spotts DE (1988) Evaluation of three experimental low-technology approaches to acid mitigation in headwater streams. Water, Air and Soil Pollution. Vol.41 pp 385-406.

Bird RB, Stewart WE, Lightfoot EN (1960) Transport Phenomena. Department of Chemical Engineering. University of Wisconsin: John Wiley & Sons.

DWA – Department of Water Affairs (2012) Feasibility study for a long-term solution to address the acid mine drainage associated with the East, Central and West Rand underground mining basins, Gauteng Province. AMD FS LTS Newsletter. Edition 1 – July 2012. Website. http://www.dwaf.gov.za/Projects/AMDFSLTS/Documents/AMD%20FS%20LTS_Newsletter%2001%20(Low%20Resolution%20-%204MB).pdf: 28/11/2012.

Fogler HS (2006) Elements of Chemical Reaction Engineering Fourth Edition. The University of Michigan: Prentice Hall Professional Technical Reference.

Galan E, Carretero MI, Fernandez-Caliani JC (1999) Effects of acid mine drainage on clay minerals suspended in the Tinto River (Rio Tinto, Spain). An experimental approach. Clay Minerals. Vol.34 pp 99-108.

Godfrey L, Hobbs P, Manders P (2009) Acid mine drainage in South Africa. CSIR Natural Resources and the Environment: Briefing Note 2009/02

Gupte SK, Advani SG (1997) Flow Near the Permeable Boundary of a Porous Medium: An Experimental Investigation using LDA. Experiments in Fluids. Vol.22 pp 408-422.

Karolia I (2011) Kromdraai Residents Concerned about Acid Mine Drainage. Website. http://acidminedrainage.wordpress.com/: 07/05/2012.

Levenspiel O (1999) Chemical Reaction Engineering Third Edition. Oregon State University: John Wiley & Sons.

McCarthy T (2010) The decanting of acid mine water in the Gauteng City-Region: analysis, prognosis and solutions. Gauteng City-Region Observatory.

Michioku K, Maeno S, Furusawa T, Haneda M (2005) Discharge through a permeable rubble mound weir. Journal of Hydraulic Engineering ASCE. Vol.131 No.1 pp 1-10.

Mulqueen J (2005) The flow of water through gravels. Irish Journal of Agricultural and Food Research. Vol.44 No.1 pp 83-94.

Persson J, Wittgren HG (2003) How hydrological and hydraulic conditions affect performance of ponds. Ecological Engineering. Vol.21 pp 259-269.

Rees SB, Bright P, Connelly R, Bowell RJ, Szabo E (2004) Application of the Welsh mine water strategy: Cwmrheidol case study. Website. http://www.imwa2013.info/docs/imwa_2004/IMWA2004_31_Rees.pdf: 26/01/2012.

Robb GA, Robinson JDF (1995) Acid drainage from mines. The Geographical Journal. Vol.161 No.1 pp 47-54.

Samani JMV, Samani HMV, Shaiannejad M (2004) Reservoir routing with outflow through rockfill dams. Journal of Hydraulic Research. Vol.42 No.4 pp 435-439.

Stephenson DA (1979) Rockfill in Hydraulic Engineering. New York: Elsevier.

Strosnider WHJ, Llanos Lopez FS, Nairn RW (2011) Acid mine drainage at Cerro Rico de Potosi II: Severe degradation of the upper Rio Pilcomayo watershed. Environ Earth Sci. Vol.64 pp 911-923.

WPCAMR – Western Pennsylvania Coalition for Abandoned Mine Reclamation (no date) Ask me about pyrite: The formation of polluted mine water. Website. http://www.amrclearinghouse.org/Sub/education/AskMeAboutPyrite/AskMeAboutPyrite.pdf: 28/11/2012.

8 BIBLIOGRAPHY

Chinnarasri C, Donjadee S, Israngkura U (2008) Hydraulic characteristics of gabion-stepped weirs. Journal of Hydraulic Engineering ASCE. Vol.134 No.8 pp 1147-1152.

Columbus N (1966) The design and construction of hele-shaw models. Ground Water. Vol.4 No.2 pp 16-22.

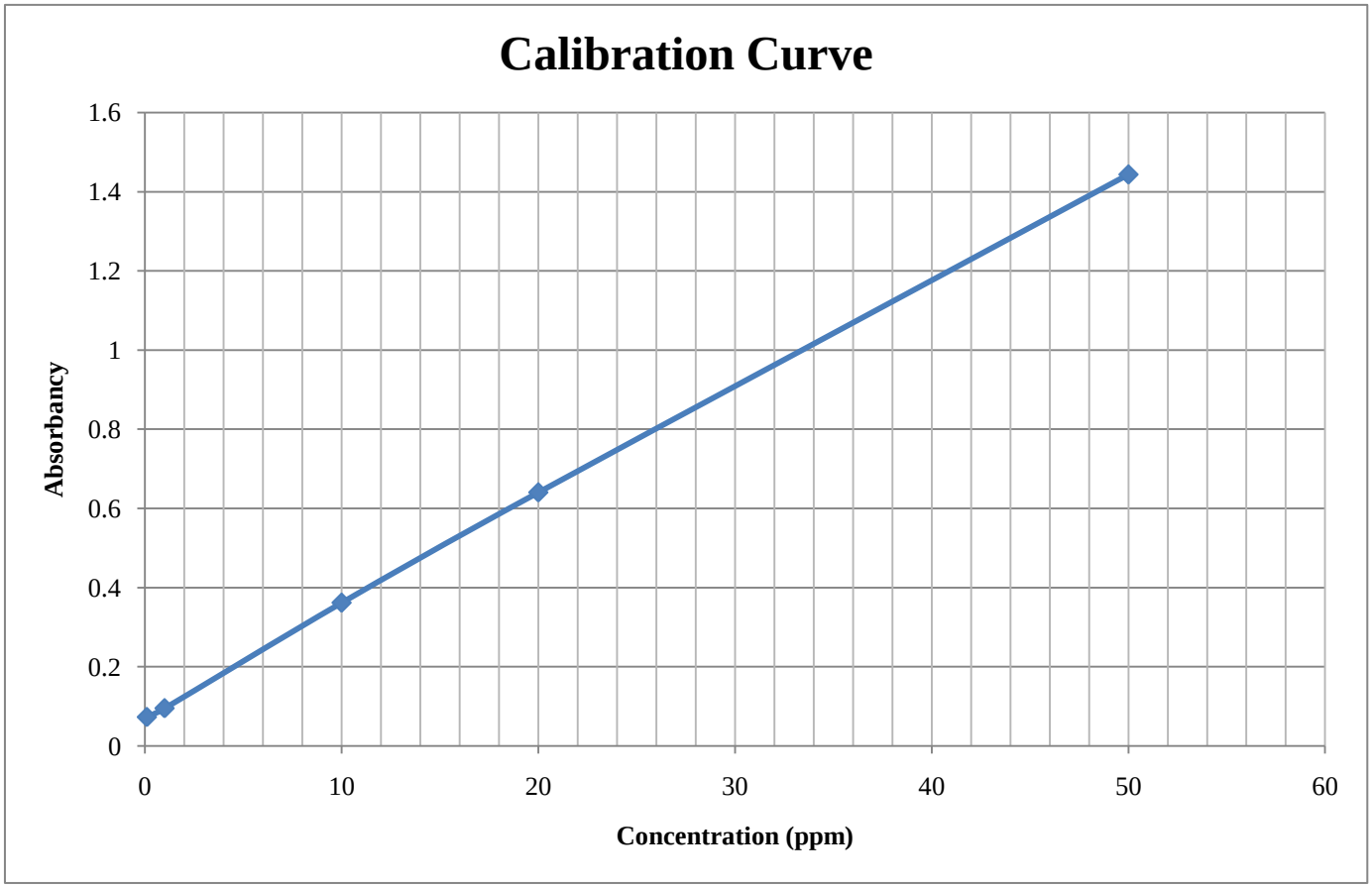
Kuma JS, Younger PL, Buah WK (2011) Numerical indices of the severity of acidic mine drainage: broadening the applicability of the Gray acid mine drainage index. Mine Water Environ. Vol.30 pp 67-74.

Murdoch AI, Soliman A (1999) On the slip-boundary condition for liquid flow over planar porous boundaries. Proceedings: Mathematical, Physical and Engineering Sciences. Vol.455 No.1984 pp 1315-1340.

Roback SS, Richardson JW (1969) The effects of acid mine drainage on aquatic insects. Proceedings of the Academy of Natural Sciences of Philadelphia. Vol.121 pp 81-107.

Siddiqua S, Blatz JA, Privat NC (2011) Evaluating turbulent flow in large rockfill. Journal of Hydraulic Engineering. Vol.137 No. 11 pp 1462-1469.

9 APPENDIX A: Spectrophotometer Calibration Curve



10 APPENDIX B: Residence Time Distribution Analysis

10.1 Empty Flume: Control

Date:	16-Oct-12	**Gabion Size (m): lxbxh**	0,29	0,29	0,175	**Total Submerged Volume (m^3):**	0,0000
		Number of Gabions:	0			**Flow Depth (m)**	0,13

Container	Time (min)	ABS	Concentration (mg/l)	Qi	Ei	ti.Ei.Δt	ti².Ei.Δt
0	0	0,0892	0	0	0	0	0
1	1,5000	0,089	0	0,00E+00	0,000	0,000	0,000E+00
2	1,6667	0,1265	1,3546	3,76E-03	23,302	0,002	4,994E-05
3	1,8333	0,25	5,8492	1,62E-02	100,618	0,009	2,609E-04
4	2,0000	0,2655	6,4132	1,78E-02	110,320	0,010	3,405E-04
5	2,1667	0,1818	3,3665	9,35E-03	57,911	0,006	2,098E-04
6	2,3333	0,1414	1,8965	5,27E-03	32,624	0,004	1,371E-04
7	2,5000	0,1134	0,8794	2,44E-03	15,128	0,002	7,295E-05
8	2,6667	0,0997	0,382	1,06E-03	6,571	0,001	3,606E-05
9	2,8333	0,1006	0,4131	1,15E-03	7,106	0,001	4,402E-05
10	3,0000	0,0924	0,1155	3,21E-04	1,987	0,000	1,380E-05
11	3,1667	0,0956	0,231	6,42E-04	3,974	0,001	3,075E-05
12	3,3333	0,0889	0	0,00E+00	0,000	0,000	0,000E+00
13	3,5000	0,0884	0	0,00E+00	0,000	0,000	0,000E+00
14	3,6667	0,09	0,0267	7,42E-05	0,459	0,000	4,765E-06
15	3,8333	0,0874	0	0,00E+00	0,000	0,000	0,000E+00

ΣQi	0,058
τm (hr)	0,034
τ(ideal)	0,033
Veff	1,046
σ^2	2,290E-05
$\sigma\theta^2$	0,019
$\sigma\theta^2=2D-2D^2*(1-e^{(-1/D)})$	
D	0,010
λ	1,026
N	51,436
N(check)	51,436

10.2 Changing the Flow Depth

Date:	20-Sep-12	**Gabion Size (m): lxbxh**	0,29	0,29	0,175		**Total Submerged Volume (m^3):**	0,1076
		Number of Gabions:	8				**Flow Depth (m)**	0,16

Container	Time (min)	ABS	Concentration (mg/l)	Qi	Ei	ti.Ei.Δt	ti^2.Ei.Δt
0	0	0,0802	0	0	0	0	0
1	0,667	0,083	0,1021	1,14E-03	1,143	0,000	1,570E-06
2	0,8667	0,1687	3,2199	1,07E-02	36,052	0,002	2,504E-05
3	1,033	0,3065	8,2341	2,28E-02	92,194	0,004	7,574E-05
4	1,2	0,2126	4,8188	1,34E-02	53,954	0,003	6,007E-05
5	1,45	0,1824	3,7173	1,55E-02	41,621	0,004	1,013E-04
6	1,667	0,1445	2,3405	8,46E-03	26,206	0,003	7,316E-05
7	1,833	0,1147	1,2569	3,48E-03	14,073	0,001	3,634E-05
8	2	0,1127	1,1814	3,29E-03	13,228	0,001	4,091E-05
9	2,333	0,0974	0,6262	3,48E-03	7,011	0,002	5,883E-05
10	2,667	0,0859	0,2087	1,16E-03	2,337	0,001	2,570E-05
11	3	0,084	0,1376	7,64E-04	1,541	0,000	2,138E-05
12	3,5	0,0831	0,1066	8,88E-04	1,194	0,001	3,384E-05
13	4	0,0801	0	0,00E+00	0,000	0,000	0,000E+00
14	5	0,0858	0,2043	3,41E-03	2,287	0,003	2,648E-04
15	6	0,0815	0,0488	8,13E-04	0,546	0,001	9,107E-05
16	8	0,0801	0	0,00E+00	0,000	0,000	0,000E+00

ΣQi	0,089
τm (hr)	0,026
τ(ideal)	0,024
Veff	1,091
σ^2	2,489E-04
$\sigma\theta^2$	0,377
$\sigma\theta^2=2D-2D^2*(1-e^{(-1/D)})$	
D	0,250
λ	0,680
N	2,654
N(check)	2,654

Percentage Bypass							
Container	**Time (min)**	**ABS**	**Concentration (mg/l)**	**Qi**	**Ei**	**ti.Ei.Δt**	**ti².Ei.Δt**
0	0	0,0802	0	0	0	0	0
1	0,667	0,083	0,1021	1,14E-03	1,200	0,000	1,648E-06
2	0,8667	0,1687	3,2199	1,07E-02	37,839	0,002	2,628E-05
3	1,033	0,3065	8,2341	2,28E-02	96,764	0,005	7,950E-05
4	1,2	0,2126	4,8188	1,34E-02	56,629	0,003	6,305E-05
5	1,45	0,1824	3,7173	1,55E-02	43,684	0,004	1,063E-04
6	1,667	0,1445	2,3405	8,46E-03	27,505	0,003	7,679E-05
7	1,833	0,1147	1,2569	3,48E-03	14,771	0,001	3,814E-05
8	2	0,1127	1,1814	3,29E-03	13,883	0,001	4,294E-05
9	2,333	0,0974	0,6262	3,48E-03	7,359	0,002	6,175E-05
10	2,667	0,0859	0,2087	1,16E-03	2,453	0,001	2,697E-05
11	3	0,084	0,1376	7,64E-04	1,617	0,000	2,244E-05
12	3,5	0,0831	0,1066	8,88E-04	1,253	0,001	3,552E-05
13	4	0,0801	0	0,00E+00	0,000	0,000	0,000E+00
14	5	0,0858	0	0,00E+00	0,000	0,000	0,000E+00
15	6	0,0815	0	0,00E+00	0,000	0,000	0,000E+00
16	8	0,0801	0	0,00E+00	0,000	0,000	0,000E+00

ΣQi	0,085
τm (hr)	0,023
τ(ideal)	0,024
Veff	0,963
σ²	6,653E-05
σθ²	0,129
σθ²=2D-2D²*(1-e^(-1/D))	
D	0,0693
λ	0,838
N	7,737
N(check)	7,737

Percentage of Interaction							
Container	**Time (min)**	**ABS**	**Concentration (mg/l)**	**Qi**	**Ei**	**ti.Ei.Δt**	**ti².Ei.Δt**
0	0	0,0802	0	0	0	0	0
1	0,667	0,083	0	0,00E+00	0,000	0,000	0,000E+00
2	0,8667	0,1687	0	0,00E+00	0,000	0,000	0,000E+00
3	1,033	0,3065	0	0,00E+00	0,000	0,000	0,000E+00
4	1,2	0,2126	0	0,00E+00	0,000	0,000	0,000E+00
5	1,45	0,1824	0	0,00E+00	0,000	0,000	0,000E+00
6	1,667	0,1445	0	0,00E+00	0,000	0,000	0,000E+00
7	1,833	0,1147	0	0,00E+00	0,000	0,000	0,000E+00
8	2	0,1127	0	0,00E+00	0,000	0,000	0,000E+00
9	2,333	0,0974	0	0,00E+00	0,000	0,000	0,000E+00
10	2,667	0,0859	0	0,00E+00	0,000	0,000	0,000E+00
11	3	0,084	0	0,00E+00	0,000	0,000	0,000E+00
12	3,5	0,0831	0	0,00E+00	0,000	0,000	0,000E+00
13	4	0,0801	0	0,00E+00	0,000	0,000	0,000E+00
14	5	0,0858	0,2043	3,41E-03	48,431	0,067	5,605E-03
15	6	0,0815	0,0488	8,13E-04	11,569	0,019	1,928E-03
16	8	0,0801	0	0,00E+00	0,000	0,000	0,000E+00

ΣQi	0,004
τm (hr)	0,087
τ(ideal)	0,024
Veff	3,673
σ²	4,323E-05
σθ²	0,006
σθ²=2D-2D²*(1-e^(-1/D))	
D	29104177,5503
λ	3,673
N	23131,223
N(check)	173,261

Date:	14-Sep-12	**Gabion Size (m): lxbxh**	0,29	0,29	0,175		**Total Submerged Volume (m^3):**	0,0875
		Number of Gabions:	8				**Flow Depth (m)**	0,13

Container	Time (min)	ABS	Concentration (mg/l)	Qi	Ei	ti.Ei.Δt	ti².Ei.Δt
0	0	0,0776	0	0	0	0	0
1	0,5	0,094	0,5951	4,96E-03	3,623	0,000	2,097E-06
2	0,667	0,2721	7,075	1,97E-02	43,071	0,001	1,481E-05
3	0,833	0,4288	12,7772	3,54E-02	77,785	0,003	4,148E-05
4	1	0,3938	11,5032	3,20E-02	70,029	0,003	5,414E-05
5	1,1667	0,248	6,2	1,72E-02	37,744	0,002	3,965E-05
6	1,333	0,2043	4,6101	1,28E-02	28,065	0,002	3,839E-05
7	1,5	0,1411	2,3095	6,43E-03	14,060	0,001	2,446E-05
8	1,667	0,1173	1,4434	4,02E-03	8,787	0,001	1,888E-05
9	1,833	0,1836	3,855	1,07E-02	23,468	0,002	6,060E-05
10	2,1667	0,087	0,342	1,90E-03	2,082	0,000	1,510E-05
11	2,33	0,0927	0,5463	1,49E-03	3,326	0,000	1,365E-05
12	2,5	0,0947	0,6218	1,76E-03	3,785	0,000	1,862E-05
13	2,833	0,1278	1,8254	1,01E-02	11,113	0,003	1,375E-04
14	4	0,0817	0,1466	2,85E-03	0,892	0,001	7,715E-05
15	5	0,0824	0,1732	2,89E-03	1,054	0,001	1,220E-04
16	6	0,0774	0,0066	1,10E-04	0,040	0,000	6,697E-06

ΣQi	0,164
τm (hr)	0,022
τ(ideal)	0,019
Veff	1,152
σ^2	1,992E-04
$\sigma\theta^2$	0,410
$\sigma\theta^2=2D-2D^2*(1-e^{(-1/D)})$	
D	0,282
λ	0,680
N	2,440
N(check)	2,440

Percentage Bypass							
Container	**Time (min)**	**ABS**	**Concentration (mg/l)**	**Qi**	**Ei**	**ti.Ei.Δt**	**ti².Ei.Δt**
0	0	0,0776	0	0	0	0	0
1	0,5	0,094	0,5951	4,96E-03	4,492	0,000	2,600E-06
2	0,667	0,2721	7,075	1,97E-02	53,409	0,002	1,837E-05
3	0,833	0,4288	12,7772	3,54E-02	96,455	0,004	5,144E-05
4	1	0,3938	11,5032	3,20E-02	86,838	0,004	6,714E-05
5	1,1667	0,248	6,2	1,72E-02	46,804	0,003	4,917E-05
6	1,333	0,2043	4,6101	1,28E-02	34,802	0,002	4,761E-05
7	1,5	0,1411	2,3095	6,43E-03	17,434	0,001	3,033E-05
8	1,667	0,1173	1,4434	4,02E-03	10,896	0,001	2,341E-05
9	1,833	0,1836	0	0,00E+00	0,000	0,000	0,000E+00
10	2,1667	0,087	0	0,00E+00	0,000	0,000	0,000E+00
11	2,33	0,0927	0	0,00E+00	0,000	0,000	0,000E+00
12	2,5	0,0947	0	0,00E+00	0,000	0,000	0,000E+00
13	2,833	0,1278	0	0,00E+00	0,000	0,000	0,000E+00
14	4	0,0817	0	0,00E+00	0,000	0,000	0,000E+00
15	5	0,0824	0	0,00E+00	0,000	0,000	0,000E+00
16	6	0,0774	0	0,00E+00	0,000	0,000	0,000E+00

ΣQi	0,132
τm (hr)	0,016
τ(ideal)	0,019
Veff	0,858
σ²	2,028E-05
σθ²	0,075
σθ²=2D-2D²*(1-e^(-1/D))	
D	0,0390
λ	0,793
N	13,303
N(check)	13,303

Percentage of Interaction							
Container	**Time (min)**	**ABS**	**Concentration (mg/l)**	**Qi**	**Ei**	**ti.Ei.Δt**	**ti².Ei.Δt**
0	0	0,0776	0	0	0	0	0
1	0,5	0,094	0	0,00E+00	0,000	0,000	0,000E+00
2	0,667	0,2721	0	0,00E+00	0,000	0,000	0,000E+00
3	0,833	0,4288	0	0,00E+00	0,000	0,000	0,000E+00
4	1	0,3938	0	0,00E+00	0,000	0,000	0,000E+00
5	1,1667	0,248	0	0,00E+00	0,000	0,000	0,000E+00
6	1,333	0,2043	0	0,00E+00	0,000	0,000	0,000E+00
7	1,5	0,1411	0	0,00E+00	0,000	0,000	0,000E+00
8	1,667	0,1173	0	0,00E+00	0,000	0,000	0,000E+00
9	1,833	0,1836	3,855	1,07E-02	306,741	0,026	7,920E-04
10	2,1667	0,087	0,342	1,90E-03	27,213	0,005	1,974E-04
11	2,33	0,0927	0	0,00E+00	0,000	0,000	0,000E+00
12	2,5	0,0947	0	0,00E+00	0,000	0,000	0,000E+00
13	2,833	0,1278	0	0,00E+00	0,000	0,000	0,000E+00
14	4	0,0817	0	0,00E+00	0,000	0,000	0,000E+00
15	5	0,0824	0	0,00E+00	0,000	0,000	0,000E+00
16	6	0,0774	0	0,00E+00	0,000	0,000	0,000E+00

ΣQi	0,013
τm (hr)	0,031
τ(ideal)	0,019
Veff	1,640
σ²	3,973E-06
σθ²	0,004
σθ²=2D-2D²*(1-e^(-1/D))	
D	579288,063
λ	1,640
N	251699,187
N(check)	248,035

Date:	20-Sep-12	**Gabion Size (m): lxbxh**	0,29	0,29	0,175		**Total Submerged Volume (m^3):**	0,0673
		Number of Gabions:	8				**Flow Depth (m)**	0,1

Container	Time (min)	ABS	Concentration (mg/l)	Qi	Ei	ti.Ei.Δt	ti².Ei.Δt
0	0	0,0847	0	0	0	0	0
1	0,5	0,2352	5,4761	4,56E-02	30,608	0,002	1,77E-05
2	0,667	0,4554	13,4886	3,75E-02	75,392	0,002	2,59E-05
3	0,833	0,3528	9,7526	2,70E-02	54,511	0,002	2,91E-05
4	1	0,2058	4,4057	1,23E-02	24,625	0,001	1,90E-05
5	1,167	0,2983	7,7722	2,16E-02	43,441	0,002	4,57E-05
6	1,333	0,114	1,0659	2,95E-03	5,958	0,000	8,14E-06
7	1,5	0,0946	0,3597	1,00E-03	2,010	0,000	3,50E-06
8	1,667	0,0912	0,2354	6,55E-04	1,316	0,000	2,83E-06
9	1,833	0,083	0	0,00E+00	0,000	0,000	0,00E+00
10	2	0,0917	0,2531	7,04E-04	1,415	0,000	4,37E-06
11	2,167	0,0878	0,111	3,09E-04	0,620	0,000	2,25E-06
12	3	0,0818	0	0,00E+00	0,000	0,000	0,00E+00
13	4	0,1249	1,4612	2,44E-02	8,167	0,009	6,05E-04
14	5	0,0862	0,0533	8,88E-04	0,298	0,000	3,45E-05
15	6	0,0913	0,2398	4,00E-03	1,340	0,002	2,23E-04

ΣQi	0,179
τm (hr)	0,023
τ(ideal)	0,015
Veff	1,533
σ²	5,120E-04
σθ²	1,005
σθ²=2D-2D²*(1-e^(-1/D))	
D	10665555,3
λ	-0,008
N	0,995
N(check)	0,995

Percentage Bypass							
Container	**Time (min)**	**ABS**	**Concentration (mg/l)**	**Qi**	**Ei**	**ti.Ei.Δt**	**ti².Ei.Δt**
0	0	0,0847	0	0	0	0	0
1	0,5	0,2352	5,4761	4,56E-02	49,711	0,003	2,877E-05
2	0,667	0,4554	13,4886	3,75E-02	122,446	0,004	4,212E-05
3	0,833	0,3528	9,7526	2,70E-02	88,532	0,003	4,721E-05
4	1	0,2058	0	0,00E+00	0,000	0,000	0,000E+00
5	1,167	0,2983	0	0,00E+00	0,000	0,000	0,000E+00
6	1,333	0,114	0	0,00E+00	0,000	0,000	0,000E+00
7	1,5	0,0946	0	0,00E+00	0,000	0,000	0,000E+00
8	1,667	0,0912	0	0,00E+00	0,000	0,000	0,000E+00
9	1,833	0,083	0	0,00E+00	0,000	0,000	0,000E+00
10	2	0,0917	0	0,00E+00	0,000	0,000	0,000E+00
11	2,167	0,0878	0	0,00E+00	0,000	0,000	0,000E+00
12	3	0,0818	0	0,00E+00	0,000	0,000	0,000E+00
13	4	0,1249	0	0,00E+00	0,000	0,000	0,000E+00
14	5	0,0862	0	0,00E+00	0,000	0,000	0,000E+00
15	6	0,0913	0	0,00E+00	0,000	0,000	0,000E+00
0	0	0	0	0,00E+00	0,000	0,000	0,000E+00

ΣQi	0,110
τm (hr)	0,011
τ(ideal)	0,015
Veff	0,723
σ²	4,858E-06
σθ²	0,043
σθ²=2D-2D²*(1-e^(-1/D))	
D	0,0310
λ	0,692
N	23,309
N(check)	23,309

Percentage of Interaction							
Container	**Time (min)**	**ABS**	**Concentration (mg/l)**	**Qi**	**Ei**	**ti.Ei.Δt**	**ti².Ei.Δt**
0	0	0,0847	0	0	0	0	0
1	0,5	0,2352	0	0,00E+00	0,000	0,000	0,000E+00
2	0,667	0,4554	0	0,00E+00	0,000	0,000	0,000E+00
3	0,833	0,3528	0	0,00E+00	0,000	0,000	0,000E+00
4	1	0,2058	4,4057	1,23E-02	114,432	0,005	8,847E-05
5	1,167	0,2983	7,7722	2,16E-02	201,873	0,011	2,126E-04
6	1,333	0,114	1,0659	2,95E-03	27,685	0,002	3,781E-05
7	1,5	0,0946	0,3597	1,00E-03	9,343	0,001	1,625E-05
8	1,667	0,0912	0,2354	6,55E-04	6,114	0,000	1,314E-05
9	1,833	0,083	0	0,00E+00	0,000	0,000	0,000E+00
10	2	0,0917	0	0,00E+00	0,000	0,000	0,000E+00
11	2,167	0,0878	0	0,00E+00	0,000	0,000	0,000E+00
12	3	0,0818	0	0,00E+00	0,000	0,000	0,000E+00
13	4	0,1249	0	0,00E+00	0,000	0,000	0,000E+00
14	5	0,0862	0	0,00E+00	0,000	0,000	0,000E+00
15	6	0,0913	0	0,00E+00	0,000	0,000	0,000E+00
0	0	0	0	0,00E+00	0,000	0,000	0,000E+00

ΣQi	0,039
τm (hr)	0,019
τ(ideal)	0,015
Veff	1,294
σ²	4,886E-06
σθ²	0,013
σθ²=2D-2D²*(1-e^(-1/D))	
D	579288,063
λ	1,294
N	204682,356
N(check)	74,370

10.3 Changing the Gabion Arrangement

Date:	25-Sep-12	**Gabion Size (m): lxbxh**	0,29	0,29	0,175		**Total Submerged Volume (m^3):**	0,0437
	Arrangement 1	**Number of Gabions:**	4				**Flow Depth (m)**	0,13

Container	Time (min)	ABS	Concentration (mg/l)	Qi	Ei	ti.Ei.Δt	$ti^2.Ei.\Delta t$
0	0	0,0809	0	0	0	0	0
1	0,5	0,0841	0,1155	9,63E-04	1,396	0,000	8,08E-07
2	0,667	0,4581	13,7233	3,82E-02	165,819	0,005	5,70E-05
3	0,833	0,2214	5,1119	1,41E-02	61,767	0,002	3,29E-05
4	1	0,1931	4,0816	1,14E-02	49,318	0,002	3,81E-05
5	1,1667	0,1345	1,9497	5,42E-03	23,558	0,001	2,47E-05
6	1,333	0,1423	2,234	6,19E-03	26,994	0,002	3,69E-05
7	1,5	0,0999	0,6884	1,92E-03	8,318	0,001	1,45E-05
8	1,667	0,0939	0,4708	1,31E-03	5,689	0,000	1,22E-05
9	1,833	0,0905	0,3464	9,58E-04	4,186	0,000	1,08E-05
10	2	0,0874	0,2354	6,55E-04	2,844	0,000	8,80E-06
11	2,1667	0,0847	0,1377	3,83E-04	1,664	0,000	6,03E-06
12	2,25	0,0825	0,0578	8,02E-05	0,698	0,000	1,36E-06
13	2,4167	0,0813	0,0133	3,70E-05	0,161	0,000	7,24E-07
14	4	0,0817	0,0267	7,05E-04	0,323	0,001	3,78E-05
15	5	0,0817	0,0267	4,45E-04	0,323	0,000	3,73E-05

ΣQi	0,083
τm (hr)	0,016
τ(ideal)	0,014
Veff	1,151
σ^2	7,381E-05
$\sigma\theta^2$	0,300
$\sigma\theta^2=2D-2D^2*(1-e^{(-1/D)})$	
D	0,1835
λ	0,806
N	3,338
N(check)	3,338

Percentage Bypass							
Container	**Time (min)**	**ABS**	**Concentration (mg/l)**	**Qi**	**Ei**	**ti.Ei.Δt**	**ti².Ei.Δt**
0	0	0,0809	0	0	0	0	0
1	0,5	0,0841	0,1155	9,63E-04	8,466	0,001	4,899E-06
2	0,667	0,4581	13,7233	3,82E-02	1005,915	0,031	3,460E-04
3	0,833	0,2214	5,1119	1,41E-02	374,701	0,014	1,998E-04
4	1	0,1931	4,0816	1,14E-02	299,180	0,014	2,313E-04
5	1,1667	0,1345	1,9497	5,42E-03	142,913	0,008	1,501E-04
6	1,333	0,1423	0	0,00E+00	0,000	0,000	0,000E+00
7	1,5	0,0999	0	0,00E+00	0,000	0,000	0,000E+00
8	1,667	0,0939	0	0,00E+00	0,000	0,000	0,000E+00
9	1,833	0,0905	0	0,00E+00	0,000	0,000	0,000E+00
10	2	0,0874	0	0,00E+00	0,000	0,000	0,000E+00
11	2,1667	0,0847	0	0,00E+00	0,000	0,000	0,000E+00
12	2,25	0,0825	0	0,00E+00	0,000	0,000	0,000E+00
13	2,4167	0,0813	0	0,00E+00	0,000	0,000	0,000E+00
14	4	0,0817	0	0,00E+00	0,000	0,000	0,000E+00
15	5	0,0817	0	0,00E+00	0,000	0,000	0,000E+00

ΣQi	0,070
τm (hr)	0,068
τ(ideal)	0,014
Veff	4,963
σ^2	-3,652E-03
$\sigma\theta^2$	-0,797
$\sigma\theta^2=2D-2D^2*(1-e^{(-1/D)})$	
D	0,0693
λ	8,916
N	-1,255
N(check)	-1,255

Percentage of Interaction							
Container	**Time (min)**	**ABS**	**Concentration (mg/l)**	**Qi**	**Ei**	**ti.Ei.Δt**	**ti².Ei.Δt**
0	0	0,0809	0	0	0	0	0
1	0,5	0,0841	0	0,00E+00	0,000	0,000	0,000E+00
2	0,667	0,4581	0	0,00E+00	0,000	0,000	0,000E+00
3	0,833	0,2214	0	0,00E+00	0,000	0,000	0,000E+00
4	1	0,1931	0	0,00E+00	0,000	0,000	0,000E+00
5	1,1667	0,1345	0	0,00E+00	0,000	0,000	0,000E+00
6	1,333	0,1423	2,234	6,19E-03	163,752	0,010	2,240E-04
7	1,5	0,0999	0,6884	1,92E-03	50,460	0,004	8,778E-05
8	1,667	0,0939	0,4708	1,31E-03	34,510	0,003	7,414E-05
9	1,833	0,0905	0,3464	9,58E-04	25,391	0,002	6,556E-05
10	2	0,0874	0,2354	6,55E-04	17,255	0,002	5,336E-05
11	2,1667	0,0847	0,1377	3,83E-04	10,093	0,001	3,657E-05
12	2,25	0,0825	0,0578	8,02E-05	4,237	0,000	8,272E-06
13	2,4167	0,0813	0,0133	3,70E-05	0,975	0,000	4,394E-06
14	4	0,0817	0,0267	7,05E-04	1,957	0,003	2,295E-04
15	5	0,0817	0,0267	4,45E-04	1,957	0,003	2,265E-04

ΣQi	0,013
τm (hr)	0,028
τ(ideal)	0,014
Veff	2,017
σ²	2,532E-04
σθ²	0,334
σθ²=2D-2D²*(1-e^(-1/D))	
D	579288,0628
λ	1,342
N	2,990
N(check)	2,990

Date:	25-Sep-12	**Gabion Size (m): lxbxh**	0,29	0,29	0,175		**Total Submerged Volume (m^3):**	0,0437
	Arrangement 2	**Number of Gabions:**	4				**Flow Depth (m)**	0,13

Container	Time (min)	ABS	Concentration (mg/l)	Qi	Ei	ti.Ei.Δt	ti².Ei.Δt
0	0	0,0812	0	0	0	0	0
1	0,41667	0,0828	0,0577	4,01E-04	0,834	0,000	2,79E-07
2	0,5833	0,2855	7,4347	2,06E-02	107,494	0,003	2,82E-05
3	0,75	0,2324	5,5028	1,53E-02	79,562	0,003	3,45E-05
4	0,91667	0,1613	2,9135	8,09E-03	42,125	0,002	2,73E-05
5	1,0833	0,1838	3,7351	1,04E-02	54,004	0,003	4,89E-05
6	1,25	0,1273	1,6788	4,66E-03	24,273	0,001	2,93E-05
7	1,41667	0,1074	0,9549	2,65E-03	13,806	0,001	2,14E-05
8	1,5833	0,1024	0,7728	2,15E-03	11,173	0,001	2,16E-05
9	1,75	0,0956	0,5241	1,46E-03	7,578	0,001	1,79E-05
10	1,833	0,0895	0,302	4,18E-04	4,366	0,000	5,64E-06
11	1,91667	0,0897	0,3109	4,34E-04	4,495	0,000	6,40E-06
12	2	0,0883	0,2576	3,58E-04	3,724	0,000	5,75E-06
13	2,1667	0,0865	0,1954	5,43E-04	2,825	0,000	1,02E-05
14	3	0,0828	0,0577	8,01E-04	0,834	0,001	2,90E-05
15	4	0,0826	0,0533	8,88E-04	0,771	0,001	5,71E-05

ΣQi	0,069
τm (hr)	0,016
τ(ideal)	0,014
Veff	1,189
σ^2	8,036E-05
$\sigma\theta^2$	0,305
$\sigma\theta^2=2D-2D^2*(1-e^{(-1/D)})$	
D	0,1875
λ	0,826
N	3,274
N(check)	3,274

Percentage Bypass							
Container	**Time (min)**	**ABS**	**Concentration (mg/l)**	**Qi**	**Ei**	**ti.Ei.Δt**	**ti².Ei.Δt**
0	0	0,0812	0	0	0	0	0
1	0,41667	0,0828	0,0577	4,01E-04	4,229	0,000	1,416E-06
2	0,5833	0,2855	7,4347	2,06E-02	544,962	0,015	1,430E-04
3	0,75	0,2324	5,5028	1,53E-02	403,354	0,014	1,751E-04
4	0,91667	0,1613	2,9135	8,09E-03	213,559	0,009	1,385E-04
5	1,0833	0,1838	0	0,00E+00	0,000	0,000	0,000E+00
6	1,25	0,1273	0	0,00E+00	0,000	0,000	0,000E+00
7	1,41667	0,1074	0	0,00E+00	0,000	0,000	0,000E+00
8	1,5833	0,1024	0	0,00E+00	0,000	0,000	0,000E+00
9	1,75	0,0956	0	0,00E+00	0,000	0,000	0,000E+00
10	1,833	0,0895	0	0,00E+00	0,000	0,000	0,000E+00
11	1,91667	0,0897	0	0,00E+00	0,000	0,000	0,000E+00
12	2	0,0883	0	0,00E+00	0,000	0,000	0,000E+00
13	2,1667	0,0865	0	0,00E+00	0,000	0,000	0,000E+00
14	3	0,0828	0	0,00E+00	0,000	0,000	0,000E+00
15	4	0,0826	0	0,00E+00	0,000	0,000	0,000E+00

ΣQi	0,044
τm (hr)	0,038
τ(ideal)	0,014
Veff	2,785
σ²	-9,851E-04
σθ²	-0,683
σθ²=2D-2D²*(1-e^(-1/D))	
D	0,0693
λ	4,685
N	-1,465
N(check)	-1,465

Percentage of Interaction							
Container	**Time (min)**	**ABS**	**Concentration (mg/l)**	**Qi**	**Ei**	**ti.Ei.Δt**	**ti².Ei.Δt**
0	0	0,0812	0	0	0	0	0
1	0,41667	0,0828	0	0,00E+00	0,000	0,000	0,000E+00
2	0,5833	0,2855	0	0,00E+00	0,000	0,000	0,000E+00
3	0,75	0,2324	0	0,00E+00	0,000	0,000	0,000E+00
4	0,91667	0,1613	0	0,00E+00	0,000	0,000	0,000E+00
5	1,0833	0,1838	3,7351	1,04E-02	273,782	0,014	2,479E-04
6	1,25	0,1273	1,6788	4,66E-03	123,056	0,007	1,484E-04
7	1,41667	0,1074	0,9549	2,65E-03	69,994	0,005	1,084E-04
8	1,5833	0,1024	0,7728	2,15E-03	56,646	0,004	1,095E-04
9	1,75	0,0956	0,5241	1,46E-03	38,416	0,003	9,080E-05
10	1,833	0,0895	0,302	4,18E-04	22,137	0,001	2,858E-05
11	1,91667	0,0897	0,3109	4,34E-04	22,789	0,001	3,243E-05
12	2	0,0883	0,2576	3,58E-04	18,882	0,001	2,914E-05
13	2,1667	0,0865	0,1954	5,43E-04	14,323	0,001	5,189E-05
14	3	0,0828	0,0577	8,01E-04	4,229	0,003	1,468E-04
15	4	0,0826	0,0533	8,88E-04	3,907	0,004	2,894E-04

ΣQi	0,025
τm (hr)	0,044
τ(ideal)	0,014
Veff	3,243
σ²	-6,744E-04
σθ²	-0,344
σθ²=2D-2D²*(1-e^(-1/D))	
D	579288,0628
λ	#DIV/0!
N	#DIV/0!
N(check)	-2,903

Date:	26-Sep-12	**Gabion Size (m): lxbxh**	0,63	0,62	0,38		**Total Submerged Volume (m^3):**	0,0437
	Single Gabion	**Number of Gabions:**	1				**Flow Depth (m)**	0,112

Container	Time (min)	ABS	Concentration (mg/l)	Qi	Ei	ti.Ei.Δt	ti².Ei.Δt
0	0	0,0824	0	0	0	0	0
1	0,25	0,1539	2,6026	1,08E-02	45,006	0,001	3,256E-06
2	0,41667	0,2505	6,1157	1,70E-02	105,756	0,002	1,417E-05
3	0,5833	0,1635	2,949	8,19E-03	50,996	0,001	1,338E-05
4	0,75	0,1309	1,7632	4,90E-03	30,490	0,001	1,324E-05
5	0,91667	0,1235	1,4967	4,16E-03	25,882	0,001	1,678E-05
6	1,0833	0,1113	1,0526	2,92E-03	18,202	0,001	1,648E-05
7	1,25	0,1057	0,8483	2,36E-03	14,669	0,001	1,769E-05
8	1,41667	0,1022	0,7195	2,00E-03	12,442	0,001	1,927E-05
9	1,5833	0,0945	0,4397	1,22E-03	7,604	0,001	1,470E-05
10	1,75	0,0979	0,5641	1,57E-03	9,755	0,001	2,306E-05
11	1,91667	0,0878	0,1954	5,43E-04	3,379	0,000	9,578E-06
12	2,0833	0,088	0,2043	5,67E-04	3,533	0,000	1,183E-05
13	2,25	0,0875	0,1865	5,18E-04	3,225	0,000	1,260E-05
14	2,5	0,0854	0,111	4,63E-04	1,919	0,000	1,389E-05
15	3,5	0,0834	0,0355	5,92E-04	0,614	0,001	3,482E-05

ΣQi	0,058
τm (hr)	0,012
τ(ideal)	0,012
Veff	1,045
σ^2	8,619E-05
$\sigma\theta^2$	0,580
$\sigma\theta^2=2D-2D^2*(1-e^{(-1/D)})$	
D	0,5234
λ	0,439
N	1,723
N(check)	1,723

Percentage Bypass							
Container	**Time (min)**	**ABS**	**Concentration (mg/l)**	**Qi**	**Ei**	**ti.Ei.Δt**	**ti².Ei.Δt**
0	0	0,0729	0	0	0	0	0
1	0,25	0,0767	2,6026	1,08E-02	223,180	0,004	1,614E-05
2	0,41667	0,264	6,1157	1,70E-02	524,439	0,010	7,026E-05
3	0,5833	0,1277	2,949	8,19E-03	252,885	0,007	6,638E-05
4	0,75	0,0994	1,7632	4,90E-03	151,199	0,005	6,564E-05
5	0,91667	0,0811	0	0,00E+00	0,000	0,000	0,000E+00
6	1,0833	0,0775	0	0,00E+00	0,000	0,000	0,000E+00
7	1,25	0,0781	0	0,00E+00	0,000	0,000	0,000E+00
8	1,41667	0,0763	0	0,00E+00	0,000	0,000	0,000E+00
9	1,5833	0,0751	0	0,00E+00	0,000	0,000	0,000E+00
10	1,75	0,0762	0	0,00E+00	0,000	0,000	0,000E+00
11	1,91667	0,0762	0	0,00E+00	0,000	0,000	0,000E+00
12	2,0833	0,0762	0	0,00E+00	0,000	0,000	0,000E+00
13	2,25	0,0762	0	0,00E+00	0,000	0,000	0,000E+00
14	2,5	0,0762	0	0,00E+00	0,000	0,000	0,000E+00
15	3,5	0,0762	0	0,00E+00	0,000	0,000	0,000E+00

ΣQi	0,041
τm (hr)	0,026
τ(ideal)	0,012
Veff	2,236
σ²	-4,612E-04
σθ²	-0,679
σθ²=2D-2D²*(1-e^(-1/D))	
D	0,0693
λ	3,753
N	-1,474
N(check)	-1,474

Percentage of Interaction							
Container	**Time (min)**	**ABS**	**Concentration (mg/l)**	**Qi**	**Ei**	**ti.Ei.Δt**	**ti².Ei.Δt**
0	0	0,0729	0	0	0	0	0
1	0,25	0,0767	0	0,00E+00	0,000	0,000	0,000E+00
2	0,41667	0,264	0	0,00E+00	0,000	0,000	0,000E+00
3	0,5833	0,1277	0	0,00E+00	0,000	0,000	0,000E+00
4	0,75	0,0994	0	0,00E+00	0,000	0,000	0,000E+00
5	0,91667	0,0811	1,4967	4,16E-03	128,346	0,005	8,322E-05
6	1,0833	0,0775	1,0526	2,92E-03	90,263	0,005	8,172E-05
7	1,25	0,0781	0,8483	2,36E-03	72,744	0,004	8,772E-05
8	1,41667	0,0763	0,7195	2,00E-03	61,699	0,004	9,555E-05
9	1,5833	0,0751	0,4397	1,22E-03	37,706	0,003	7,292E-05
10	1,75	0,0762	0,5641	1,57E-03	48,373	0,004	1,143E-04
11	1,91667	0,0762	0,1954	5,43E-04	16,756	0,001	4,750E-05
12	2,0833	0,0762	0,2043	5,67E-04	17,519	0,002	5,866E-05
13	2,25	0,0762	0,1865	5,18E-04	15,993	0,002	6,248E-05
14	2,5	0,0762	0,111	4,63E-04	9,519	0,002	6,886E-05
15	3,5	0,0762	0,0355	5,92E-04	3,044	0,003	1,726E-04

ΣQi	0,017
τm (hr)	0,034
τ(ideal)	0,012
Veff	2,947
σ²	-2,356E-04
σθ²	-0,199
σθ²=2D-2D²*(1-e^(-1/D))	
D	579288,0628
λ	#DIV/0!
N	#DIV/0!
N(check)	-5,014

10.4 Changing the Number of Gabions

Date:	25-Sep-12	**Gabion Size (m): lxbxh**	0,29	0,29	0,175		**Total Submerged Volume (m^3):**	0,0437
		Number of Gabions:	4				**Flow Depth (m)**	0,13

Container	Time (min)	ABS	Concentration (mg/l)	Qi	Ei	ti.Ei.Δt	ti².Ei.Δt
0	0	0,0809	0	0	0	0	0
1	0,5	0,0841	0,1155	9,63E-04	1,396	0,000	8,08E-07
2	0,667	0,4581	13,7233	3,82E-02	165,819	0,005	5,70E-05
3	0,833	0,2214	5,1119	1,41E-02	61,767	0,002	3,29E-05
4	1	0,1931	4,0816	1,14E-02	49,318	0,002	3,81E-05
5	1,1667	0,1345	1,9497	5,42E-03	23,558	0,001	2,47E-05
6	1,333	0,1423	2,234	6,19E-03	26,994	0,002	3,69E-05
7	1,5	0,0999	0,6884	1,92E-03	8,318	0,001	1,45E-05
8	1,667	0,0939	0,4708	1,31E-03	5,689	0,000	1,22E-05
9	1,833	0,0905	0,3464	9,58E-04	4,186	0,000	1,08E-05
10	2	0,0874	0,2354	6,55E-04	2,844	0,000	8,80E-06
11	2,1667	0,0847	0,1377	3,83E-04	1,664	0,000	6,03E-06
12	2,25	0,0825	0,0578	8,02E-05	0,698	0,000	1,36E-06
13	2,4167	0,0813	0,0133	3,70E-05	0,161	0,000	7,24E-07
14	4	0,0817	0,0267	7,05E-04	0,323	0,001	3,78E-05
15	5	0,0817	0,0267	4,45E-04	0,323	0,000	3,73E-05

ΣQi	0,083
τm (hr)	0,016
τ(ideal)	0,014
Veff	1,151
σ^2	7,381E-05
$\sigma\theta^2$	0,300
$\sigma\theta^2=2D-2D^2*(1-e^{(-1/D)})$	
D	0,1835
λ	0,806
N	3,338
N(check)	3,338

Percentage Bypass							
Container	**Time (min)**	**ABS**	**Concentration (mg/l)**	**Qi**	**Ei**	**ti.Ei.Δt**	**ti².Ei.Δt**
0	0	0,0809	0	0	0	0	0
1	0,5	0,0841	0,1155	9,63E-04	8,466	0,001	4,899E-06
2	0,667	0,4581	13,7233	3,82E-02	1005,915	0,031	3,460E-04
3	0,833	0,2214	5,1119	1,41E-02	374,701	0,014	1,998E-04
4	1	0,1931	4,0816	1,14E-02	299,180	0,014	2,313E-04
5	1,1667	0,1345	1,9497	5,42E-03	142,913	0,008	1,501E-04
6	1,333	0,1423	0	0,00E+00	0,000	0,000	0,000E+00
7	1,5	0,0999	0	0,00E+00	0,000	0,000	0,000E+00
8	1,667	0,0939	0	0,00E+00	0,000	0,000	0,000E+00
9	1,833	0,0905	0	0,00E+00	0,000	0,000	0,000E+00
10	2	0,0874	0	0,00E+00	0,000	0,000	0,000E+00
11	2,1667	0,0847	0	0,00E+00	0,000	0,000	0,000E+00
12	2,25	0,0825	0	0,00E+00	0,000	0,000	0,000E+00
13	2,4167	0,0813	0	0,00E+00	0,000	0,000	0,000E+00
14	4	0,0817	0	0,00E+00	0,000	0,000	0,000E+00
15	5	0,0817	0	0,00E+00	0,000	0,000	0,000E+00

ΣQi	0,070
τm (hr)	0,068
τ(ideal)	0,014
Veff	4,963
σ²	-3,652E-03
σθ²	-0,797
σθ²=2D-2D²*(1-e^(-1/D))	
D	0,0693
λ	8,916
N	-1,255
N(check)	-1,255

Percentage of Interaction							
Container	**Time (min)**	**ABS**	**Concentration (mg/l)**	**Qi**	**Ei**	**ti.Ei.Δt**	**ti².Ei.Δt**
0	0	0,0809	0	0	0	0	0
1	0,5	0,0841	0	0,00E+00	0,000	0,000	0,000E+00
2	0,667	0,4581	0	0,00E+00	0,000	0,000	0,000E+00
3	0,833	0,2214	0	0,00E+00	0,000	0,000	0,000E+00
4	1	0,1931	0	0,00E+00	0,000	0,000	0,000E+00
5	1,1667	0,1345	0	0,00E+00	0,000	0,000	0,000E+00
6	1,333	0,1423	2,234	6,19E-03	163,752	0,010	2,240E-04
7	1,5	0,0999	0,6884	1,92E-03	50,460	0,004	8,778E-05
8	1,667	0,0939	0,4708	1,31E-03	34,510	0,003	7,414E-05
9	1,833	0,0905	0,3464	9,58E-04	25,391	0,002	6,556E-05
10	2	0,0874	0,2354	6,55E-04	17,255	0,002	5,336E-05
11	2,1667	0,0847	0,1377	3,83E-04	10,093	0,001	3,657E-05
12	2,25	0,0825	0,0578	8,02E-05	4,237	0,000	8,272E-06
13	2,4167	0,0813	0,0133	3,70E-05	0,975	0,000	4,394E-06
14	4	0,0817	0,0267	7,05E-04	1,957	0,003	2,295E-04
15	5	0,0817	0,0267	4,45E-04	1,957	0,003	2,265E-04

ΣQi	0,013
τm (hr)	0,028
τ(ideal)	0,014
Veff	2,017
σ²	2,532E-04
σθ²	0,334
σθ²=2D-2D²*(1-e^(-1/D))	
D	579288,0628
λ	1,342
N	2,990
N(check)	2,990

Date:	14-Sep-12	**Gabion Size (m): lxbxh**	0,29	0,29	0,175		**Total Submerged Volume (m^3):**	0,0875
		Number of Gabions:	8				**Flow Depth (m)**	0,13

Container	Time (min)	ABS	Concentration (mg/l)	Qi	Ei	ti.Ei.Δt	ti².Ei.Δt
0	0	0,0776	0	0	0	0	0
1	0,5	0,094	0,5951	4,96E-03	3,623	0,000	2,097E-06
2	0,667	0,2721	7,075	1,97E-02	43,071	0,001	1,481E-05
3	0,833	0,4288	12,7772	3,54E-02	77,785	0,003	4,148E-05
4	1	0,3938	11,5032	3,20E-02	70,029	0,003	5,414E-05
5	1,1667	0,248	6,2	1,72E-02	37,744	0,002	3,965E-05
6	1,333	0,2043	4,6101	1,28E-02	28,065	0,002	3,839E-05
7	1,5	0,1411	2,3095	6,43E-03	14,060	0,001	2,446E-05
8	1,667	0,1173	1,4434	4,02E-03	8,787	0,001	1,888E-05
9	1,833	0,1836	3,855	1,07E-02	23,468	0,002	6,060E-05
10	2,1667	0,087	0,342	1,90E-03	2,082	0,000	1,510E-05
11	2,33	0,0927	0,5463	1,49E-03	3,326	0,000	1,365E-05
12	2,5	0,0947	0,6218	1,76E-03	3,785	0,000	1,862E-05
13	2,833	0,1278	1,8254	1,01E-02	11,113	0,003	1,375E-04
14	4	0,0817	0,1466	2,85E-03	0,892	0,001	7,715E-05
15	5	0,0824	0,1732	2,89E-03	1,054	0,001	1,220E-04
16	6	0,0774	0,0066	1,10E-04	0,040	0,000	6,697E-06

ΣQi	0,164
τm (hr)	0,022
τ(ideal)	0,019
Veff	1,152
σ^2	1,992E-04
$\sigma\theta^2$	0,410
$\sigma\theta^2=2D-2D^2*(1-e^{(-1/D)})$	
D	0,282
λ	0,680
N	2,440
N(check)	2,440

Percentage Bypass							
Container	**Time (min)**	**ABS**	**Concentration (mg/l)**	**Qi**	**Ei**	**ti.Ei.Δt**	**ti².Ei.Δt**
0	0	0,0776	0	0	0	0	0
1	0,5	0,094	0,5951	4,96E-03	4,492	0,000	2,600E-06
2	0,667	0,2721	7,075	1,97E-02	53,409	0,002	1,837E-05
3	0,833	0,4288	12,7772	3,54E-02	96,455	0,004	5,144E-05
4	1	0,3938	11,5032	3,20E-02	86,838	0,004	6,714E-05
5	1,1667	0,248	6,2	1,72E-02	46,804	0,003	4,917E-05
6	1,333	0,2043	4,6101	1,28E-02	34,802	0,002	4,761E-05
7	1,5	0,1411	2,3095	6,43E-03	17,434	0,001	3,033E-05
8	1,667	0,1173	1,4434	4,02E-03	10,896	0,001	2,341E-05
9	1,833	0,1836	0	0,00E+00	0,000	0,000	0,000E+00
10	2,1667	0,087	0	0,00E+00	0,000	0,000	0,000E+00
11	2,33	0,0927	0	0,00E+00	0,000	0,000	0,000E+00
12	2,5	0,0947	0	0,00E+00	0,000	0,000	0,000E+00
13	2,833	0,1278	0	0,00E+00	0,000	0,000	0,000E+00
14	4	0,0817	0	0,00E+00	0,000	0,000	0,000E+00
15	5	0,0824	0	0,00E+00	0,000	0,000	0,000E+00
16	6	0,0774	0	0,00E+00	0,000	0,000	0,000E+00

ΣQi	0,132
τm (hr)	0,016
τ(ideal)	0,019
Veff	0,858
σ²	2,028E-05
σθ²	0,075
σθ²=2D-2D²*(1-e^(-1/D))	
D	0,0390
λ	0,793
N	13,303
N(check)	13,303

Percentage of Interaction							
Container	**Time (min)**	**ABS**	**Concentration (mg/l)**	**Qi**	**Ei**	**ti.Ei.Δt**	**ti².Ei.Δt**
0	0	0,0776	0	0	0	0	0
1	0,5	0,094	0	0,00E+00	0,000	0,000	0,000E+00
2	0,667	0,2721	0	0,00E+00	0,000	0,000	0,000E+00
3	0,833	0,4288	0	0,00E+00	0,000	0,000	0,000E+00
4	1	0,3938	0	0,00E+00	0,000	0,000	0,000E+00
5	1,1667	0,248	0	0,00E+00	0,000	0,000	0,000E+00
6	1,333	0,2043	0	0,00E+00	0,000	0,000	0,000E+00
7	1,5	0,1411	0	0,00E+00	0,000	0,000	0,000E+00
8	1,667	0,1173	0	0,00E+00	0,000	0,000	0,000E+00
9	1,833	0,1836	3,855	1,07E-02	306,741	0,026	7,920E-04
10	2,1667	0,087	0,342	1,90E-03	27,213	0,005	1,974E-04
11	2,33	0,0927	0	0,00E+00	0,000	0,000	0,000E+00
12	2,5	0,0947	0	0,00E+00	0,000	0,000	0,000E+00
13	2,833	0,1278	0	0,00E+00	0,000	0,000	0,000E+00
14	4	0,0817	0	0,00E+00	0,000	0,000	0,000E+00
15	5	0,0824	0	0,00E+00	0,000	0,000	0,000E+00
16	6	0,0774	0	0,00E+00	0,000	0,000	0,000E+00

ΣQi	0,013
τm (hr)	0,031
τ(ideal)	0,019
Veff	1,640
σ^2	3,973E-06
$\sigma\theta^2$	0,004
$\sigma\theta^2=2D-2D^2*(1-e^{(-1/D)})$	
D	579288,063
λ	1,640
N	251699,187
N(check)	248,035

Date:	09-Oct-12	**Gabion Size (m): lxbxh**	0,29	0,29	0,175		**Total Submerged Volume (m^3):**	0,1312
		Number of Gabions:	12				**Flow Depth (m)**	0,13

Container	Time (min)	ABS	Concentration (mg/l)	Qi	Ei	ti.Ei.Δt	ti².Ei.Δt
0	0	0,0883	0	0	0	0	0
1	0,7500	0,1033	0,5463	6,83E-03	4,152	0,001	8,110E-06
2	0,9167	0,1838	3,4775	9,66E-03	26,433	0,001	1,714E-05
3	1,0833	0,3215	8,4873	2,36E-02	64,512	0,003	5,842E-05
4	1,2500	0,334	8,9403	2,48E-02	67,956	0,004	8,193E-05
5	1,4167	0,3232	8,5495	2,37E-02	64,985	0,004	1,006E-04
6	1,5833	0,2323	5,2407	1,46E-02	39,835	0,003	7,706E-05
7	1,7500	0,1919	3,7706	1,05E-02	28,661	0,002	6,773E-05
8	1,9167	0,1466	2,1229	5,90E-03	16,136	0,001	4,574E-05
9	2,0833	0,1299	1,5145	4,21E-03	11,512	0,001	3,855E-05
10	2,2500	0,1163	1,0215	2,84E-03	7,764	0,001	3,033E-05
11	2,5000	0,0997	0,4175	1,74E-03	3,173	0,001	2,296E-05
12	2,7500	0,1094	0,7683	3,20E-03	5,840	0,001	5,112E-05
13	3,0833	0,0875	0	0,00E+00	0,000	0,000	0,000E+00
14	4,0833	0,0859	0	0,00E+00	0,000	0,000	0,000E+00
15	5,0833	0,0859	0	0,00E+00	0,000	0,000	0,000E+00

ΣQi	0,132
τm (hr)	0,023
τ(ideal)	0,025
Veff	0,952
σ^2	4,933E-05
$\sigma\theta^2$	0,090
$\sigma\theta^2=2D-2D^2*(1-e^{(-1/D)})$	
D	0,047
λ	0,867
N	11,157
N(check)	11,157

Percentage Bypass							
Container	**Time (min)**	**ABS**	**Concentration (mg/l)**	**Qi**	**Ei**	**ti.Ei.Δt**	**ti².Ei.Δt**
0	0	0,0883	0	0	0	0	0
1	0,7500	0,1033	0,5463	6,83E-03	4,256	0,001	8,313E-06
2	0,9167	0,1838	3,4775	9,66E-03	27,092	0,001	1,757E-05
3	1,0833	0,3215	8,4873	2,36E-02	66,121	0,003	5,988E-05
4	1,2500	0,334	8,9403	2,48E-02	69,651	0,004	8,397E-05
5	1,4167	0,3232	8,5495	2,37E-02	66,606	0,004	1,031E-04
6	1,5833	0,2323	5,2407	1,46E-02	40,828	0,003	7,898E-05
7	1,7500	0,1919	3,7706	1,05E-02	29,375	0,002	6,942E-05
8	1,9167	0,1466	2,1229	5,90E-03	16,539	0,001	4,688E-05
9	2,0833	0,1299	1,5145	4,21E-03	11,799	0,001	3,951E-05
10	2,2500	0,1163	1,0215	2,84E-03	7,958	0,001	3,109E-05
11	2,5000	0,0997	0,4175	1,74E-03	3,253	0,001	2,353E-05
12	2,7500	0,1094	0	0,00E+00	0,000	0,000	0,000E+00
13	3,0833	0,0875	0	0,00E+00	0,000	0,000	0,000E+00
14	4,0833	0,0859	0	0,00E+00	0,000	0,000	0,000E+00
15	5,0833	0,0859	0	0,00E+00	0,000	0,000	0,000E+00

ΣQi	0,128
τm (hr)	0,023
τ(ideal)	0,025
Veff	0,929
σ²	3,777E-05
σθ²	0,072
σθ²=2D-2D²*(1-e^(-1/D))	
D	0,0390
λ	0,862
N	13,889
N(check)	13,889

Percentage of Interaction							
Container	**Time (min)**	**ABS**	**Concentration (mg/l)**	**Qi**	**Ei**	**ti.Ei.Δt**	**ti².Ei.Δt**
0	0	0,0883	0	0	0	0	0
1	0,7500	0,1033	0	0,00E+00	0,000	0,000	0,000E+00
2	0,9167	0,1838	0	0,00E+00	0,000	0,000	0,000E+00
3	1,0833	0,3215	0	0,00E+00	0,000	0,000	0,000E+00
4	1,2500	0,334	0	0,00E+00	0,000	0,000	0,000E+00
5	1,4167	0,3232	0	0,00E+00	0,000	0,000	0,000E+00
6	1,5833	0,2323	0	0,00E+00	0,000	0,000	0,000E+00
7	1,7500	0,1919	0	0,00E+00	0,000	0,000	0,000E+00
8	1,9167	0,1466	0	0,00E+00	0,000	0,000	0,000E+00
9	2,0833	0,1299	0	0,00E+00	0,000	0,000	0,000E+00
10	2,2500	0,1163	0	0,00E+00	0,000	0,000	0,000E+00
11	2,5000	0,0997	0	0,00E+00	0,000	0,000	0,000E+00
12	2,7500	0,1094	0,7683	3,20E-03	240,000	0,046	2,101E-03
13	3,0833	0,0875	0	0,00E+00	0,000	0,000	0,000E+00
14	4,0833	0,0859	0	0,00E+00	0,000	0,000	0,000E+00
15	5,0833	0,0859	0	0,00E+00	0,000	0,000	0,000E+00

ΣQi	0,003
τm (hr)	0,046
τ(ideal)	0,025
Veff	1,860
σ^2	0,000E+00
$\sigma\theta^2$	0,000
$\sigma\theta^2=2D-2D^2*(1-e^{(-1/D)})$	
D	579288,063
λ	#DIV/0!
N	#DIV/0!
N(check)	#DIV/0!

Date:	08-Oct-12	**Gabion Size (m): lxbxh**	0,29	0,29	0,175		**Total Submerged Volume (m^3):**	0,1749
		Number of Gabions:	16				**Flow Depth (m)**	0,13

Container	Time (min)	ABS	Concentration (mg/l)	Qi	Ei	ti.Ei.Δt	ti².Ei.Δt
0	0	0,0907	0	0	0	0	0
1	0,75	0,0914	0,0267	3,34E-04	0,391	0,000	7,642E-07
2	0,916666667	0,1185	1,0126	2,81E-03	14,839	0,001	9,621E-06
3	1,083333333	0,1719	2,9535	8,20E-03	43,283	0,002	3,920E-05
4	1,25	0,2085	4,2859	1,19E-02	62,809	0,004	7,572E-05
5	1,416666667	0,2174	4,6101	1,28E-02	67,560	0,004	1,046E-04
6	1,583333333	0,1849	3,4287	9,52E-03	50,247	0,004	9,720E-05
7	1,75	0,1595	2,5049	6,96E-03	36,709	0,003	8,674E-05
8	1,916666667	0,1432	1,9098	5,31E-03	27,988	0,002	7,933E-05
9	2,083333333	0,1371	1,6877	4,69E-03	24,733	0,002	8,283E-05
10	2,25	0,105	0,5196	1,44E-03	7,615	0,001	2,974E-05
11	2,416666667	0,1187	1,0171	2,83E-03	14,905	0,002	6,717E-05
12	2,75	0,0968	0,2221	1,23E-03	3,255	0,001	3,799E-05
13	2,916666667	0,0917	0,0355	9,86E-05	0,520	0,000	3,415E-06
14	3,083333333	0,0917	0,0355	9,86E-05	0,520	0,000	3,816E-06
15	3,25	0,0878	0	0,00E+00	0,000	0,000	0,000E+00
16	4,25	0,0883	0	0,00E+00	0,000	0,000	0,000E+00

ΣQi	0,068
τm (hr)	0,026
τ(ideal)	0,030
Veff	0,859
σ^2	4,797E-05
$\sigma\theta^2$	0,072
$\sigma\theta^2=2D-2D^2*(1-e^{(-1/D)})$	
D	0,037
λ	0,797
N	13,970
N(check)	13,970

Percentage Bypass							
Container	**Time (min)**	**ABS**	**Concentration (mg/l)**	**Qi**	**Ei**	**ti.Ei.Δt**	**ti².Ei.Δt**
0	0	0,0907	0	0	0	0	0
1	0,75	0,0914	0,0267	3,34E-04	0,462	0,000	9,015E-07
2	0,916666667	0,1185	1,0126	2,81E-03	17,504	0,001	1,135E-05
3	1,083333333	0,1719	2,9535	8,20E-03	51,055	0,003	4,623E-05
4	1,25	0,2085	4,2859	1,19E-02	74,088	0,004	8,932E-05
5	1,416666667	0,2174	4,6101	1,28E-02	79,692	0,005	1,234E-04
6	1,583333333	0,1849	3,4287	9,52E-03	59,270	0,004	1,146E-04
7	1,75	0,1595	2,5049	6,96E-03	43,301	0,004	1,023E-04
8	1,916666667	0,1432	1,9098	5,31E-03	33,014	0,003	9,358E-05
9	2,083333333	0,1371	0	0,00E+00	0,000	0,000	0,000E+00
10	2,25	0,105	0	0,00E+00	0,000	0,000	0,000E+00
11	2,416666667	0,1187	0	0,00E+00	0,000	0,000	0,000E+00
12	2,75	0,0968	0	0,00E+00	0,000	0,000	0,000E+00
13	2,916666667	0,0917	0	0,00E+00	0,000	0,000	0,000E+00
14	3,083333333	0,0917	0	0,00E+00	0,000	0,000	0,000E+00
15	3,25	0,0878	0	0,00E+00	0,000	0,000	0,000E+00
16	4,25	0,0883	0	0,00E+00	0,000	0,000	0,000E+00

ΣQi	0,058
τm (hr)	0,024
τ(ideal)	0,030
Veff	0,785
σ²	2,140E-05
σθ²	0,038
σθ²=2D-2D²*(1-e^(-1/D))	
D	0,0390
λ	0,755
N	26,184
N(check)	26,184

Percentage of Interaction							
Container	**Time (min)**	**ABS**	**Concentration (mg/l)**	**Qi**	**Ei**	**ti.Ei.Δt**	**ti².Ei.Δt**
0	0	0,0907	0	0	0	0	0
1	0,75	0,0914	0	0,00E+00	0,000	0,000	0,000E+00
2	0,916666667	0,1185	0	0,00E+00	0,000	0,000	0,000E+00
3	1,083333333	0,1719	0	0,00E+00	0,000	0,000	0,000E+00
4	1,25	0,2085	0	0,00E+00	0,000	0,000	0,000E+00
5	1,416666667	0,2174	0	0,00E+00	0,000	0,000	0,000E+00
6	1,583333333	0,1849	0	0,00E+00	0,000	0,000	0,000E+00
7	1,75	0,1595	0	0,00E+00	0,000	0,000	0,000E+00
8	1,916666667	0,1432	0	0,00E+00	0,000	0,000	0,000E+00
9	2,083333333	0,1371	1,6877	4,69E-03	275,256	0,027	9,218E-04
10	2,25	0,105	0,5196	1,44E-03	84,744	0,009	3,310E-04
11	2,416666667	0,1187	0	0,00E+00	0,000	0,000	0,000E+00
12	2,75	0,0968	0	0,00E+00	0,000	0,000	0,000E+00
13	2,916666667	0,0917	0	0,00E+00	0,000	0,000	0,000E+00
14	3,083333333	0,0917	0	0,00E+00	0,000	0,000	0,000E+00
15	3,25	0,0878	0	0,00E+00	0,000	0,000	0,000E+00
16	4,25	0,0883	0	0,00E+00	0,000	0,000	0,000E+00

ΣQi	0,006
τm (hr)	0,035
τ(ideal)	0,030
Veff	1,173
σ²	1,389E-06
σθ²	0,001
σθ²=2D-2D²*(1-e^(-1/D))	
D	579288,063
λ	1,173
N	720051,128
N(check)	901,122

11 APPENDIX C: Model Coding in VBA

```
Option Base 1
Option Explicit

Dim arrZones(4, 20)
Dim flume(4, 20, 35) 'Pathways / zones / time
Dim probTimes(4)
Dim numZones As Integer
Dim time As Integer
Dim particles As Double

Sub clearOutput()

    Sheets("Output-Data").Select

    Range("A1").Select
    Range(Selection, Selection.End(xlDown)).Select
    Range(Selection, Selection.End(xlToRight)).Select
    Selection.Clear

End Sub

Sub GetData()

    Dim R As Range
    Dim i As Integer
    Dim j As Integer

    Sheets("Input").Select

    time = Cells(2, 2)
```

```
    particles = Cells(2, 5)

    probTimes(1) = Cells(5, 2)
    probTimes(2) = Cells(6, 2)
    probTimes(3) = Cells(7, 2)
    probTimes(4) = Cells(8, 2)

    Range("B11").Select
    Range(Selection, Selection.End(xlDown)).Select
    Range(Selection, Selection.End(xlToRight)).Select
    Set R = Selection

    numZones = R.Columns.Count

    For i = 1 To 20
       arrZones(1, i) = 0
       arrZones(2, i) = 0
       arrZones(3, i) = 0
       arrZones(4, i) = 0

For j = 1 To 35
          flume(1, i, j) = 0
          flume(2, i, j) = 0
          flume(3, i, j) = 0
          flume(4, i, j) = 0
       Next j
    Next i

    For i = 1 To numZones
       arrZones(1, i) = R(1, i)
       arrZones(2, i) = R(2, i)
```

```
        arrZones(3, i) = R(3, i)
        arrZones(4, i) = R(4, i)
    Next i

End Sub

Sub sim()

    Dim j As Integer
    Dim k As Integer

    clearOutput
    GetData

    flume(1, 1, probTimes(1)) = flume(1, 1, probTimes(1)) + arrZones(1, 1) *
particles
    flume(2, 1, probTimes(2)) = flume(2, 1, probTimes(2)) + arrZones(2, 1) *
particles
    flume(3, 1, probTimes(3)) = flume(3, 1, probTimes(3)) + arrZones(3, 1) *
particles
    flume(4, 1, probTimes(4)) = flume(4, 1, probTimes(4)) + arrZones(4, 1) *
particles

    For j = 2 To time
        For k = 2 To numZones
            particles = flume(1, k - 1, j - 1) + flume(2, k - 1, j - 1) + flume(3, k - 1, j -
1) + flume(4, k - 1, j - 1)
            flume(1, k, j - 1 + probTimes(1)) = flume(1, k, j - 1 + probTimes(1)) +
arrZones(1, k) * particles
            flume(2, k, j - 1 + probTimes(2)) = flume(2, k, j - 1 + probTimes(2)) +
arrZones(2, k) * particles
```

```
        flume(3, k, j - 1 + probTimes(3)) = flume(3, k, j - 1 + probTimes(3)) +
arrZones(3, k) * particles
        flume(4, k, j - 1 + probTimes(4)) = flume(4, k, j - 1 + probTimes(4)) +
arrZones(4, k) * particles
      Next k
   Next j

   Sheets("Output-Data").Select

   For j = 1 To time
      For k = 1 To numZones
         Cells(k, j) = flume(1, k, j) + flume(2, k, j) + flume(3, k, j) + flume(4, k, j)
      Next k
   Next j

End Sub
```